Report 3883

NAVAL SHIP RESEARCH AND DEVELOPMENT CENTER
Bethesda, Md. 20034

DESIGN HISTORY OF THE RIGID VINYL MODEL OF THE HYDROFOIL PLAINVIEW (AGEH-1)

by
Steven L. Austin

APPROVED FOR PUBLIC RELEASE: DISTRIBUTION UNLIMITED

STRUCTURES DEPARTMENT
RESEARCH AND DEVELOPMENT REPORT

October 1972

Report 3883

DESIGN HISTORY OF THE RIGID VINYL MODEL OF THE HYDROFOIL PLAINVIEW (AGEH-1)

The Naval Ship Research and Development Center is a U. S. Navy center for laboratory effort directed at achieving improved sea and air vehicles. It was formed in March 1967 by merging the David Taylor Model Basin at Carderock, Maryland with the Marine Engineering Laboratory at Annapolis, Maryland.

Naval Ship Research and Development Center

Bethesda, Md. 20034

MAJOR NSRDC ORGANIZATIONAL COMPONENTS

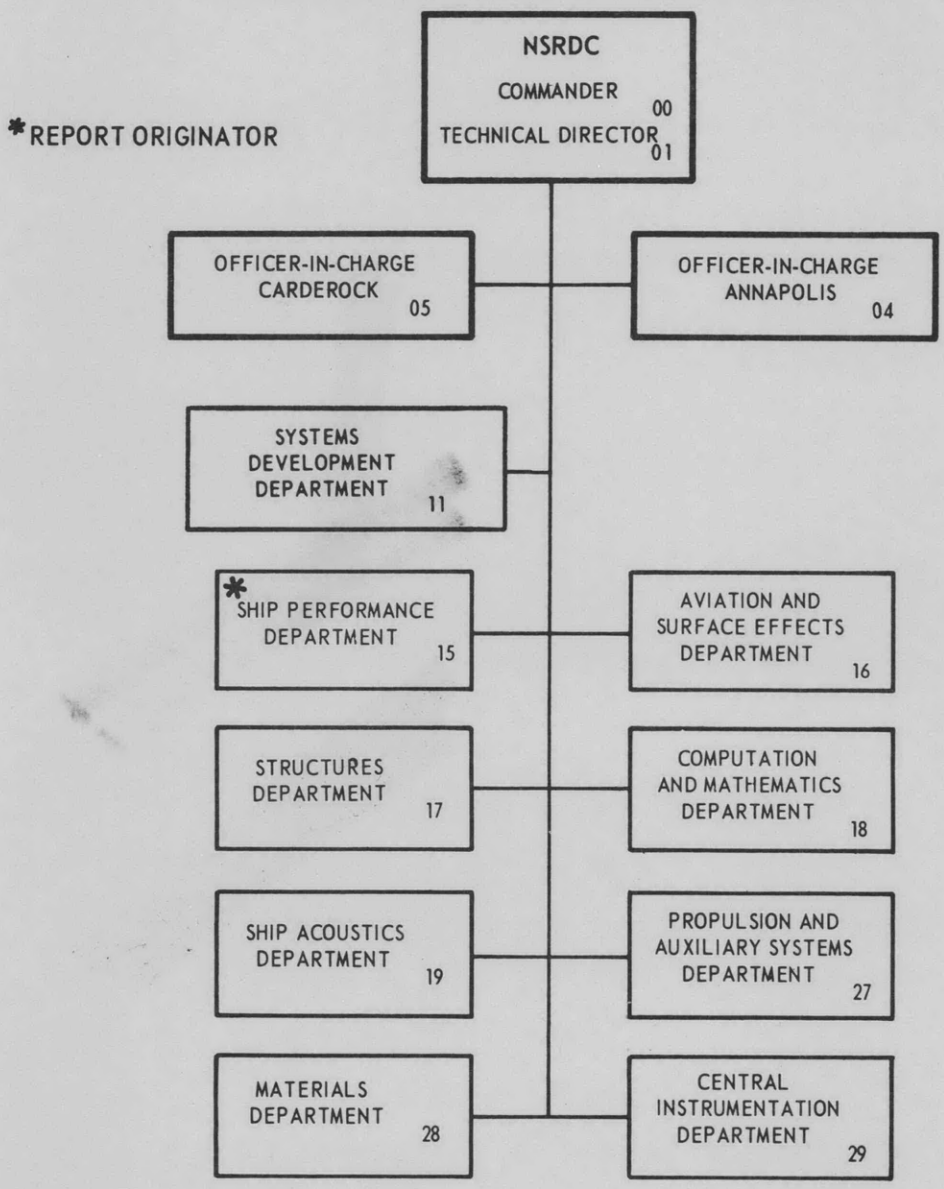

NDW-NSRDC 3960/43b (Rev. 3-72)

GPO 928-108

DEPARTMENT OF THE NAVY
NAVAL SHIP RESEARCH AND DEVELOPMENT CENTER
BETHESDA, MD. 20034

DESIGN HISTORY OF THE RIGID VINYL MODEL OF THE HYDROFOIL PLAINVIEW (AGEH-1)

by

Steven L. Austin

APPROVED FOR PUBLIC RELEASE: DISTRIBUTION UNLIMITED

October 1972

Report 3883

TABLE OF CONTENTS

LIST OF FIGURES

LIST OF TABLES

ABSTRACT

This report presents the method and the rationale used in the design and construction of a small-scale rigid vinyl (PVC) statically loaded, elastic structural model of the hydrofoil PLAINVIEW (AGEH-1).

ADMINISTRATIVE INFORMATION

The work reported herein was authorized under the Hydrofoil Advanced Development Program of the Naval Ship Research and Development Center (NSRDC). Funding was provided by Project S46-06X, Task 1707.

INTRODUCTION

Modeling of complete ship structures in a thermoplastic is a relatively quick and efficient prediction method that affords economy of material, time, and manpower as well as ease of modification and instrumentation. Such a technique is desirable in view of the current emphasis on unconventional, high performance ships.

NSRDC recommended a structural modeling of the experimental hydrofoil PLAINVIEW (AGEH-1) and suggested rigid vinyl (PVC) as the most practical thermoplastic for that purpose.* Basic studies in PVC material behavior had to be performed prior to any modeling effort. Final verification of modeling accuracy, however, will be obtained from the prototype AGEH-1 by virtue of the availability of extensive sea trials data. The experimentally verified model of the prototype would then be used to analyze its unique construction as well as to provide feedback for future prototype modification.

This report deals with the design, construction, and instrumentation of the 1/20-scale AGEH-1 rigid vinyl model. It discusses each step and decision together with the assumptions made to design a statically loaded, elastic structural model which would provide representative strain and

*As reported informally in NSRDC Tech Note SD n-148 of August 1969.

deflection data under longitudinal (vertical) and lateral bending and torsion. In short, the report identifies the steps of designing and fabricating a rigid vinyl model and the means by which problems inherent in small-scale modeling were resolved.

PLAINVIEW (AGEH-1) STRUCTURAL CONFIGURATION

The PLAINVIEW (AGEH-1), a research hydrofoil ship, is shown in its two operational modes in Figure 1. The AGEH-1 was selected for verification of the rigid vinyl modeling technique by virtue of its extensive analysis and documentation which would allow for detailed comparison of model and prototype strain and deflection data. A model of the AGEH-1 would also provide supplemental strain data near the numerous discontinuities in the ship. The strut attachment foundations, which are regions of high load, were located in discontinuous areas of the hull structure. These areas are shown in Figures 2 and 3.

Like most other hydrofoil craft, PLAINVIEW is a weight-critical structure. Therefore, all heavy equipment had to be placed in optimum locations. For this reason, the main engines were located on the lower deck adjacent to drive shaft housings which are in the main struts. This is very near the center of gravity of the ship. Because of the operational requirements of the two engines, air intakes and exhaust openings are in juxtaposition at midship. These four large openings must penetrate the three levels of the ship above the engine, including the highly stressed 0-1 level. Figure 4 indicates the orientation of the 0-1 level decking and openings that require further investigation. The air intakes, exhaust openings, and other numerous openings indicated in Figure 4 are shown photographically in Figures 5-9.

The prototype hull plating and decking are comprised of four basic extruded aluminum plate configurations. Figure 10 shows a typical plating section which is extruded with its stiffeners in place. These panels are then welded into place and the extruded stiffeners become the ship "stringers" which run continuously in the longitudinal direction. The AGEH-1 prototype utilizes 71 transverse frames spaced typically at 3-ft intervals over its 212-ft overall length. During foilborne operations,

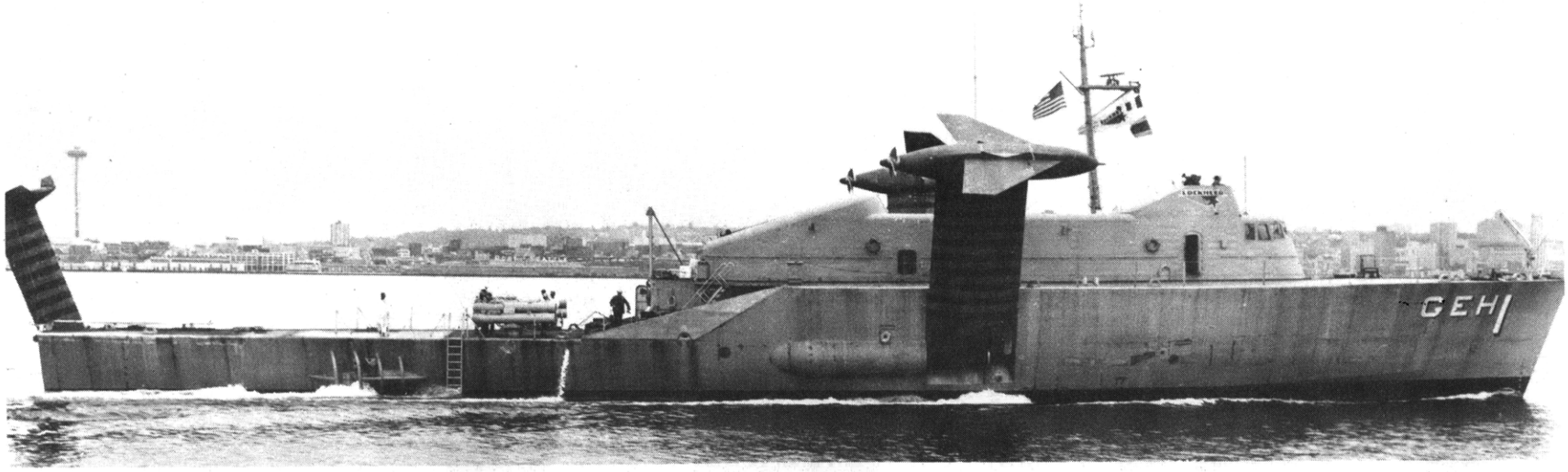

Figure 1a - Struts and Foils Retracted

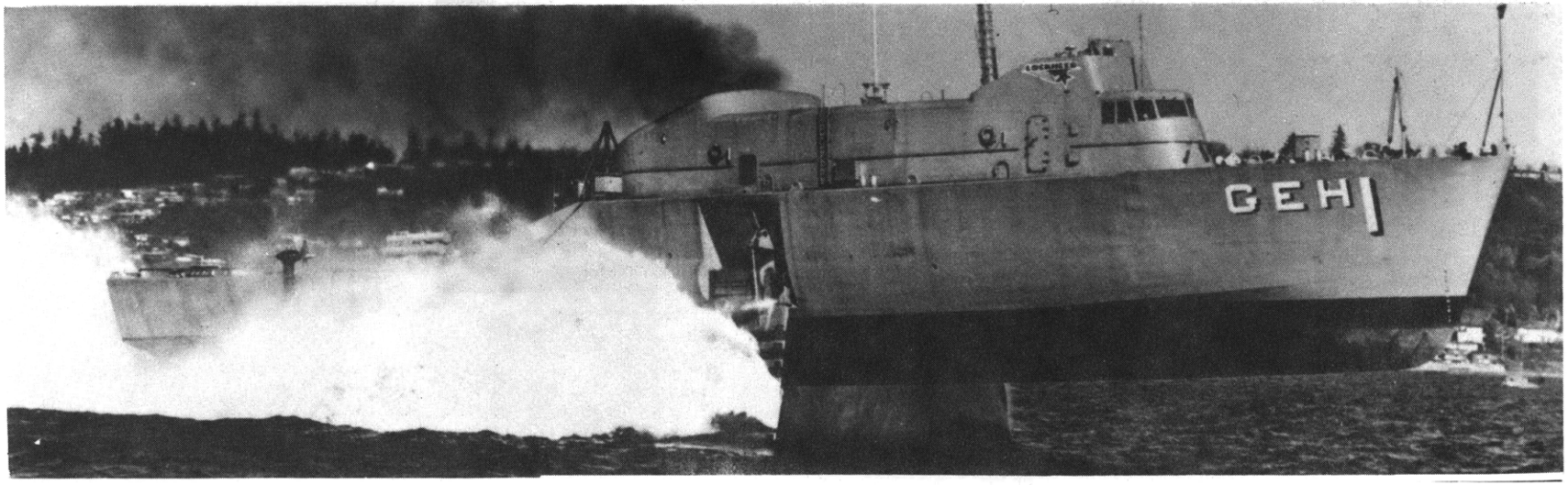

Figure 1b - Struts and Foils Extended

Figure 1 - Two Operational Modes of the AGEH-1 Prototype

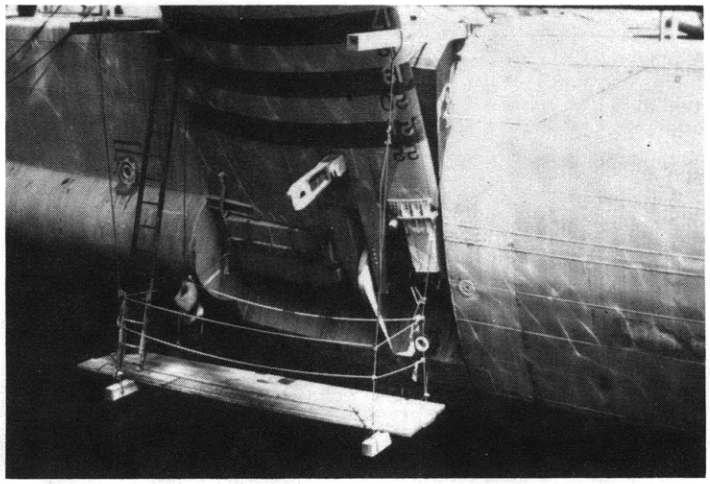

Figure 2 - Retracted Main Starboard Strut and Strut Support Area

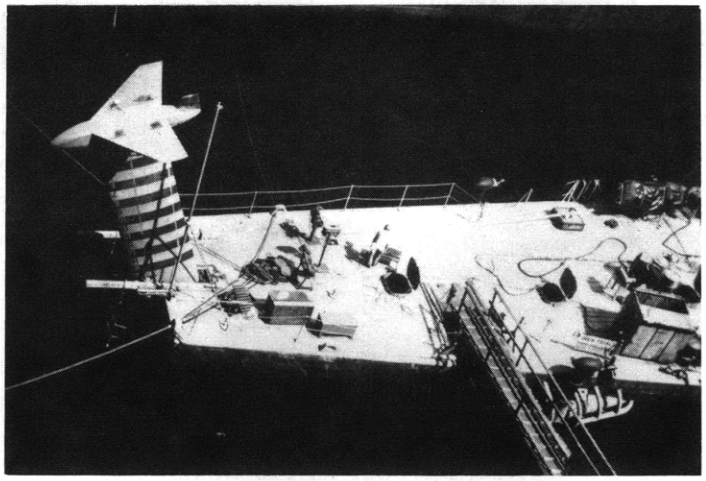

Figure 3 - Retracted Tail Strut and Foil in Recessed Foundation Area

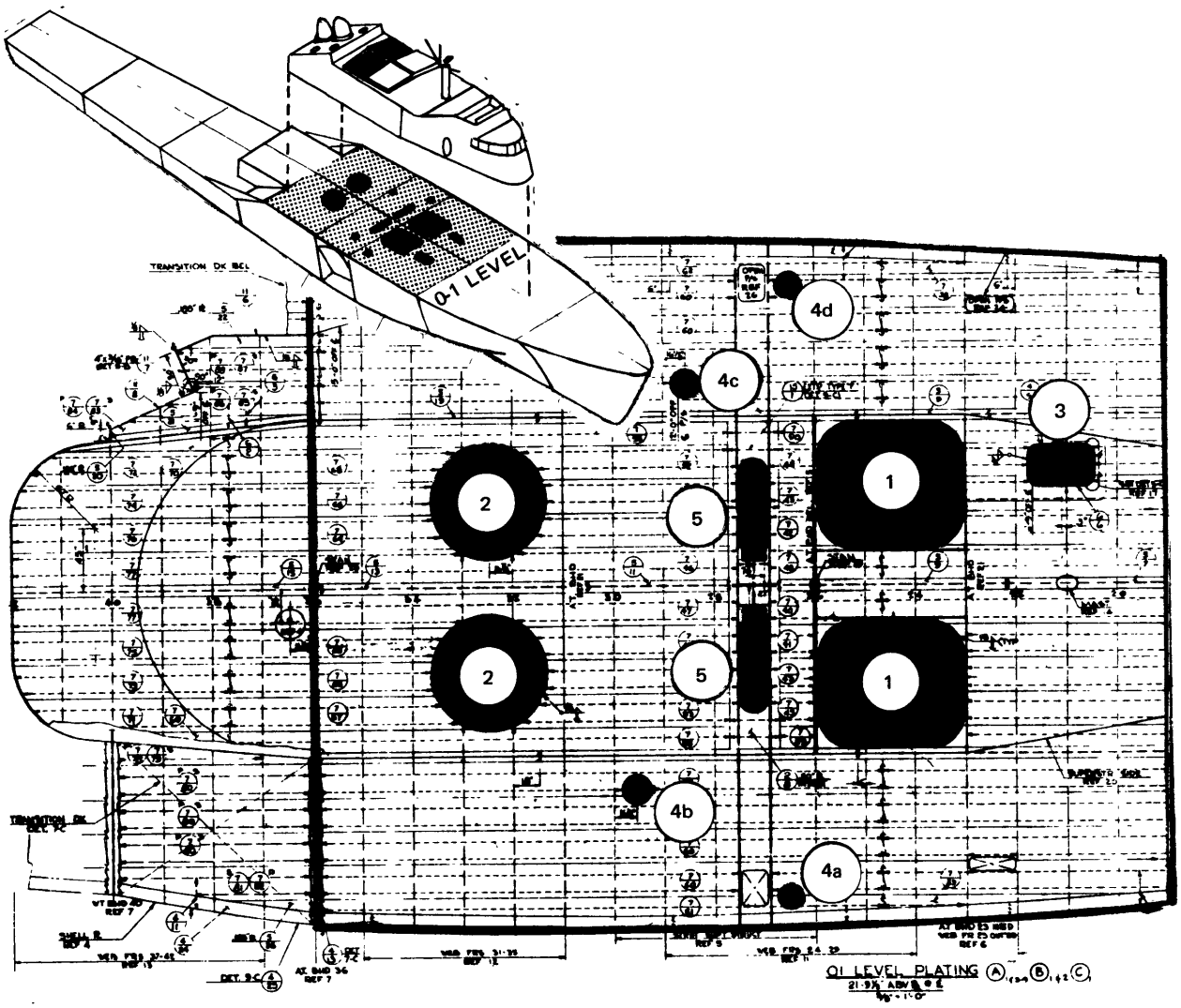

NOTES: A) FOR DETAILS SEE AGEH-1
PLANS 108-2206548

0-1 LEVEL PLATING AND FRAMING

B) LEGEND

1. AIR INTAKE OPENINGS (SEE FIGURE 5)
2. EXHAUST OPENINGS (SEE FIGURE 6)
3. HATCHWAY (SEE FIGURE 7)
4. MANHOLES (SEE FIGURE 8)
5. MAIN FOIL RETRACTION MECHANISM SLOTS (SEE FIGURE 9)

Figure 4 - Openings under Investigation for the 0-1 Level Decking

(See AGEH-1 Plan 800-2206548 for details of 0-1 level plating and framing)

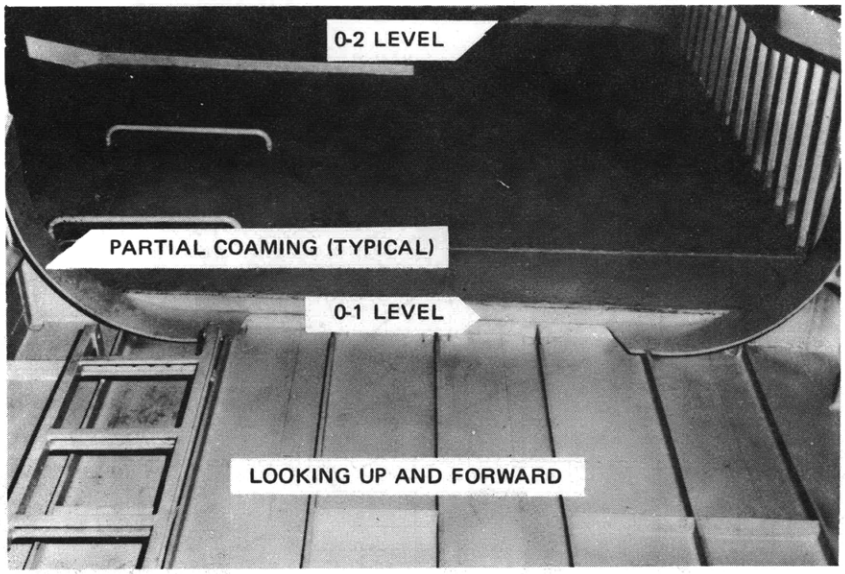

Figure 5 - 0-1 Level Air Intake Opening

Figure 6 - 0-1 Level Exhaust Openings

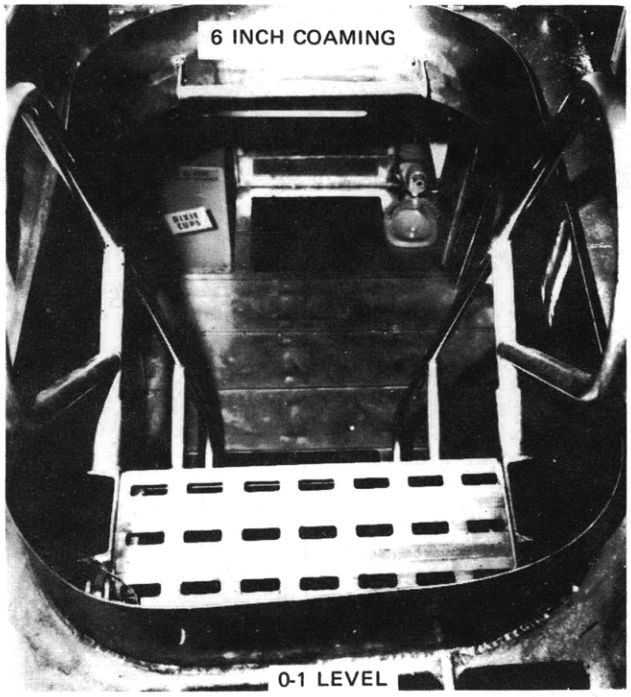

Figure 7 - Typical Hatchway

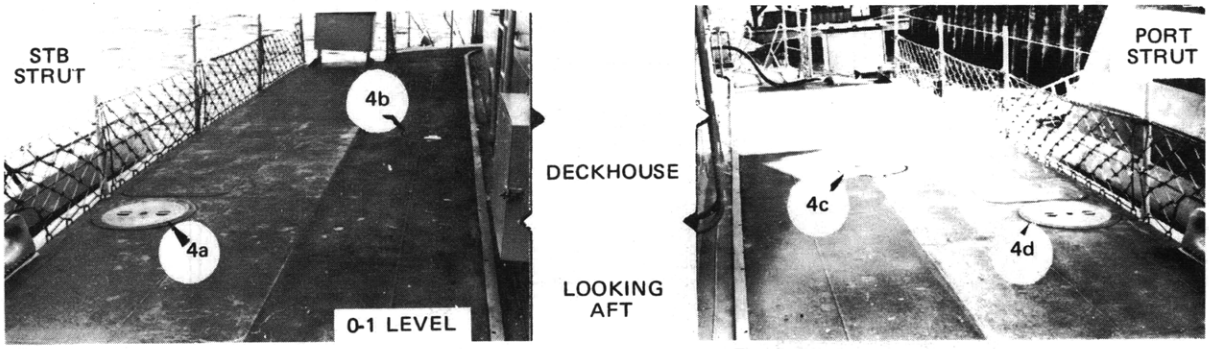

Figure 8 - 0-1 Level Access Manholes
(Manholes are indicated by the circled areas)

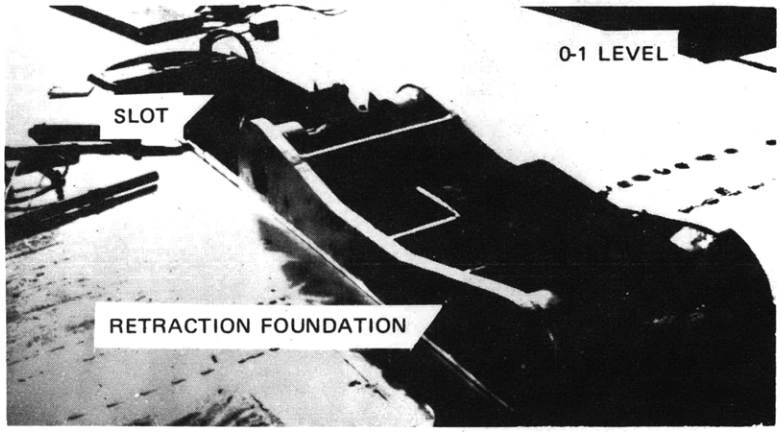

Figure 9 - Main Foil Retraction Mechanism Slots
during Construction

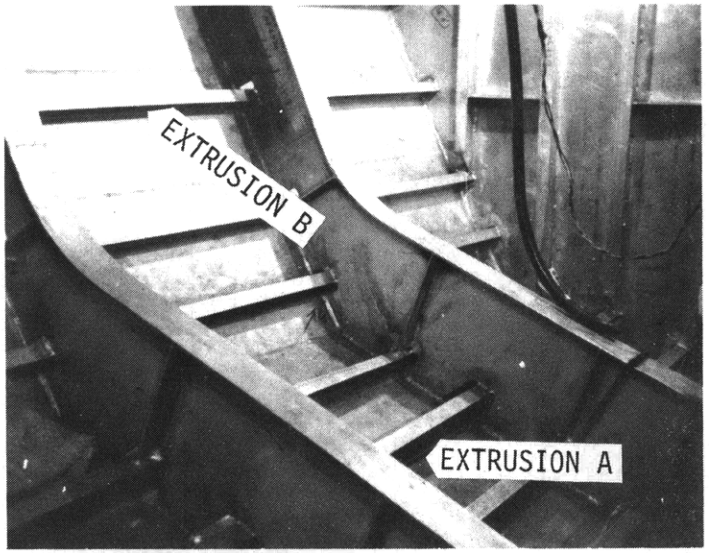

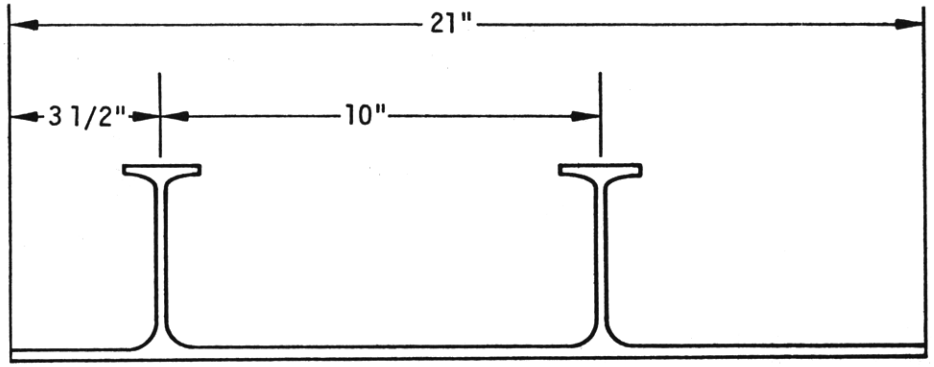

PANEL EXTRUSION (A)
3" = 1'-0"

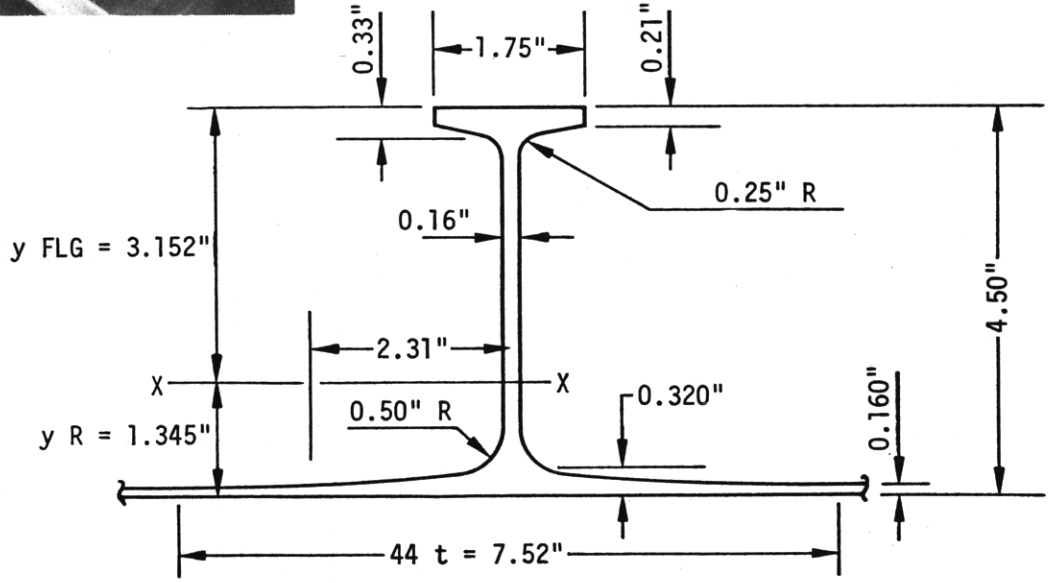

TEE SECTION

Figure 10 - Typical Extruded Stiffener

the main structural support is provided by Frame 27. Figure 11 presents the plan for the main strut/foil support, structural Frame 27, and Figure 12 identifies its ship orientation. Hull strength longitudinals consists primarily of six girders, two longitudinal bulkheads, a center vertical keel, and the extruded stringers of the hull skin and decks.

DESIGN

The accurate prediction of full-scale structural performance through the use of models is a function of a properly scaled model design, precise fabrication, representative loading and support, and the correct interpretation of the experimental results. The design stage is the foundation of any modeling effort since it determines the plan for construction and the procedure for data analysis. The development of a model design requires an understanding of the structure to be represented, the material that will be used in the model, the scaling relationships, and the amount of detail required for the desired level of investigation.

RIGID VINYL MATERIAL PROPERTIES

Rigid vinyl is one of the more dimensionally stable, nonhygroscopic and isotropic plastics on the market. Limited and conflicting documentation of PVC mechanical behavior necessitated additional investigation for data verification. Table 1 gives the experimentally verified basic material properties of commercially available "Bakelite" rigid vinyl at a temperature of 73 F. Even though PVC is a relatively stable plastic, its modulus of

TABLE 1 - MATERIAL PROPERTIES OF RIGID VINYL ("BAKELITE") AT A TEMPERATURE OF 73 F

Specific Gravity	1.35
Tensile Strength, psi	9,000
Elastic Limit, psi	4,000
Modulus of Elasticity E, psi	5×10^{5}*
Coefficient of Linear Expression α, in./deg F	38×10^{-6}
Poisson's Ratio, μ	0.325

*0.015 in. thick PVC--see Figure 14.

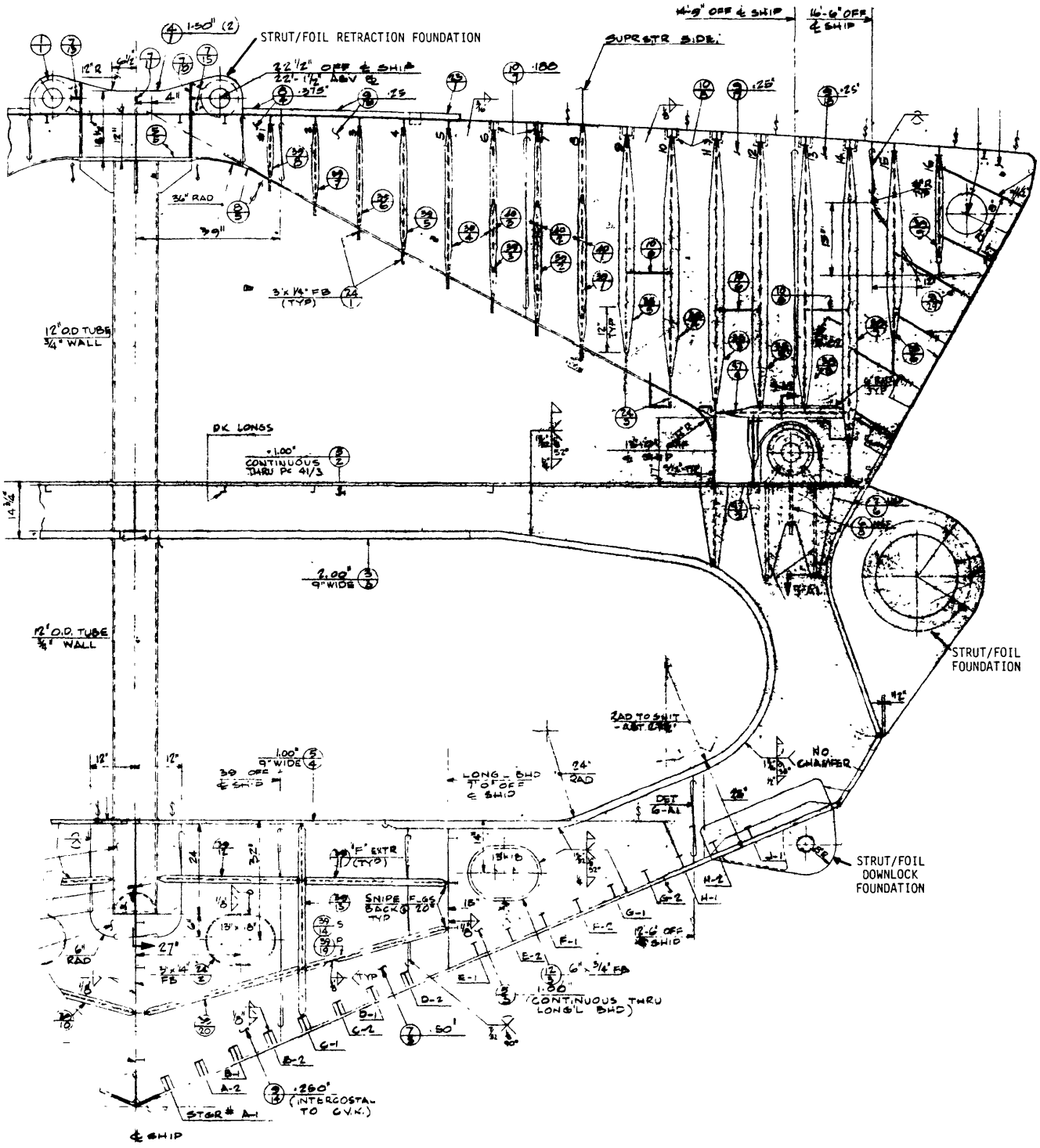

Figure 11 - AGEH-1 Main Strut/Foil Support, Structural Frame 27

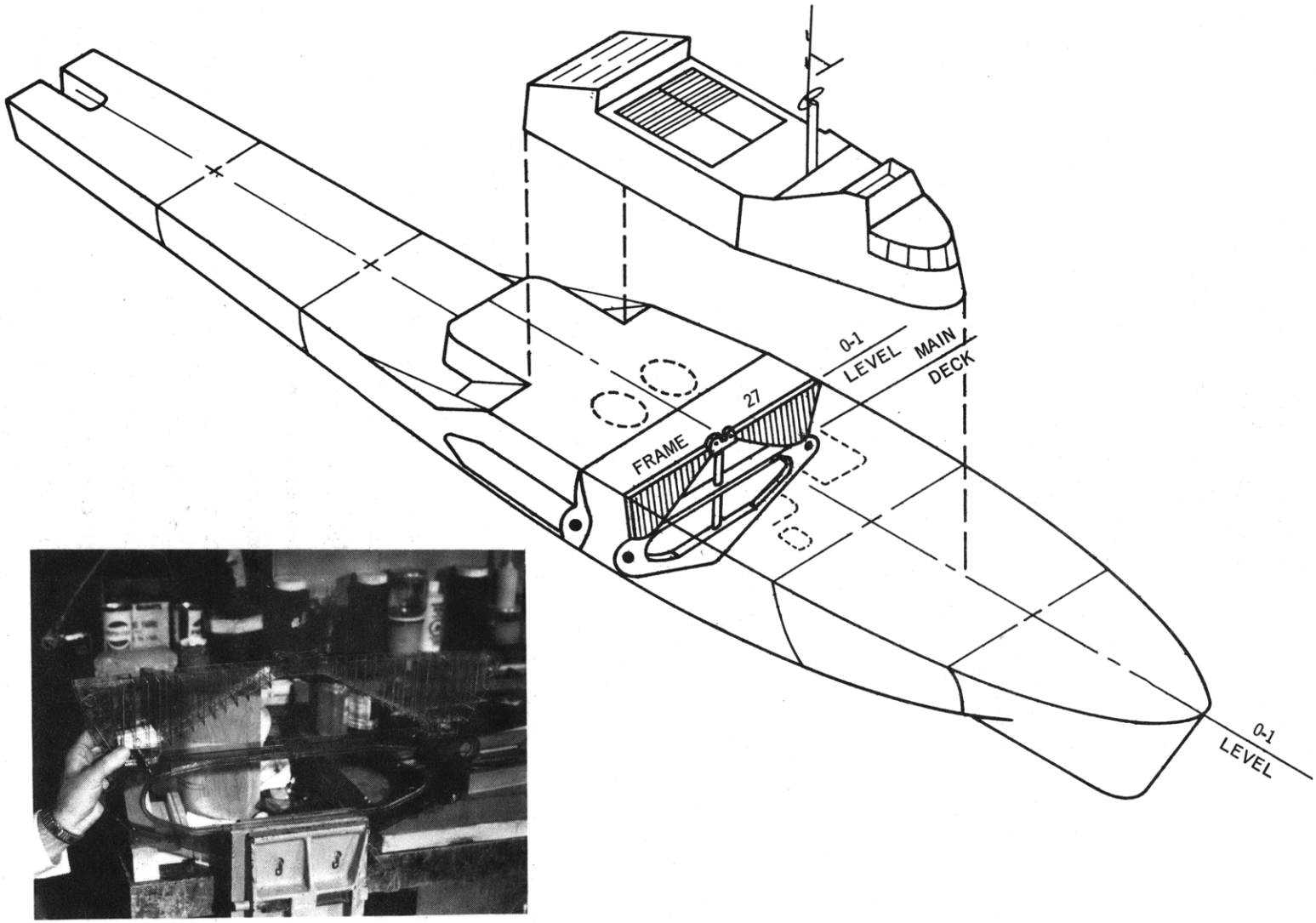

Figure 12 - Frame 27 Model Replica and Ship Orientation

elasticity E fluctuates (< 1 percent/deg F) with temperature. Figure 13 shows the variation of E for 0.015-in.-thick PVC as a function of temperature. In order to ensure consistency of experimental results and to reduce undesirable variables, an environmentally controlled room was developed.

It was also observed that the modulus of elasticity was slightly higher for the thin PVC stock. Figure 14 shows the modulus of elasticity E_{PVC} versus plastic thickness at a temperature of 73 F. The curve was experimentally determined by optical deflection measurements. The second curve, labeled E_{GAGED}, represents a quasi-modulus of elasticity that reflects the local stiffening effect of a strain gage. This curve is used only for conversion of strain-gage data to stress. The actual strain in the plastic is not truly that read by the gage but must be calculated in the following manner:

1. Determine strain from gage measurement (see section on instrumentation and test preparation).

2. Calculate stress (this is the true stress) by using Hooke's Law and E_{GAGED} of Figure 14.

3. Calculate the strain by using Hooke's Law, the stress determined in Step 2), and E_{PVC} of Figure 14.

Previous experience with plastics suggested that the creep rate of PVC could be a serious problem in the highly stressed region. Further investigation indicated that creep was virtually nonexistent for loadings up to 500 psi. To reduce any possibility for material creep and thus to stabilize the results, it was decided to reduce all scaled loads to a magnitude where the highest stressed region would be less than or equal to 500 psi. The strain which accompanies this stress level is 1000 μin./in.; this is more than adquate for reliable data acquisition and provides an equivalent stress of nearly 20 ksi for the aluminum prototype.

Regrettably, the amount of time available for material research was limited to that required for the design and construction of the AGEH-1 model. In many cases, such as in creep, threshold values were deemed sufficient for design purposes. For extensive use of rigid vinyl in structural modeling, however, complete data on PVC material behavior must

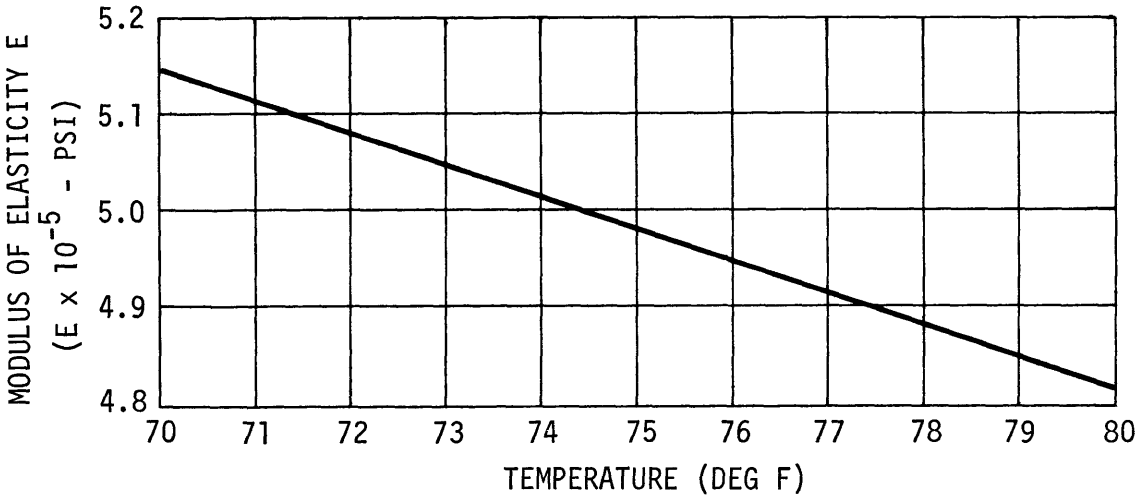

Figure 13 - Modulus of Elasticity versus Temperature for 0.015-Inch-Thick Rigid Vinyl

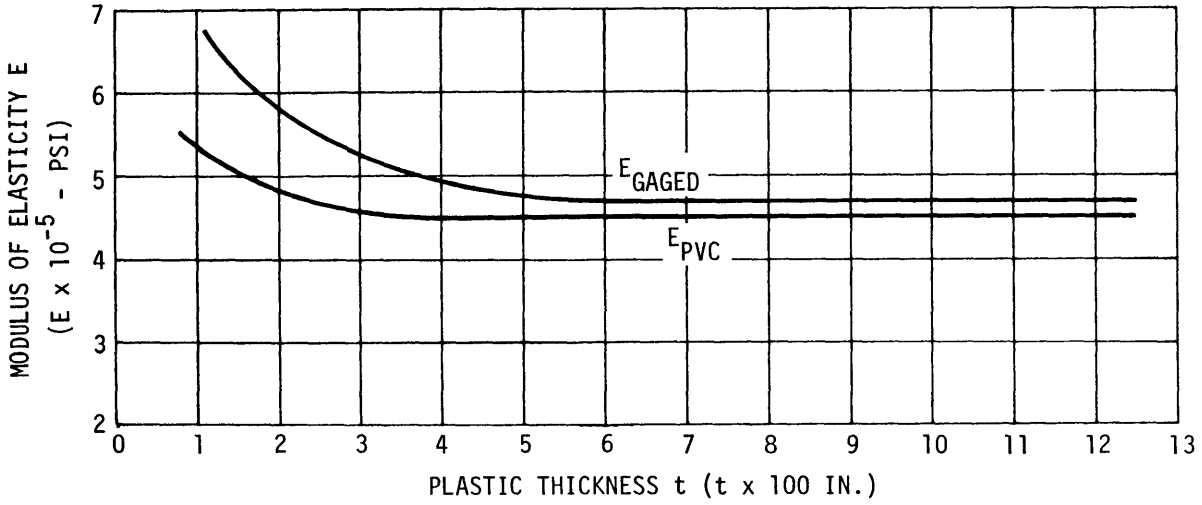

Figure 14 - Modulus of Elasticity versus Plastic Thickness at a Temperature of 73 F

be developed. Such an extensive research program is underway and the results will be reported independently.

MODEL DESIGN DEVELOPMENT

The development of a representative model design is twofold. It requires (1) the establishment of design criteria to fulfill the model objectives and (2) a design procedure which satisfies these design criteria.

Definition of Test Objectives

In order to establish detailed design criteria for the model, its test objectives must be defined. These goals, and consequently the gross model design guidelines, can be defined through the development of the following model considerations:

1. Design stresses - stress output investigation level:
   a. Primary stress - stresses resulting from bending or torsion of the entire structure as a result of applied loads. Stress distribution does not require modeling of all stiffeners, etc., but gross cross-sectional representation is required.
   b. Secondary stress - stresses resulting from bending of the plate stiffener and its effective width under normal pressure. True-to-scale modeling is required.
   c. Tertiary stress - stresses occurring in plate between stiffeners due to normal pressure loads. True-to-scale modeling is required.
2. Scaling relationships -

Suppose that one object is located with reference to three coordinate axes, which we may take for convenience to be mutually perpendicular. Each point on the object can be specified by its coordinates (x, y, z). If we now construct a second object, located with respect to the same coordinate axes, but having its various points defined by $x_1 = \lambda x$, $y_1 = \lambda y$, $z_1 = \lambda z$, this second object will be geometrically similar to the first object. Since all coordinates are changed in the same ratio (λ), all linear dimensions are also changed in this ratio, and the second object will be λ times as large as the first. Each point so located on the second object corresponds to the point on the first object from which its

coordinates were derived, and the two are said to be corresponding points. The lengths on the two objects, defined by pairs of corresponding points, are known as corresponding lengths. The ratios of all corresponding lengths are equal to λ, which is termed the scale factor.

The conditions governing model tests of statically loaded elastic structures are readily derived because the equations of mechanics and elasticity are known. Since the same equations apply to all structures, it is a comparatively simple matter to deduce the relations existing between a model and its prototype. The scaling relationships given in Table 2 are

TABLE 2 - SCALING RELATIONSHIPS FOR PROTOTYPE AND MODEL

Measured Quantity	Prototype	Model
Length	L_p	$L_m = \lambda L_p$
Strain	ε_p	$\varepsilon_m = \varepsilon_p$
Stress	σ_p	$\sigma_m = e\,\sigma_p$
Force	F_p	$F_m = e\,\lambda^2\,F_p$
Moment	M_p	$M_m = e\,\lambda^3\,M_p$
Moment of Inertia	I_p	$I_m = \lambda^4\,I_p$
Section Modulus	S_p	$S_m = \lambda^3\,S_p$
Polar Moment of Inertia	J_p	$J_m = \lambda^4\,J_p$
Torque	T_p	$T_m = e\,\lambda^3\,T_p$
Shear	τ_p	$\tau_m = e\,\tau_p$
Unit Angle of Twist	θ_p	$\theta_m = \frac{e}{\lambda g}\,\theta_p$
Total Angle of Twist	ϕ_p	$\phi_m = \frac{e}{g}\,\phi_p$
Axial Deformation	δ_p	$\delta_p = \lambda\,\delta_p$

Note: In the relationships given above,

$\lambda = L_m/L_p$

$e = E_m/E_p$

$g = G_m/G_p$

$G = E/[2(1 + \mu)]$

derived by assuming that the strain of the model (ε_m) is equivalent to the strain of the geometrically similar prototype (ε_p) or $\varepsilon_m = \varepsilon_p$. A portion of the derived equations is given in Appendix A. The resulting model is not dynamically scaled since it will not have the correct density. It will, however, possess the proper mass ratio and can be used in certain vibrational experiments. Detailed information concerning dynamic and hydrodynamic structural models that incorporate rigid vinyl will be reported at a later date.

3. Model Size -

A model 15 to 25 ft in length would simplify the construction and increase the possibilities for structural detail. However, it would also be a very difficult model to handle in rooms of limited space. A 10-ft model of the AGEH seemed desirable for ease of handling and testing. An investigation of the prototype plans suggested a scaling factor of 1/20. This would scale the 212-ft AGEH to a model of 10.6 ft between perpendiculars.

4. Loading Procedure -

By applying design loads at discrete points or by pressure bags, any desired strain level can be obtained by adjusting the magnitude of the loads. They may, however, create local stress concentrations which could be catastrophic to the model if not considered in the model design.

Design Procedure

The design flow chart of Figure 15 graphically illustrates the repetitive design procedure as applied to the AGEH-1 rigid vinyl model. The basis for the design of the AGEH-1 model is to permit the primary stresses to be obtained under quasi-static representation of loads experienced by the prototype. The following steps outline the procedure for performing model design:

1. Hull Girder Design - the governing maxims for hull plating design or in fact the design of any longitudinal stiffening members are:

   a. The cross-sectional areas of the model must be in predictable ratios of those for the prototype.
   b. The members must take all necessary loads without model buckling.

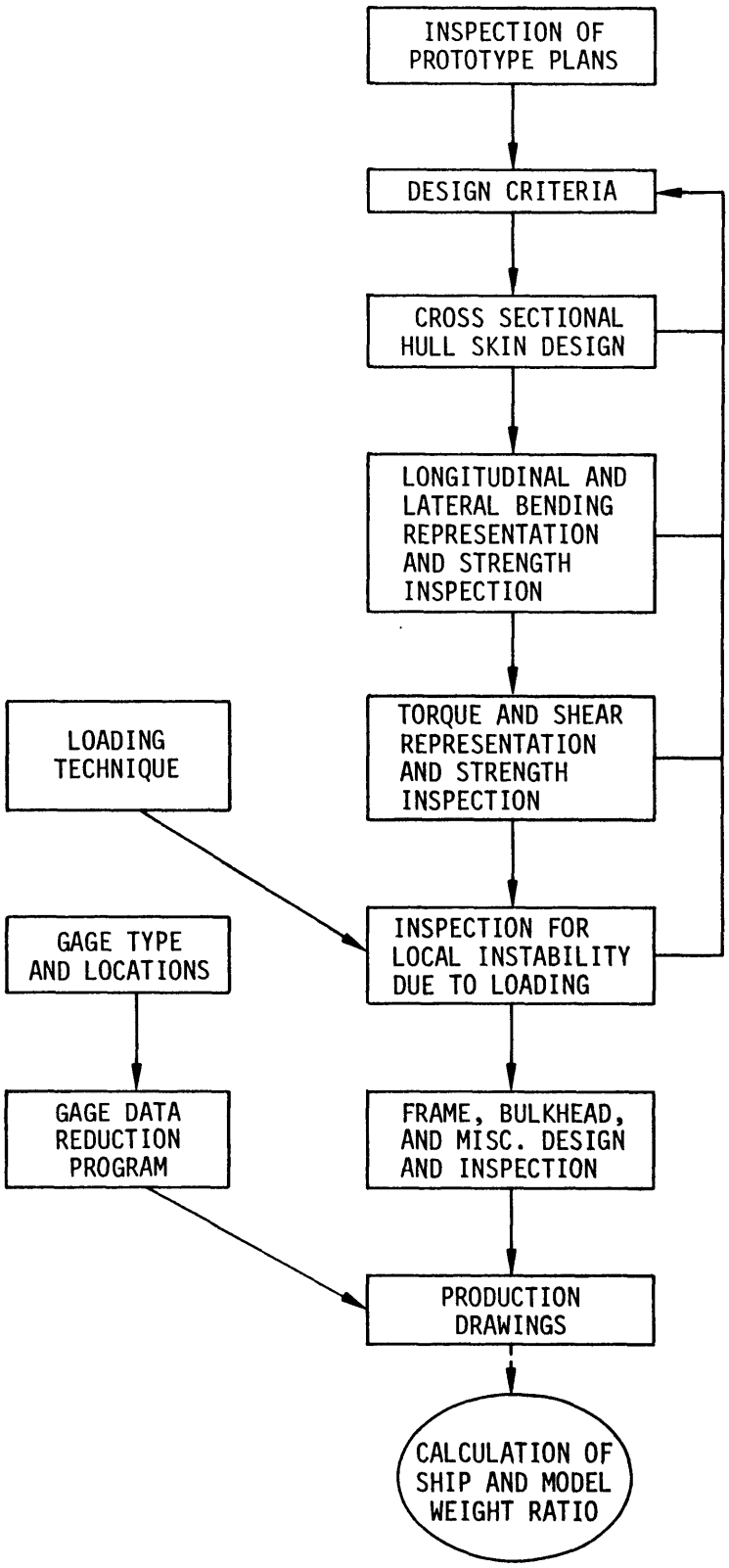

Figure 15 - Design Flow Chart

The latter rule is obvious since a model which buckles due to changed geometry does not predict the response of a nonbuckling prototype. Throughout design, it will be assumed that the ship behaves according to elastic beam theory. This assumption is necessary so that stresses can be predicted and checked against buckling criteria.

The first rule is necessary for the accurate distribution of primary stresses under quasi-static loading and for providing the correct area moments of inertia. The moments of inertia are correct without regard to geometry *if and only if* it can be assumed that the local moment of inertia is negligible compared with the moment of inertia of that member about the neutral axis of the ship.

2. Frame Design - the basis for frame design is:

   a. To provide the strength necessary for the hull skin to retain its shape.

   b. To transmit loadings in the same manner as the prototype.

The first of these criteria is easily achieved because it states only a minimum boundary condition. The upper boundary would be that both prototype and model must buckle at the same loading. The latter condition will never be tested. Therefore, any framework can be used as long as the minimum boundary is satisfied. The latter criterion is more complicated because frame bending is involved when the ship is loaded in bending and torsion. Representative local inertias must be obtained to ensure proper bending.

3. Scaling Factor - the overall scaling factor of 1/20 was chosen for the design of the AGEH-1 rigid vinyl model because it gives a manageable size (L_{pp} = 10.6 ft) yet is large enough to allow the incorporation of sufficient detail to accurately determine the principal stresses of the ship.

Table 3 indicates the proportional relationships of Table 2 to be used for a 1/20 true-to-scale model.

TABLE 3 - SCALING RELATIONSHIPS FOR
1/20-SCALE MODEL

Measured Quantity	Relationship
Length	$L_m = 0.05\ L_p$
Strain	$\varepsilon_m = \varepsilon_p$
Stress	$\sigma_m = 0.05\ \sigma_p$
Force	$F_m = 0.125 \times 10^{-3}\ F_p$
Moment	$M_m = 0.625 \times 10^{-5}\ M_p$
Moment of Inertia	$I_m = 0.625 \times 10^{-5}\ I_p$
Section Modulus	$S_m = 0.125 \times 10^{-3}\ S_p$
Polar Moment of Inertia	$J_m = 0.625 \times 10^{-5}\ J_p$
Torque	$T_m = 0.625 \times 10^{-5}\ T_p$
Shear	$\tau_m = 0.05\ \tau_p$
Unit Angle of Twist	$\theta_m = 20.0\ \theta_p$
Total Angle of Twist	$\phi_m = \phi_p$
Axial: Deformation	$\delta_m = 0.05\ \delta_p$
Note: In the above relationships, $\lambda = 1/20$ $e \cong E_m/E_p = \frac{\approx .5 \times 10^6}{\approx 10 \times 10^6} \cong 1/20$ $g \cong 1/20$	

Hull Girder Design

The previously discussed criteria for hull cross-sectional design can be expanded as follows:

1. To maintain model to prototype area relationships.
2. To obtain sectional moments-of-inertia according to the scaling relationships.
3. To simplify for construction and cost purposes in a manner which would not affect prototype predictions.

4. To satisfy the above without buckling.

When a scale of 1:20 was decided on, the detail design could then be examined and the above goals obtained by using the guidelines of the previous section. An examination of Extrusion A, previously shown in Figure 10, reveals that the plate thickness for the 1:20 model would be 0.008 in. Also, the T's of this, the largest of the four basic panel extrusions, would be 0.22 in. high and 0.008 in. thick. These dimensions would be difficult and expensive to model. Since only primary stress levels were to be investigated, it was assumed that the extruded plates could be "smeared" into a plate with an effective thickness. To do this, however, changes in model behavior must be considered. The model must be scaled to give a representative response to (1) axial loading, (2) bending, and (3) torsional loading and the model must be able to take these loading conditions without buckling because of this plating simplification.

Consider the rectangular coordinate system nomenclature and sign convention given for the model (Figure 16). This convention will be used throughout the report. Also, by considering only primary stresses and the ideal case where the ship behaves according to simple beam theory, it can be assumed that the following stress predictions can be used:

$$\text{Axial Loading: } \sigma = F/A \tag{1}$$

$$\text{Bending Moment: } \sigma = Mc/I \quad [c = f(y, z)] \tag{2}$$

$$\text{Torsional Loading: } \tau = Tr/J \quad [r = f(y, z)] \tag{3}$$

Inspection of Equation (1) requires only that the area in a given location be correct to obtain correct principal primary stresses for a given load. The detailed geometry of this area is not a factor when averaged stresses are under consideration; therefore plating simplification with unchanged area values will still give representative loading response in the axial mode. Similarly, in Equation (2), the moment M and the arm c are not affected by the area; only the scaled cross-sectional moment of inertia must be obtained. If this value can be duplicated with a simplified cross section, then all primary stresses due to bending will be correct. Finally, for torsional consideration, the stresses will be in the form of shear

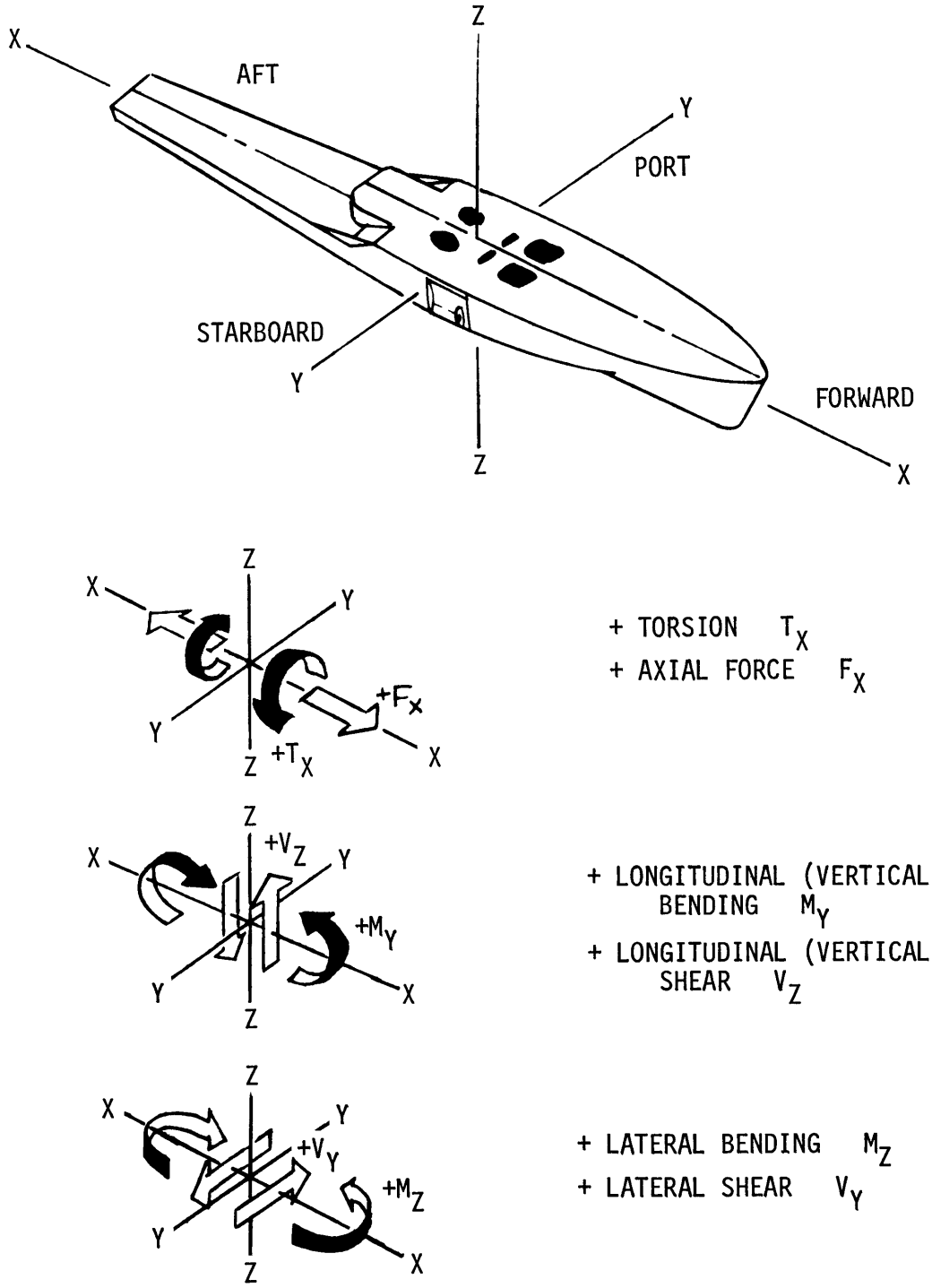

Figure 16 - Nomenclature and Sign Convention for AGEH-1 PVC Model

stresses. For torsional loading, the torque T and the arm r of Equation (3) are not affected by plate simplification. The polar moment of inertia J of the multicelled ship structure will increase, however, when the longitudinals, ineffective in torsional stiffness, are smeared into affective thickness. The increase in stiffness is uniform and is predictable; therefore the simplification process for plate smearing holds as shown in the ideal case. Since the ship is a very complex structure, it does not truly behave according to simple beam theory. It is assumed, however, that on the primary stress level of investigation, the assumption is adequate for justification of plating simplification.

Some geometric buckling criteria must be adopted in order to investigate the elastic instability. The buckling behavior of ship plating experimentally determined by St. Denis[1] was verified analytically and computerized.[2,3] The geometry and boundary conditions used are given in **Figure 17.** The critical buckling stress is mathematically defined by the empirical equation:

$$\sigma_{cr} = \frac{4\pi^2 D}{3tB^2}\left(3\frac{A^2}{B^2} + 3\frac{B^2}{A^2} + 2\right)$$

where σ_{cr} is the critical stress for buckling,

D is the flexure rigidity of the plating = $Et^3/[12(1 - \mu^2)]$,

t is the plating thickness,

μ is Poisson's ratio, and

A,B is as defined in Figure 17.

---

[1]St. Denis, M., "On the Structural Design of the Midship Section," David Taylor Model Basin Report C-555 (DECLASSIFIED) (Oct 1954).

[2]Timoskenko, S.T. and J.M. Gere, "Theory of Elastic Stability," McGraw Hill Book Company (1961); see Chapter 9, page 348 (Buckling of Thin Plates).

[3]Roark, R.J., "Formulas for Stress and Strain," McGraw Hill Book Company (1965) pp. 348-354.

The results are shown graphically in Figure 18 for the 1:20 scaled AGEH frame spacing of 1.8 in. The curves plot critical stress versus plate width B for all available plating thickness up to 0.030 in. The critical stresses for the thicker plastics are larger than the maximum stress level of 500 psi set for the model; theoretically then, buckling will not occur in these thicknesses. The design flow chart of Figure 15 graphically illustrates the repetitive design process as applied to the AGEH-1 rigid vinyl model. For the first cycle of the design flow chart, the previously justified plating simplification process was considered. By using the "true-to-scale" relationships of Table 3 and smearing the plating of Extrusion A, the effective plating thickness becomes 0.016 in. This size plating would be unsatisfactory for the main plating of the hull for two reasons:

1. The outermost fibers at the ship hull will buckle at a stress below 500 psi unless the plating is restiffened at 1.6-in. intervals (obtained from Figure 18).
2. The thickness would limit modeling of thinner plating thickness because of the limited availability of thinner PVC stock (the available thicknesses of PVC is listed in the construction section of this report.)

One way to reduce the possibility of model buckling after cross-sectional simplification is to increase the plastic thickness to a level which would give a critical stress value above 500 psi for widely spaced stiffener intervals.

Inspection of the critical stress curves (Figure 18) suggests a minimum plating thickness of 0.030 in. for a nonbuckling condition for any arbitrary plate width for loading stresses up to 500 psi. This increased plating thickness would also widen the selection of thinner rigid vinyl stock (i.e., 0.010, 0.015, 0.020, and 0.025 in.) and allow for the construction of a more representative model. To incorporate this increased thickness without changing the overall dimensions or scantlings of the ship would require the adoption of a second scaling factor and modified scaling relationships. Table 4 gives the modified model-to-prototype relationships in terms of an additional scaling factor, or K factor. This K factor is the ratio of the increased thickness to true-to-scale thickness. Table 4

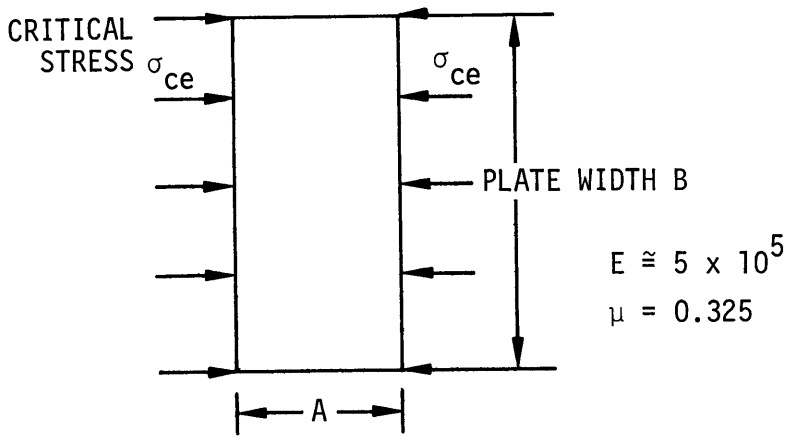

Figure 17 - Geometry for Determining Critical Buckling Stress

Note: (All edges are assumed to be rigidly attached)

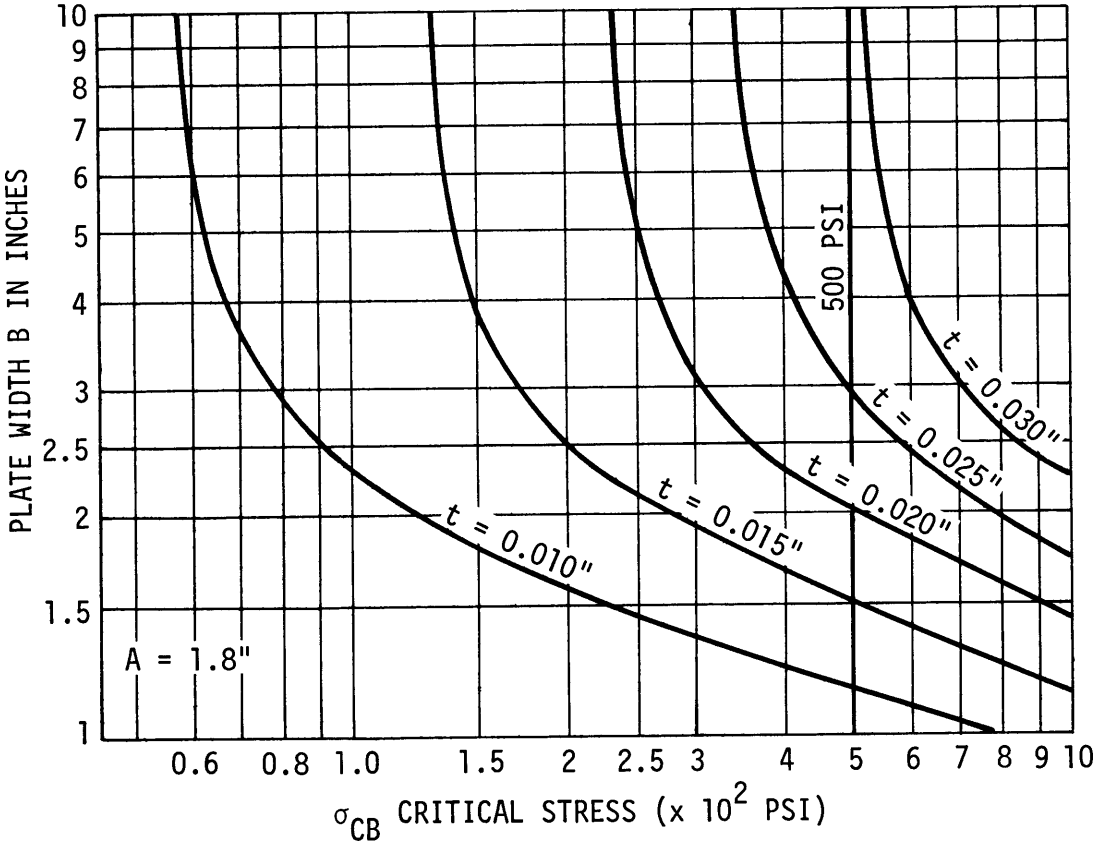

Figure 18 - Critical Buckling Stress versus Plating Width B

TABLE 4 - MODEL TO PROTOTYPE SCALING RELATIONSHIPS
IN TERMS OF THE ADDITIONAL SCALING FACTOR
(K FACTOR)

Measured Quantity	Prototype	Model
Length	L_p	$L_m = \lambda L_p$
Strain	ε_p	$\varepsilon_m = \varepsilon_p / K$
Stress	σ_p	$\sigma_m = e\, \sigma_p / K$
Force	F_p	$F_m = \lambda^2 e\, F_p$
Moment	M_p	$M_m = \lambda^3 e\, M_p$
Moment of Inertia	I_p	$I_m = K \lambda^4 I_p$
Section Modulus	S_p	$S_m = K \lambda^3 S_p$
Polar Moment of Inertia*	J_p	$J_m = K \lambda^4 J_p$
Torque	T_p	$T_m = \lambda^3 e\, T_p$
Shear	τ_p	$\tau_m = e\, \tau_p / K$
Unit Angle of Twist	θ_p	$\theta_m = e\, \theta_p / K \lambda g$
Total Angle of Twist	ϕ_p	$\phi_m = e\, \phi_p / K g$
Axial Deformation	δ_p	$\delta_m = \lambda \delta_p / K$

Note: In the above relationships,

$\lambda = L_m / L_p$

$e = E_m / E_p$

$g = G_m / G_p$

$G = \dfrac{E}{2(1 + \mu)}$

$K = \begin{cases} = 1 \text{ for true-to-scale model} \\ = t_2 / t_1 \quad t_1 = \lambda t_p \end{cases}$.

t_2 = increased thickness

*If longitudinals are smeared into effective plating, the value for the polar moment of inertia must be calculated and effected quantities (i.e., τ, θ, ε, ϕ) adjusted.

reduces to Table 2 when the thickness ratio K = 1. The derivation of the modified scaling relationships is given with the true-to-scale relationship derivation in Appendix A.

Based on a desired hull plating thickness of 0.030 in., the second scaling factor is calculated in Appendix B and the two scaling factors for the AGEH-1 model are given as:

$$\text{Overall scaling factor } \lambda = 1/20$$

$$\text{Thickness scaling factor } \lambda_t = 1/10.634 = 0.09404$$

and the K factor of Table 4 is K = 1.881. Substitution of these values into the relationships of Table 4 results in the numerical design ratios presented in Table 5.

The use of these scaling relationships enables conversion of prototype dimensional characteristics into values for model design. It is important to remember that once the second scaling factor λ_t is incorporated into a design, it must be retained throughout the entire design process. For example, all scantlings of a ship model are in terms of the overall scaling factor λ whereas all the thicknesses and resulting areas of any cross section are increased by the factor K ($\lambda_t = K\lambda$). As a result, all of the basic extrusions of the PLAINVIEW were rescaled in this manner (Appendix B) and are summarized in Table 6. The use of the linearly scaled hull plating satisfies the requirement for maintaining the local area relationships.

It would be impractical to describe every step on the transformation from prototype to model because of the extremely large number of cross referencing of prototype plans. Therefore only typical studies will be shown for explanatory purposes. In actuality, each structural member of the model was studied and scaled. Figure 19, for example, illustrates how the main girder under the 0-1 level decking at Frame 16 was converted from a wide flange beam to a rectangular one. It is important to remember that the local moment of inertia is not retained, but only the scaled area.

The model design can be considered representative in bending when there is quantitative agreement between the model and scaled prototype moments of inertia. Table 7 presents the longitudinal and lateral moments of inertia together with the distance from the neutral axis and the keel

TABLE 5 - NUMERICAL DESIGN RATIOS BASED ON RELATIONSHIPS OF TABLE 4

Measured Quantity	Relationship
Length*	$L_m = 0.05\ L_p$
Strain	$\varepsilon_m = 0.532\ \varepsilon_p$
Stress	$\sigma_m = 0.0266\ \sigma_p$
Force*	$F_m = 0.125 \times 10^{-3}\ F_p$
Moment*	$M_m = 0.625 \times 10^{-5}\ M_p$
Moment of Inertia	$I_m = 1.176 \times 10^{-5}\ I_p$
Section Modulus	$S_m = 0.235 \times 10^{-3}\ S_p$
Polar Moment of Inertia**	$J_m = 1.176 \times 10^{-5}\ J_p$
Torque*	$T_m = 0.625 \times 10^{-5}\ T_p$
Shear	$\tau_m = 0.0266\ \tau_p$
Unit Angle of Twist	$\theta_m = 10.633\ \theta_p$
Total Angle of Twist	$\phi_m = 0.532\ \phi_p$
Axial Deformation	$\delta_m = 0.0266\ \delta_p$

*Value to be used affected by overall scaling factor; do not use for plating, etc.

**See Table 4. J_m was found to be 1.956 stiffer than true-to-scale cross section (at Frame 42.5) therefore $J_{m_{actual}} = (1.956)(1/20)^4\ J_p = 1.222 \times 10^{-5}\ J_p$.

Note: In the above relationships,

$\lambda = 0.05$

$K = 1.881$

$e \cong 0.05,\ g \cong 0.05$

TABLE 6 - RESCALED BASIC EXTRUSIONS

Basic Extrusion*	Prototype Effective Thickness in.	Model Effective Thickness in.	Available Rigid Vinyl Thickness in.
A	0.319	0.030	0.030
B	0.2267	0.0213	0.020
C	0.191	0.0179	0.015/0.020**
D	0.1175	0.011	0.010

*Puget Sound Bridge and Dry Dock Co., Hydrofoil Research Ship Plans AGEH-1-800-2206521-B.

**Dictated by local design problem.

and weather deck for several typical frames in terms of prototype and model values. The geometric definition of the parameters used in Table 7 is illustrated in Figure 20. The model values of Table 7 provide a quantitative goal during the iterative process for determining the best representation of plating for satisfying all of the design criteria. The model moments of inertia were obtained in a fashion similar to the segment calculation method used for prototype calculations by making the following assumptions:

1. The cross section of the hull is symmetrical about the Z-axis (see Figure 20).
2. The local moment of inertia is negligible in comparison to the moment of inertia created by the area at a given distance from the neutral axis. This assumption is valid for all structural members of the ship except those that are very near the neutral axis. There are, however, very few significant members with high local moments of inertia and for this reason, the moment of inertia about the neutral axis is essentially the same when calculated with and without the local moment of inertia of an individual structural member.

The segment calculation method consists of the application of these assumptions to the parallel axis theorem to develop the equations for:

TABLE 7 - AGEH-1 MODEL DESIGN PARAMETERS

Frame	Station	$I_{\bar{y}\bar{y}}$		$I_{\bar{z}\bar{z}}$		y_k		y_{wd}	
		Proto* in^2-ft^2	Model $in.^4$	Proto* in^2-ft^2	Model $in.^4$	Proto* ft	Model in.	Proto* ft	Model in.
5	0.73	16.0	27.09	14.80	25.05	13.77	8.76	8.02	4.81
12	1.76	19.75	33.44	36.14	61.19	11.84	7.10	9.95	5.97
16	2.35	21.1	35.72	49.60	83.97	11.49	6.89	10.30	6.18
19	2.79	22.9	38.77	56.80	96.16	11.57	6.94	10.22	6.13
25	3.66	20.1	34.03	63.30	107.16	10.25	6.15	11.53	6.92
27	4.00	22.8	38.60	--	--	11.04	6.62	10.75	6.45
33	4.79	21.4	36.23	68.20	115.46	10.44	6.26	11.18	6.70
35	5.08	23.4	39.61	67.30	113.93	10.85	6.51	10.44	6.26
37	5.38	13.6	23.02	49.50	83.80	9.11	5.47	10.14	6.08
42	6.10	6.6	11.17	28.90	48.92	7.15	4.29	5.55	3.33
48	6.93	5.3	8.97	22.00	37.24	6.60	3.96	5.17	3.10
55	8.00	4.4	7.45	14.10	23.87	6.32	3.79	4.40	2.64
62	9.03	3.2	5.42	8.00	13.54	5.96	3.58	3.69	2.21

*See Appendix C.

Note: The AGEH consists of 71 frames and 10 stations

$I_{\bar{y}\bar{y}}$ = Longitudinal Moment of Inertia about $\bar{y}\bar{y}$

$I_{\bar{z}\bar{z}}$ = Lateral Moment of Inertia about $\bar{z}\bar{z}$

y_k = Distance from neutral axis (N.A.) to keel

y_{wd} = Distance from neutral axis to weather deck

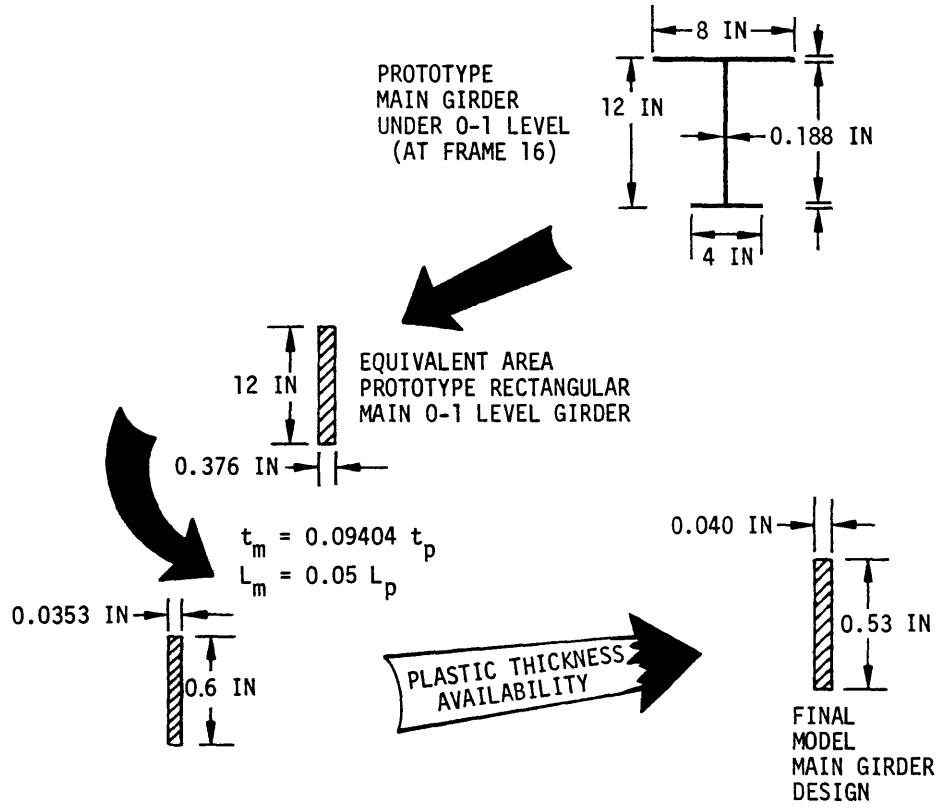

Figure 19 - Design Procedure for Longitudinal Member Simplification

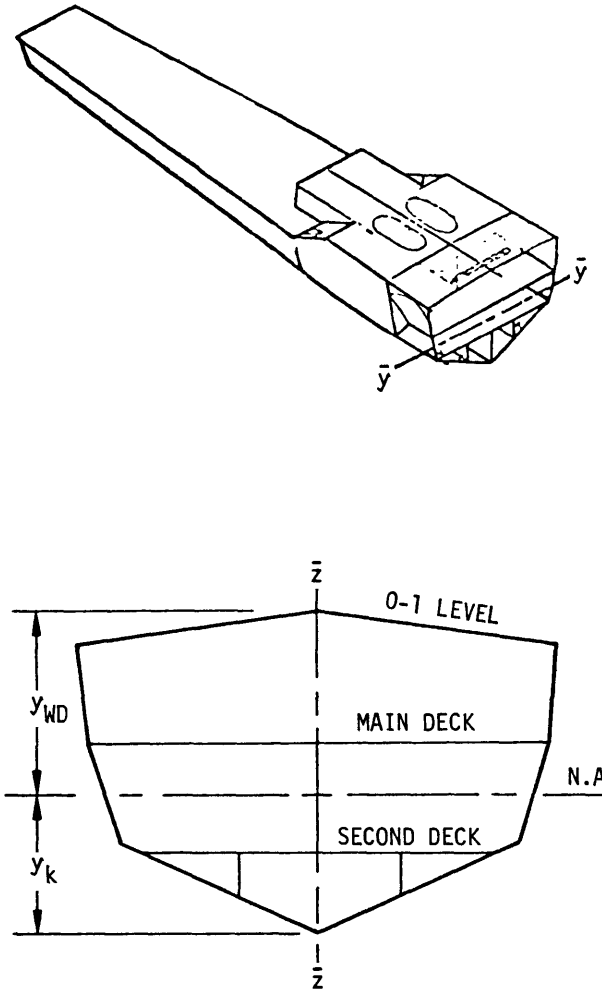

Figure 20 - Geometric Definition of AGEH-1 Cross Section

1. The longitudinal moment of inertia about the neutral axis $\bar{y}$-$\bar{y}$:

$$I_{\bar{y}\bar{y}} = \Sigma\, Az^2 - (\Sigma A)\bar{z}_{\bar{y}}^2$$

2. The lateral moment of inertia about the centerline $\bar{z}$-$\bar{z}$:

$$I_{\bar{z}\bar{z}} = \Sigma\, Ay^2$$

The definitions of these terms are presented in the simplified descriptive example of Figure 21. The example illustrates the solution of the neutral axis and the moments of inertia through the table summation of the properties of segmented cross-sectional elements.

The development of a model with representative bending stiffness without local buckling required three geometric configuration modifications including the installation of longitudinal 0-1 level stiffeners. The structural configuration developed for Frame 16 is illustrated in Figure 22. In order to verify the stability of the simplified model hull girder, two additional inspections must be performed: (1) the model must resist shear stresses as a result of torsional loading without buckling and (2) it must be capable of resisting the local instability resulting from the loading technique.

The design values for torsional loading were obtained from Puget Sound Bridge and Dry Dock Company Drawing AGEH-1-800-2006520-A. It was assumed that the most critical area for torsional shear flow would occur just aft of the transition area as a result of high torsion and low cross-sectional area at that region near Frame 42. The values given in Appendix D for shear flow at Frame 42.5 were calculated by using multicelled shear flow theory and the cross section shown in Figure 23. The stress values were very low and were determined as safe on the basis of the buckling criteria established by Roark.[3]

A network of "loading-rings" was developed as a means of producing static or quasi-static loads in the hull girder. The removable loading rings, shown in Figure 24, were constructed of reinforced 0.070 in. PVC seats and were fitted snugly around the hull at bulkhead locations with the aid of large rubber "bands," allowing for shear, bending, and torsional loadings.

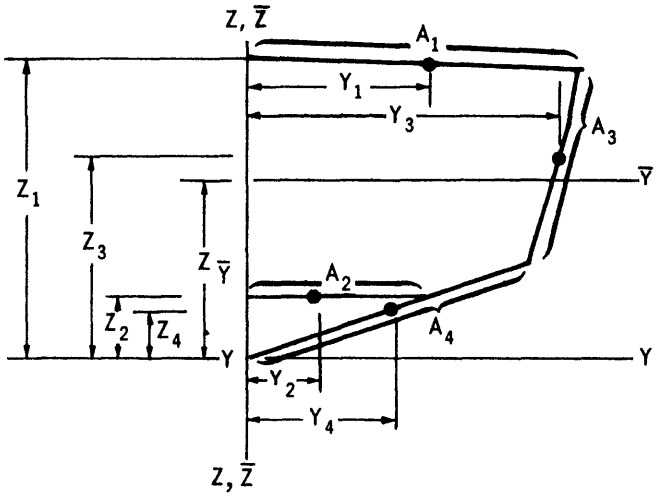

A = AREA OF ONE-HALF THE SYMMETRICAL HULL

$A_i \equiv$ ELEMENT AREA FOR AREAS i = 1, 2, 3, 4

● INDICATES LOCAL ELEMENT CENTROIDS

ID	AREA (A)	Z	AZ	AZ^2	Y	AY^2
DECK 1	A_1	Z_1	A_1Z_1	$A_1Z_1^2$	Y_1	$A_1Y_1^2$
DECK 2	A_2	Z_2	A_2Z_2	$A_2Z_2^2$	Y_2	$A_2Y_2^2$
HULL SIDE	A_3	Z_3	A_3Z_3	$A_3Z_3^2$	Y_3	$A_3Y_3^2$
HULL BOTTOM	A_4	Z_4	A_4Z_4	$A_4Z_4^2$	Y_4	$A_4Y_4^2$
	ΣA		ΣAZ	ΣAZ^2		ΣAY^2

$$\bar{Y} = Z_{\bar{Y}} = \frac{\Sigma AZ}{\Sigma A}$$

$$I_{\bar{Y}\bar{Y}} = 2\left[\Sigma AZ^2 - (\Sigma A)\, Z_{\bar{Y}}^2\right]$$

$$I_{\bar{Z}\bar{Z}} = 2\left[\Sigma AY^2\right]$$

Figure 21 - Calculation of the Hull Girder Bending Properties

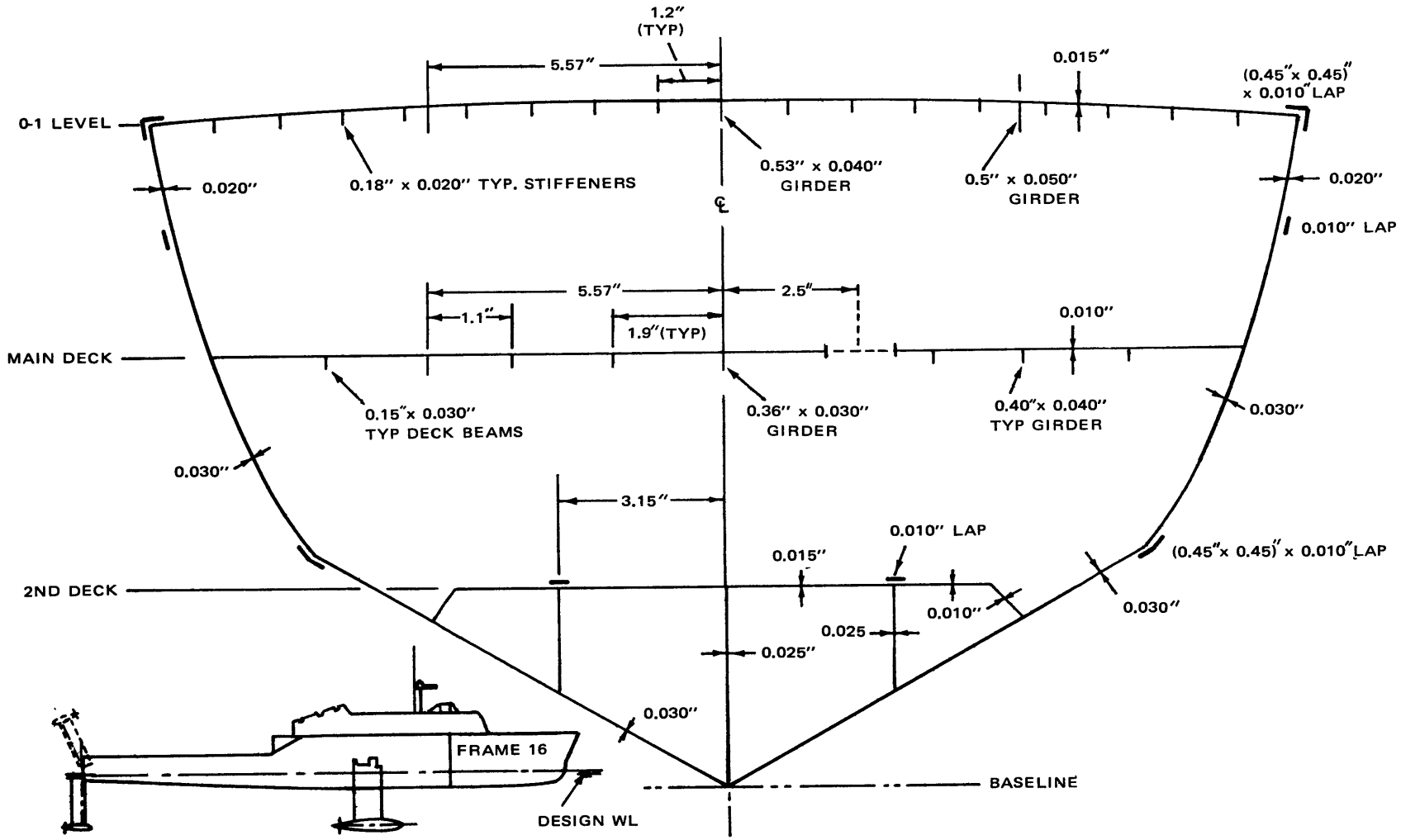

Figure 22 - Decking and Plating of 1:20 AGEH Rigid Vinyl Model at Frame 16

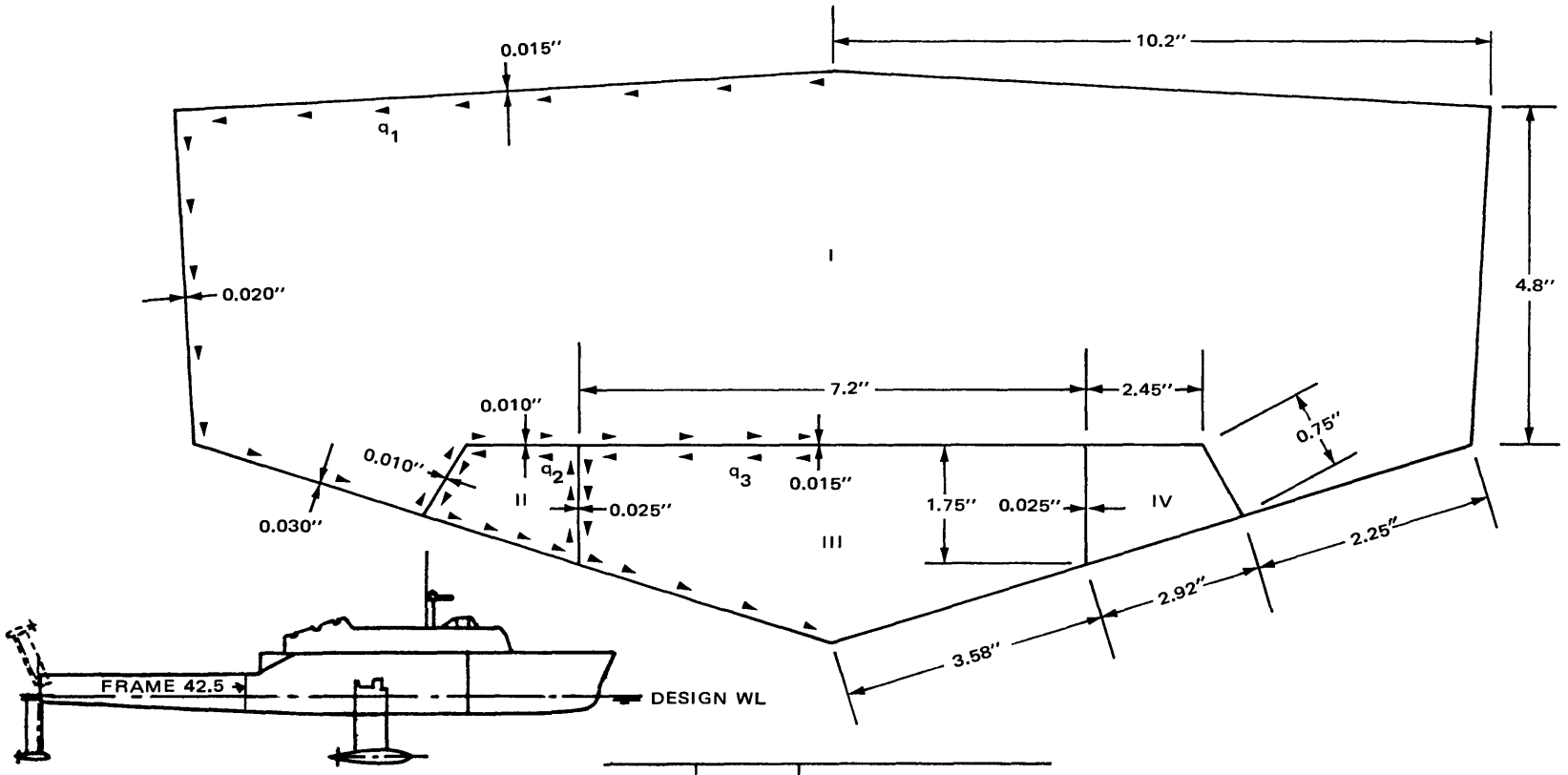

Area Ω_i	Area, $in.^2$	Shear Flow at Maximum Torsion, lb/in.
I	93.836	0.156
II	3.370	0.149
III	17.974	0.175
IV	3.370	0.149

Figure 23 - Shear Flow Inspection for 1:20 AGEH Model at Frame 42.5

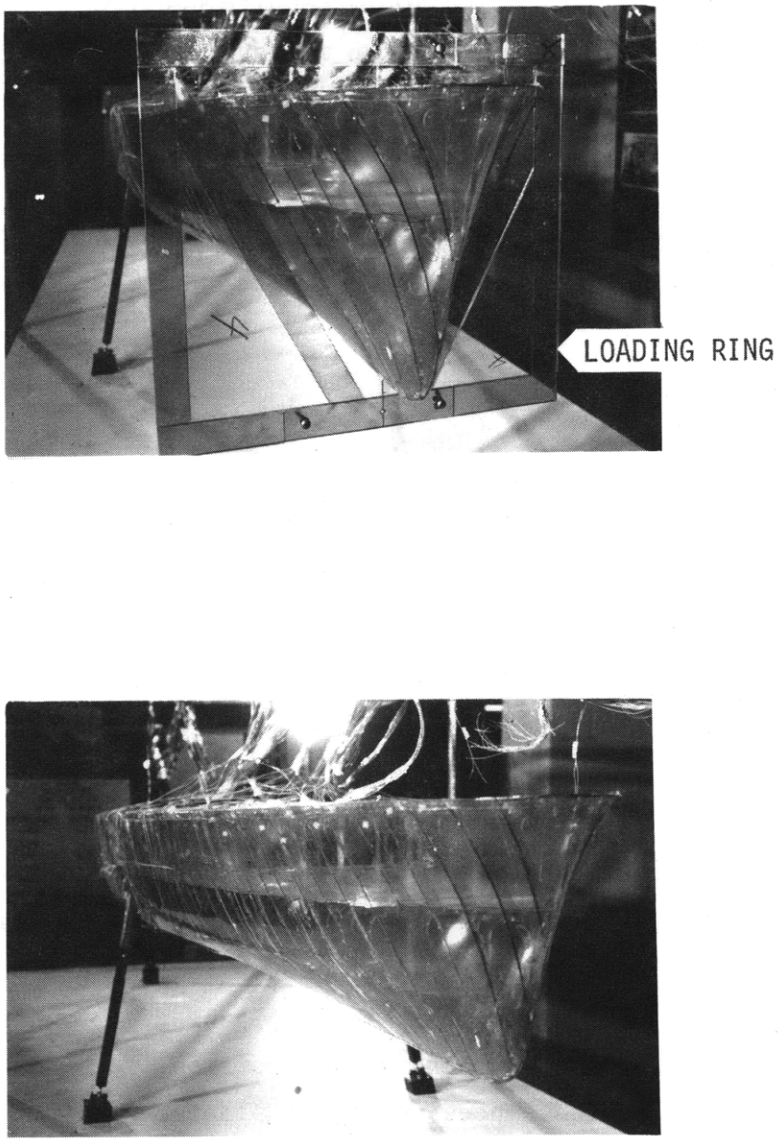

Figure 24 - AGEH-1 PVC Model with
and without Loading Rings

To establish insight into the stability of the hull with the application of the concentrated loads, experimental verification was favored over an analytical check which would require questionable assumptions. The test incorporated a load ring mockup and an existing six-frame fabrication study model (see Figure 25). The model was loaded well beyond the anticipated test spectrum with no structural deformation for shear forces in excess of 100 lb. Therefore, the loading concept was considered adequate, and ten loading locations (comprised of solid bulkheads and load bearing frames) were selected to describe the design loading conditions; see Figure 26.

Frame Design

The AGEH prototype utilizes 71 transverse frames spaced typically at 3-ft intervals. In order to obtain correct values of skin stress under the various loading conditions, these frames must behave correctly in bending. For the frame design, therefore, the problem becomes local rather than gross as was the case for the skin inertias. The basis for frame design is (1) to provide the strength necessary for the hull skin to retain its shape and (2) to transmit loadings in the same manner as the prototype.

Consider the geometry of Figure 27. The bending inertia to provide the strength necessary for the hull skin to retain its shape is that about axis I. The loads the frame will encounter is a result of (1) local deck and hull loading, (2) athwartship bending, and (3) structural contraction due to large deflections in bending and torsion.

The first of these need not be considered for primary stress distribution. The values for athwartship bending are considered to be insignificant because of the AGEH geometry. To obtain structural contraction large enough to influence stress distribution would require bending and torsional loadings far beyond the proposed testing range. Therefore, the only requirement for model design is the provision of a minimum bending strength that is equal to the design strength of the scaled prototype.

Figure 25 - Study Model for Loading Ring/Hull Stability Verification

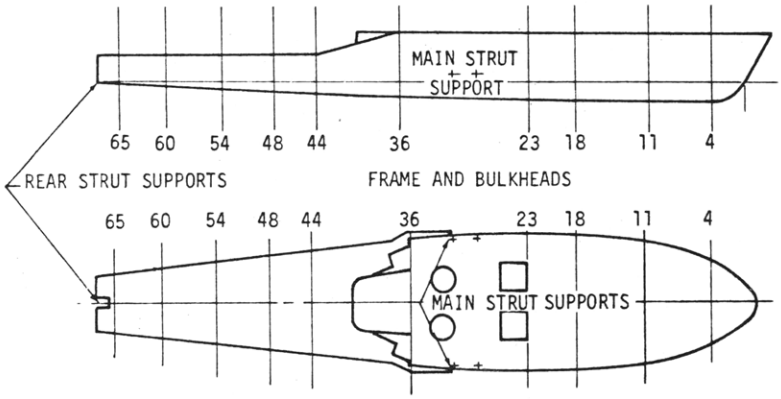

Figure 26 - Loading Ring Orientation

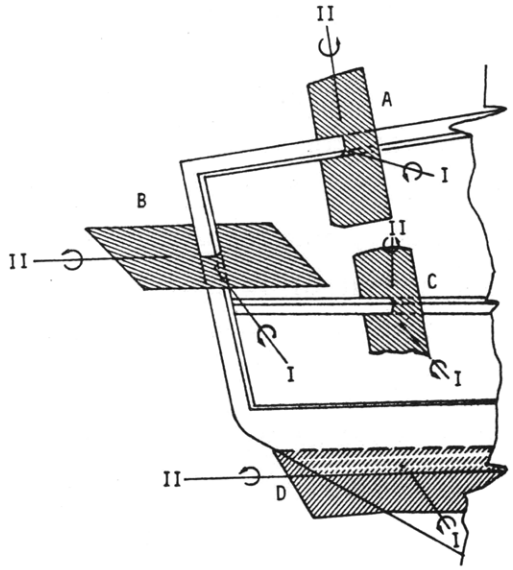

Figure 27 - Planes of Inertia for Frame Design

The second criterion for frame design, namely, to transmit loadings in the same manner as the prototype, is the critical factor that *must* be obtained. To determine whether loads are correctly transmitted, one must evaluate all possible loadings and consider which could involve frame interaction. The two loadings whose response were considered most affected by frame strength are:

1. Longitudinal bending at the transition area between Frames 36 and 40, as shown in Figure 28, where the loads carried by the 0-1 level are transmitted to the aft main deck by the skin stiffened frames.
2. Torsion in the area just after the transition deck; where the cross section is most "out-of-round," the frames will tend to bend as shown in Figure 29.

To ensure correct stress distribution, the scaled inertia of the frames must be adjusted by the same factor as used in the skin design. Therefore, the moment of inertia about axis II of Figure 27 is scaled according to the scaling relationships of Table 5 or

$$I_m = 1.176 \times 10^{-5} I_p$$

A direct reduction of girders and plating according to the previously discussed scaling factors would give an exact representation of the prototype response. However, construction complexity would increase the cost of the model to the point where such direct reduction would not be advantageous as a cost-effective structural evaluation tool. Accordingly, to speed construction time, a procedure was investigated whereby the AGEH framework was converted into mass producible equivalent channel sections. A fabrication study proved that this technique was faster than direct scaling; however, it would be far from economical for 71 frames.

To represent the frames, consideration was given to modeling solid frames with local bending moment of inertias scaled about all axes as presented in Figure 27. This would be advantageous for both design and installation. The design could be automated to convert the previously scaled inertias into rectangular geometries of equivalent inertias. The major disadvantage is that this procedure would involve a great deal of drafting time and expense. To combat this disadvantage, consideration was also given to modeling solid frames cut from scaled prototype plans with

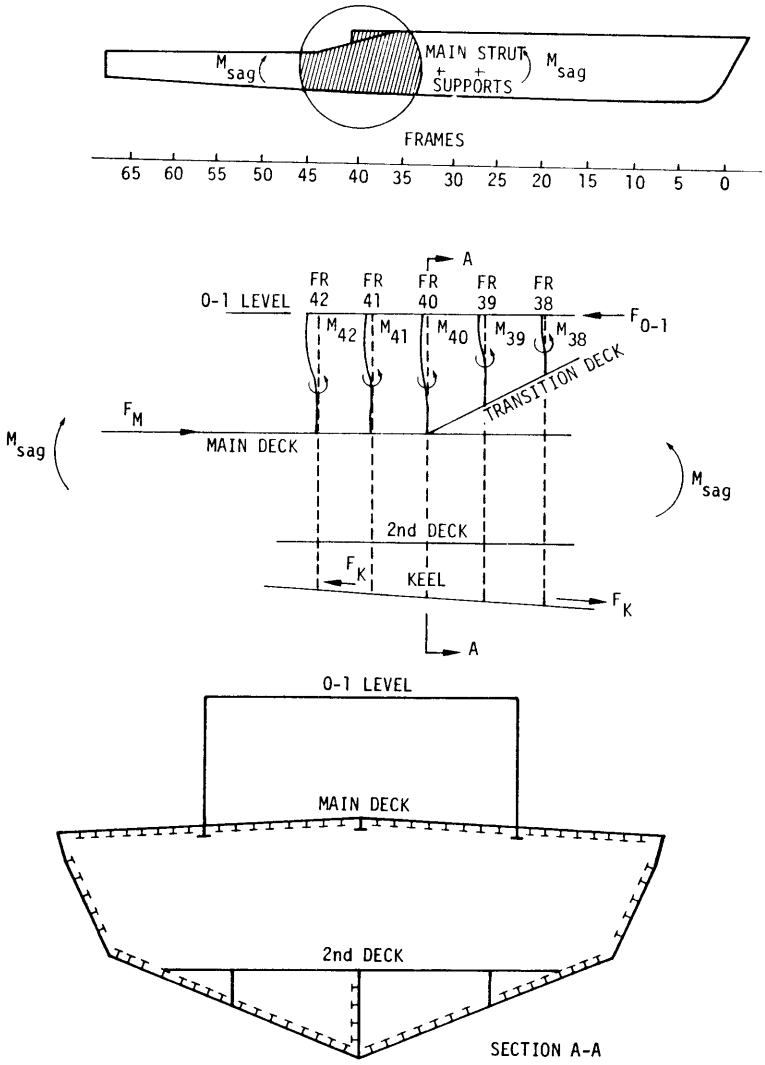

Figure 28 - Frame Interaction during Longitudinal Bending at Transition Deck

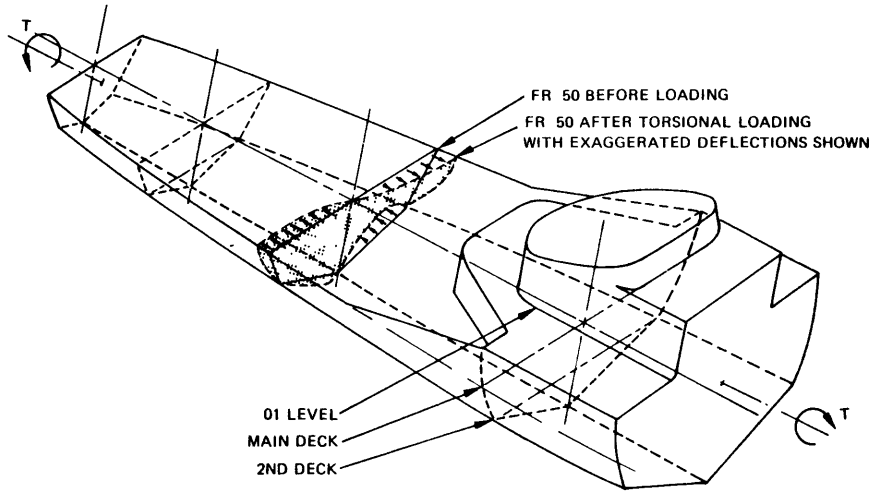

Figure 29 - Torsional Deflection of a Frame at the Aft End of the AGEH as a Result of Cross-Sectional Out-of-Roundness

thicknesses cut so as to accurately predict only one of the two moments of inertia. The major advantages of simple design and installation are retained but drafting time will be minimized since the solid frames could be cut directly from scaled prototype drawings with inertias determined by frame thickness. The moment-of-inertia about the II-axis of Figure 27 would be scaled exactly as was previously justified, with a check to ensure that the I-axis strength was at least equal to the prototypes designed stiffness. A frame-by-frame inspection for bending strength was made for the planes A, B, C, and D, described in Figure 27 by utilizing this method for frame and bulkhead representation. An inspection of the prototype frame drawings suggest three frame groups:

1. Group I - Standard Frames and Bulkheads (A, 0, 1-29, 31-35, 42-67)
2. Group II - Load Distribution Frame (36-41, 68, transom)
3. Group III - Specialized Frames (27, 30)

Group I prototype frames are all made from basic structural components. Observation of calculations show that the thickness for the entire frame (or bulkhead) averages 0.070 in. This thickness is more critical for Group II frames, especially in the region of load distribution. For this reason, these frames must correctly scale these structural components exactly. The transition frames (36-41) are constructed so as to enable the frame cross-sectional thickness to be modeled by 0.090 in. rigid vinyl sheets. Frames 68 and the transom, the aft load bearing frames, was also scaled to a thickness of 0.090 in.

By definition, Group III frames must be evaluated on an individual basis. Frame 27, the major load-bearing structure of the entire ship, was modeled in its entirety by the scaling relationships given in Table 5. This was done to give the exact load distribution of the ship. Model plans of Frame 27 (Figure 30) when compared to corresponding prototype plans (Figure 11) illustrate the amount of detail PVC modeling allows.

Frame 30 is basically a reinforced Group II frame. The strut support area was scaled by the derived relationships and the frame is 0.090 in. thick with 0.030 in. doubler plating fore and aft at the strut support region.

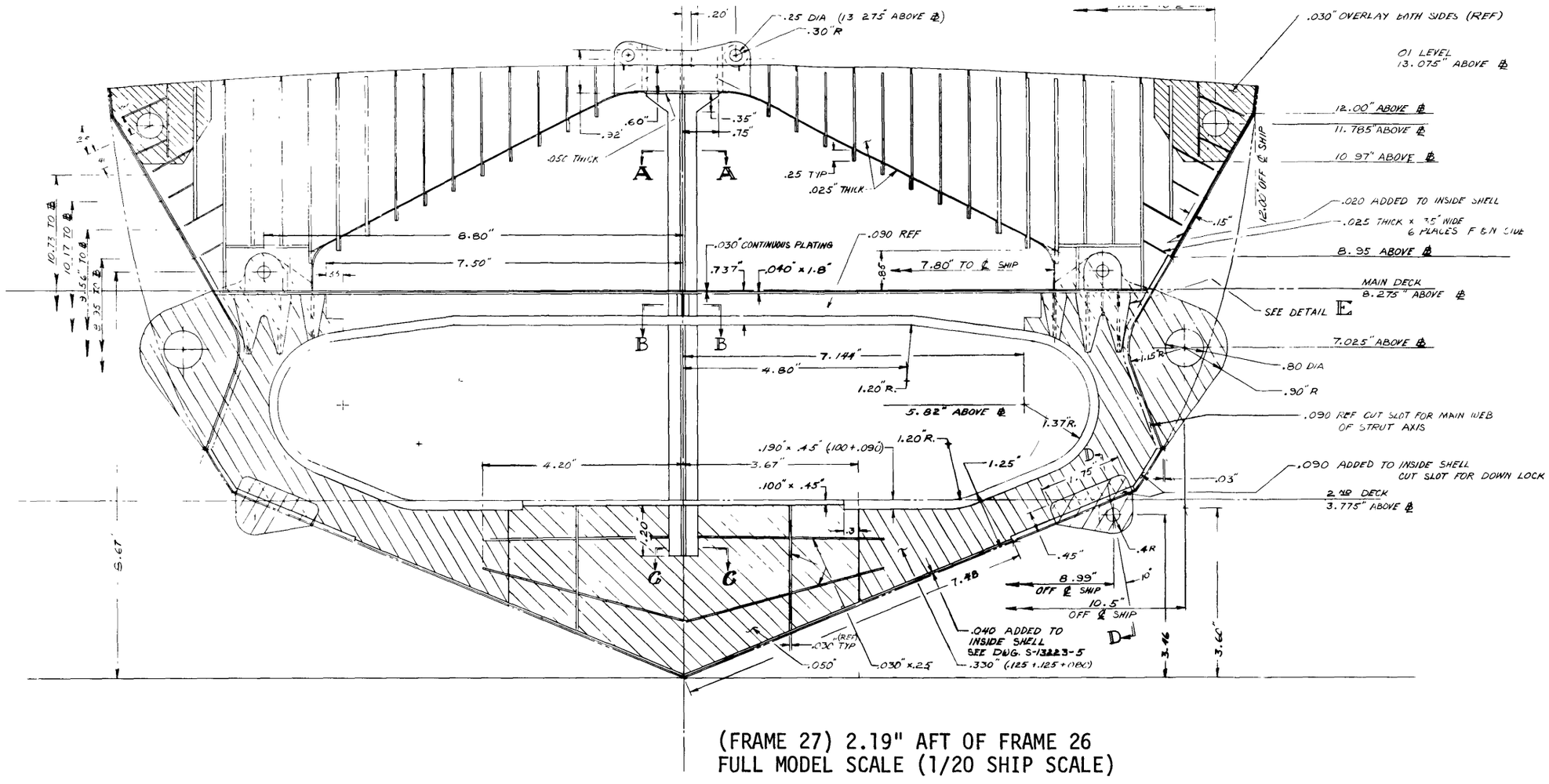

(FRAME 27) 2.19" AFT OF FRAME 26
FULL MODEL SCALE (1/20 SHIP SCALE)

Figure 30 - Frame 27 of 1:20 AGEH PVC Model

It would be impracticable to describe the scaling of each detail of the AGEH-1, such as foundations,* etc.; however, the procedure followed involved individual detail inspection and scaling if the item under consideration was felt to influence the response of the ship. After the design work was finished, a complete set of construction drawings was developed,** and the model was ready for construction.

CONSTRUCTION

A complete photographic description of the construction of the 1:20 AGEH-1 rigid vinyl model is given in Appendix E. The photographs illustrate and supplement the previous design sections. They are the most effective presentation of the steps performed by the modelmakers in constructing the complex structural model. This section will therefore be limited to a description of the materials used and the bonding techniques incorporated in the model construction.

MATERIALS

The material used in the construction of the AGEH model was Bakelite rigid vinyl sheets with a clear, planished, press polished (both sides) finish. Table 8 lists the properties as given by the distributor. The rigid vinyl is available as 21- x 51-in. sheets in thicknesses of 0.010, 0.015, 0.020, 0.025, and 0.030 in. and as 20- x 50-in. sheets in thicknesses of 0.040, 0.050, 0.060, 0.070, 0.080, 0.090, 0.100, and 0.125 in.

The thickness tolerance is ± 10 percent of nominal thickness (actual thickness was found to be ± 0.002 in. for the majority of the plastic sheets measured). The cost per sheet is under $10.00.

The following adhesives were used:

Solvent - CADCO SC-201

Bodied solvent - CADCO SC-202

---

*Puget Sound Bridge and Dry Dock Company Drawings AGEH-1-112-2206549-550 and AGEH-1-113-2206551-556 (Foundations et al.)

**NSRDC Drawing S-13223-1-24(AG(EH)-1 PVC Model Structural Drawings).

TABLE 8 - PROPERTIES OF RIGID VINYL SHEETS

(From CADCO® Plastics Catalog)

Properties	ASTM Test Method	Polyvinyl Chloride Rigid
Specific gravity	D792	1.35-1.45
Specific volume, cu in/lb	D792	20.5-19.1
Refractive index, nD	D542	1.52-1.55
Tensile strength (at yield) psi	D638, D651	5000-9000
Elongation, %	D638	2.0-40
Modulus of elasticity in tension, 10^5 psi	D747	3.5-6
Compressive strength psi	D695	8000-13000
Flexural strength, psi	D790	10000-16000
Impact strength, ft-lb/in. of notch (1/2 x 1/2 in. notched bar, izod test)	D256	0.4-20
Hardness, Rockwell	D785	70-90(Shore)
Thermal conductivity	C177	3.0-7.0
Specific heat, cal/°C/gm	-	0.2-0.28
Thermal expansion, 10^{-5}/°C	D696	5-18.5
Resistance to heat, °F (continuous)	-	120-160
Heat distortion temp., °F	D648	130-165
Volume resistivity	D257	$>10^{16}$
Dielectric strength	D149	425-1300
Dielectric strength	D149	375-750
Dielectric constant, 60 cycles	D150	3.2-3.6
Dielectric constant, 10^3 cycles	D150	3.0-3.3
Dielectric constant, 10^6 cycles	D150	2.8-3.1
Dissipation (power) factor, 60 cycles	D150	0.007-0.02
Dissipation (power) factor, 10^3 cycles	D150	0.009-0.17
Dissipation (power) factor, 10^6 cycles	D150	0.006-0.019
Arc resistance, sec	D495	60-80
Water absorption, 24 hr 1/8-in. thickness, percent	D570	0.07-0.4
Burning rate	D635	Self-extinguishing
Effect of sunlight	-	Darkness on prolonged intense exposure
Effect of weak acids	D543	None
Effect of strong acids	D543	None
Effect of weak alkalies	D543	None
Effect of strong alkalies	D543	None
Effect of organic solvents	D543	Resists alchols, eliphatic hydrocarbons and oils. Soluble in keytones and esters; sweels in aromatic hydrocarbons
Clarity	-	Transparent to opaque

Distributor's note: These values are representative of those obtained under standard ASTM conditions, and should not be used to design parts which function under different conditions. Since they are average values, they should not be used as minimums for material specifications.

Bodied solvent/nonvinyl-to-vinyl applications - CADCO SC-203

Epoxy - CADCO BA 470

BASIC ASSEMBLY PROCEDURE

The most attractive feature of rigid vinyl modeling is its workability. The AGEH-1 model was fabricated from heated PVC by a hand-draping vacuum-forming process over wooden molds. For the most part, the form material used was mahogany wood finished to a smooth surface. Almost any material can be used as a form as long as it has some structural integrity and can be finished to a smooth surface. Any imperfection or unfilled grain will show up on the plastic part. The forms were made as male forms so that the heated material could be hand draped over the form with less material thinning and wrinkling than possible with a female form.

The lines were scribed onto the wooden hull form; they were then transferred to the plastic part and this helped to match up parts during assembly. Small holes were drilled into the form from the outside surface through to the chambers in the mold in order that the air could be evacuated during the forming operation. The sheet of plastic is placed in the oven and hung vertically; a special clamping device keeps the plastic from folding back and welding itself together. The plastic is heated to its forming temperature (250 F) in 2 to 4 min. The plastic is then taken from the oven and hand draped over the wooden form so that it takes the general shape of the form, then pulled around the form to prevent wrinkles and to help in the sealing of the vacuum. The vacuum is then applied and is held until the plastic is cool. Special care must be taken in the vacuum-forming operation to avoid successive thinning. Sealing of the plastic to the vacuum mold is important so that the full vacuum is pulled quickly while the plastic is hot.

A part that is not formed correctly will be sloppy and out of tolerance. In certain cases, a part that does not form perfectly in localized areas, such as fillets, may be finished by applying local heat with a blower and by using a forming tool to force the material to take the shape of the form.

The formed parts must be inspected carefully for excessive thinning and compared to the prototype part. The hand-draping operation can be

done in various ways to eliminate unwanted thinning, but in certain cases the original gage material must be increased to obtain the required final thickness.[4]

After forming, the plastic parts are trimmed. It is possible to cut the thinner rigid vinyl stock by using only a pair of hand shears. All work can be accomplished with basic plastic or woodworking tools. The basic tools needed for cutting, clamping, and gluing are shown in Figure 31.

The way that the cut pieces of a model can be bonded depends on the loading requirement and accessability of the joint. For example, it would not be advisable to use an epoxy bond where there is a "peeling" type of load, because the epoxy-vinyl bond cannot tolerate such loadings. Moreover, in most cases, it would not be possible to "close out" a model with a solvent where a joint could not be reached with all pieces of rigid vinyl in place; the solvent evaporates too quickly for preattachment adhesive application.

Solvent cementing depends on the intermingling of the two surfaces to be joined so that there is actual cohesion, as contrasted with the adhesion of the gluing of two pieces of wood. To effect this intermingling and cohesion, the surfaces to be joined are softened and swollen into a "cushion" by contact with a liquid organic solvent. After assembly, the solvent evaporates or dissipates through the material to form a hard clear joint.

In the preparation of the joint, the vinyl surfaces to be connected should be lightly sanded so that they fit accurately without forcing. In butt joints, for example, edges should be true and matched. It should not

Figure 31 - Tools for Rigid Vinyl Modelmaking

[4]Blackburn, R.J., "Plastic Model Techniques for Structural Analysis," Ford Motor Company, Car Systems Research Technical Memorandum (Dec 1969).

be necessary to flex either piece more than a few thousands of an inch in order to make two curved pieces come into complete contact.

The temperature and humidity conditions of the cementing room and the temperature of the parts being cemented are important. The ideal conditions are a temperature of 80 to 90 F and a low relative humidity. Conditions of high relative humidity will tend to produce cloudy, unattractive joints due to the moisture condensed from the air by the cooling effect of cement evaporation. Low temperatures retard the solvent action and increase the necessity for repeated soakings. No attempt should be made to cement the vinyl below a temperature of 65 F because a weak bond will result.

A capillary action method is used for attachment of parts on the AGEH-1 model. The cement is introduced to the joint by means of a brush or hypodermic needle, as shown in Figure 32. It is necessary to introduce additional cement only at various points since capillary action will spread the solvent sufficiently to wet the area to be bonded if the two surfaces are well matched. To allow the cushions to form, the joining surfaces are held together gently for 30 to 60 sec before pressure is applied.

The success of a cementing job often depends on the design of the jig that holds the two sections in place while the joint hardens. The jig should keep the two pieces firmly together but should not force either of them out of shape. If the part is flexed or forced out of shape, local areas will be stressed and will almost certainly be crazed when brought in contact with cement.

The pressure should (1) be great enough to squeeze all air bubbles from the joint and ensure thorough intermingling of the cushions, (2) be applied evenly all along the joints to avoid stress concentration at any point, and (3) be maintained to compensate for the shrinkage that takes place in the joints during setting or hardening. Since the swelling action of the cement in forming a cushion causes an increase of volume, the cushion will shrink as the solvent evaporates. Unless the two pieces can move together while the joint is contracting, as the cushion shrinks, it will draw the extruded material or bead back into the joint. The joint will then be marked with a curve or dimple, or even by bubbles or voids.

The three vital conditions listed above are best met by jigs that incorporate spring clips, spring clothes pins, battery clamps, or air

Figure 32a - Capillary Action Method of Applying Solvent with a Hypodermic Needle

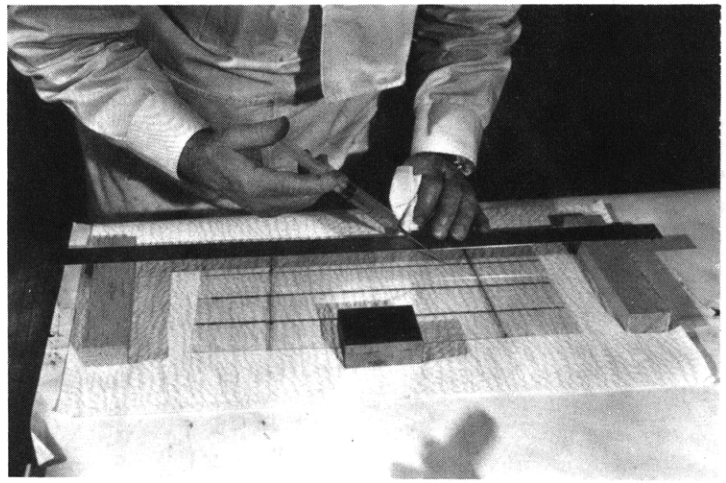

Figure 32b - "Bead" of Epoxy Being Applied to Deck Using Modified Hypodermic Needle

Figure 32 - Rigid Vinyl Bonding Techniques--Use of Syringe for Application of Solvent and Epoxy

pressure. For cementing a rib in position, for example, a jig could be constructed with a bar directly above the rib; then pressure between the bar and the rib could be applied by battery clips inserted at about 2 in. intervals.

A uniform pressure of approximately 1-2 psi of cementing area has been found satisfactory for most joints, provided, however, that this pressure does not force either of the parts appreciably out of shape. Excessive or uneven pressure may force all the cement or cushion out of the joint and result in "dry" areas which will not bond. Stress induced by high local pressure combined with the solvent action of the cement may cause immediate crazing in the cement joint area.

It is advisable to examine the joints carefully when the assembly is placed in the jig and at intervals thereafter. If slipping is noted before the joint has set, the pressure can be readjusted or the parts taken apart for reassembly. Just as soon as the assembly has been locked in its jig, any excess cement and cushion which have extruded from the joint should be scraped onto the masking tape and the tape removed quickly. When ribs are cemented to panels, it may be well not to remove the extruded cushion since it may act as a fillet and reduce stress concentrations along the edges of the rib.

The joint should be allowed to harden thoroughly before trimming or moving. If the joint is trimmed too soon, a visible recessive scar will be left along the joint. After assembly, the cement joints should be allowed to stand in a jig for at least 4 hr before removal. Furthermore, the joints should not be loaded for 24 hr at which time the strength is 1000 psi or two-thirds of the totally cured strength obtained in 3 to 5 days.

Bodied solvent is used when it is necessary to fill small gaps. Its slower drying time and thicker consistency allow a little more workability, but it must be used sparingly since an excess could cause softening of the rigid vinyl. Application is similar to unbodied solvent except that a larger bore hypodermic needle is needed for the thicker consistency of the bonding agent.

Epoxy is used when a long working time is needed. The modelmaker is allowed approximately 45 min of working time instead of the seconds available with solvent. Two major disadvantages in the use of epoxy are that the almost invisible glue line of solvent cannot be obtained and the set time is more critical and longer than for solvent. Epoxy is, however, the only reliable way to bond large areas of rigid vinyl without causing material deformation. For pregluing large areas of decking, it was found that a modified hypodermic needle (Figure 32b) would allow the application of a controlled "bead" of epoxy.

INSTRUMENTATION AND TEST PREPARATIONS

The designs for the model, its instrumentation, and testing facility are a function of the experiments to be performed. The Phase 1 test plan incorporated four major static loading programs. The experiments will involve:

1. Response of the ship due to uniform longitudinal and lateral bending and torsional loads, independent of the strut supports.
2. Prototype design loading conditions.
3. Investigation of a hull calibration loading matrix.
4. Introduction of deckhouse to the model to investigate hull-deckhouse interaction.

The model was designed as previously described with the above experiments in mind. To enable the proper load dissipation of the model in the foilborne configuration, the strut design allows only for axial support through the use of ball bearings. This support, along with moments created by thrust/drag, sideloads, and asymmetric lift are the only loads transmitted by the struts of the prototype. These additional bending moments are applied to the model through loading points on the model struts just above the ball-bearing supports.

To allow for the use of the loading rings, an interchangable "erector set" type of framework was constructed for supporting the model and pulleys for load application. Figure 33 shows the completed model mounted in the foilborne configuration on the rigid "honeycomb" test bed. The strain-gage lead wires are shown supported by the test bed framework prior to the data acquisition interfacing.

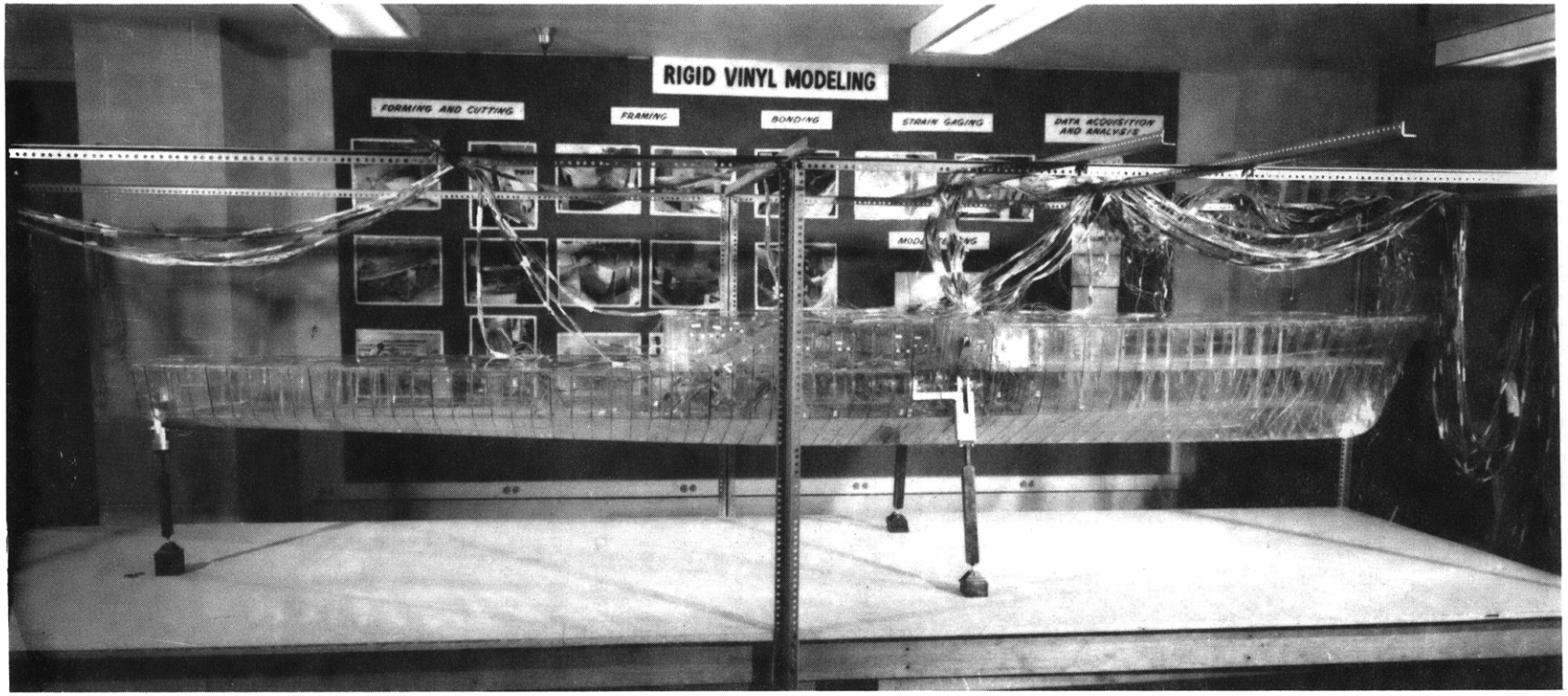

Figure 33 - Completed 1:20 AGEH PVC Model before Data Acquisition System Interfacing

The instrumentation consists of strain gages for stress analysis, deflection transducers for hull deflection in the Z-direction (Figure 16), and load cells for measurement of axial strut loads. The 23 prototype strain-gage locations are represented in the model as well as additional complementary strain gages for a total of approximately 400 investigation locations. Small foil-type strain gages especially designed for plastic are used on the model. Investigation for the majority of these locations consist of two strain gages mounted back-to-back on each side of the plastic and wired in the balanced bridge to enable local buckling to be neglected. Locations that were considered to be stiffened against buckling were not backed by an additional gage. The strain gages were applied to the model with Eastman 910 adhesive; however the adhesive and accelerator were applied directly to the gage and not the plastic because prolonged exposure to the adhesive fumes created PVC embrittlement.

The majority of the gages were mounted internally and therefore required installation during construction of the model. The lead wires were coiled and routed through the ship as additional sections were completed. Figure 34 shows a typical internal installation of strain gages. All internal gage wires eventually pass through the ships air intake openings, where they are joined by the external strain-gage lead wires as shown in Figure 35. The collection of wires is supported by the facility framework and leads to one of the two ship model computer data acquisition system interface junction boxes. Figure 36 shows the connection of a lead wire with the junction box. The junction box interfaces with a completely automated data acquisition system. The system shown in Figure 37 consists of a scanner, a digital voltmeter for digitizing the analog strain-gage signal, and a minicomputer which drives the entire system. The input-output is via a teletype system. Since the plastic material is an insulator and heat-sensitive, it was necessary to allow current to flow to all the gages at once so that a steady-state condition could be reached before scanning. This condition along with the specially constructed 1 V d-c power supply for lower heat generation allows for excellent strain results with amazing repeatability.

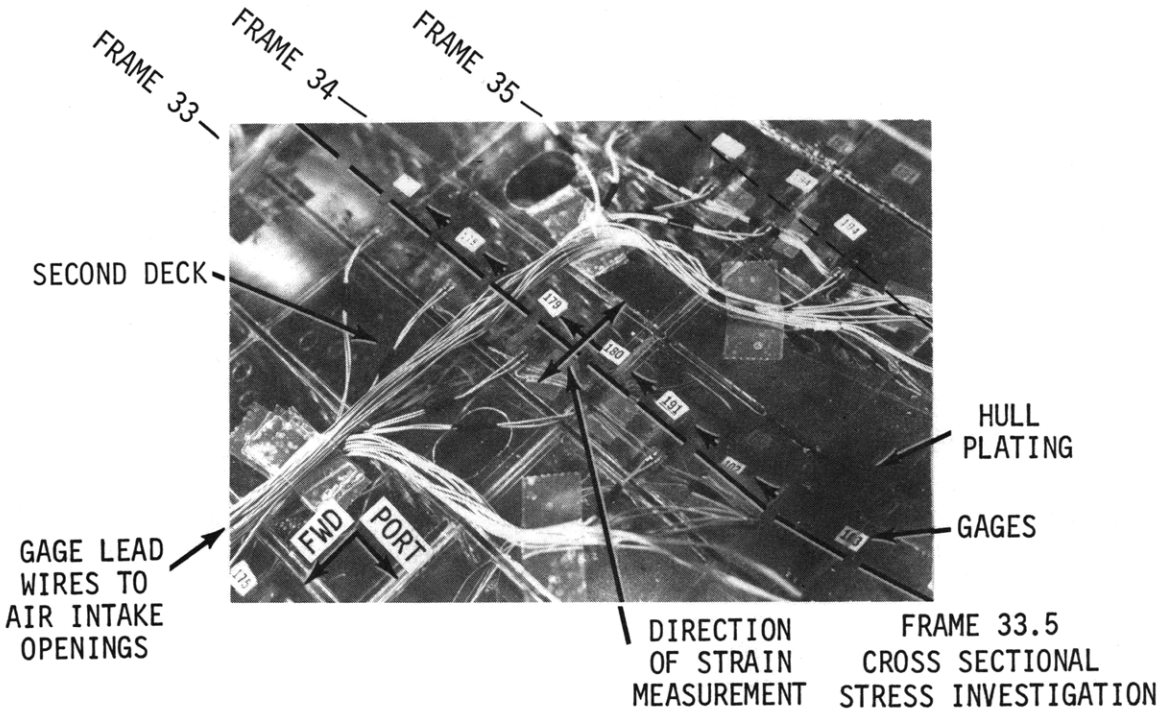

Figure 34 - Installation of Internal Strain Gages for the Cross-Sectional Investigation of Frame 33.5

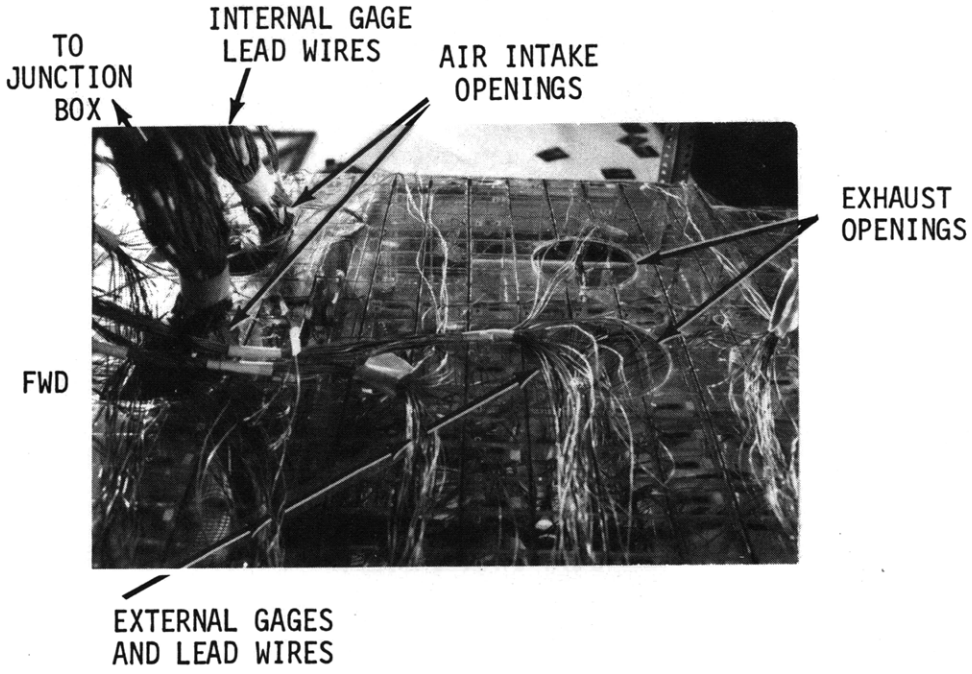

Figure 35 - Collection of Strain-Gage Lead Wires

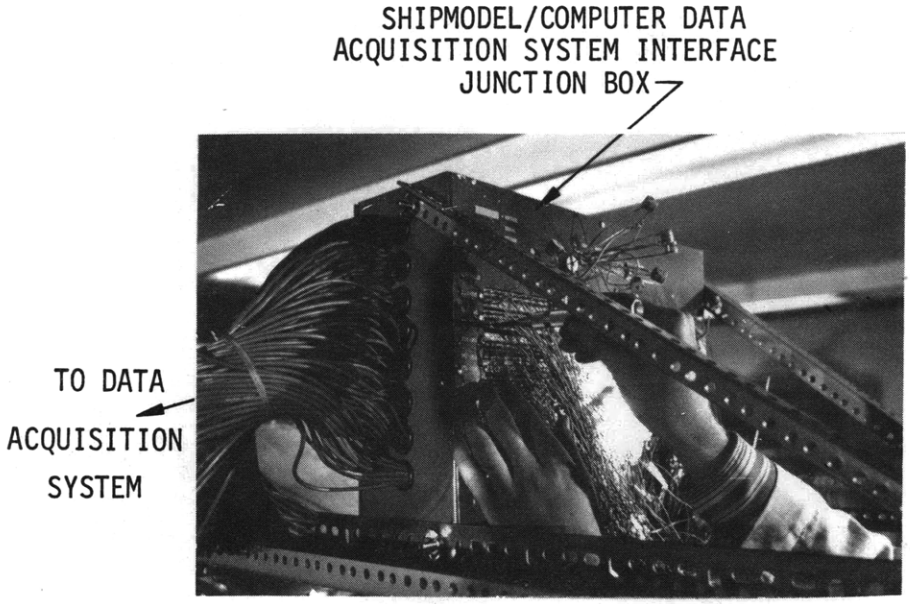

Figure 36 - Junction Box for Interfacing the Model to the Automatic Data Acquisition System

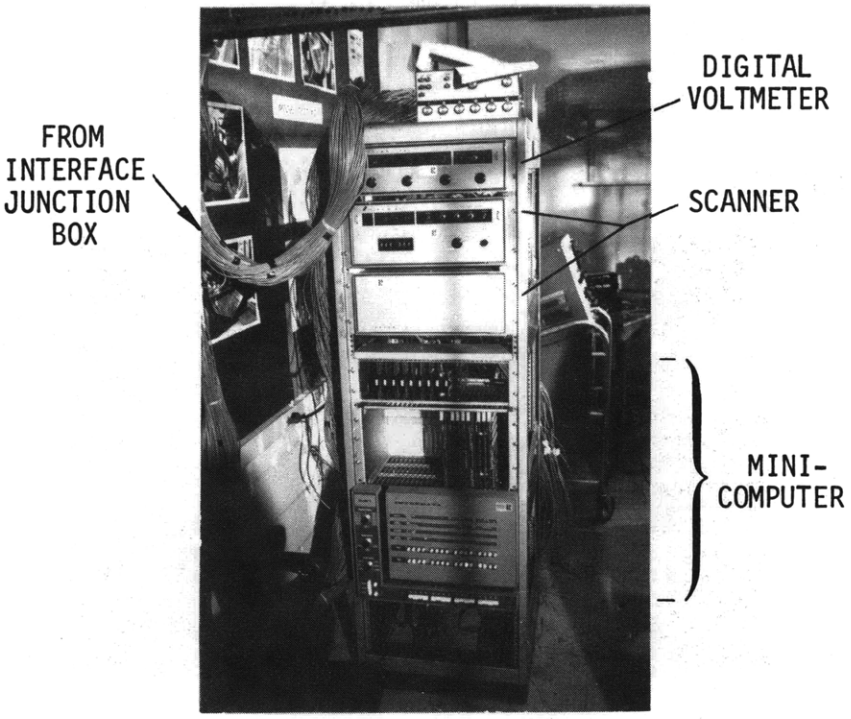

Figure 37 - Data Acquisition System

The stress analysis is divided into six areas of investigation:

1. Cross-sectional stress distribution where entire cross sections are gaged to read strain in a fore-to-aft direction. The nine cross sectional locations are shown in Figure 38 with the installation at Frame 33.5 shown in Figure 34.

2. Longitudinal bending analysis through instrumentation of center vertical keel, main deck, and 0-1 level girders at locations presented in Table 9.

3. Lateral bending analysis using outer fiber gages at the cross-sectional investigation.

4. Shear stress distribution at locations shown in Figure 38.

5. Two-dimensional stress distribution at discontinuity and the transition area using rosettes.

6. Detailed stress analysis at the main load-bearing structure, Frame 27, and at the transition deck, Frame 37.5

The exact locations of the above gages can be found in Appendix F.

The experimental data are automatically reduced; output is in the form of model and prototype equivalent stresses and catagorized as to the analysis interest areas described above. The conversion of model effective strain as read by the system to actual model stress and consequently prototype equivalent stress involves the application of the empirical modulus of elasticity, E_{gaged}, of Figure 14. The use of this value in determining actual model stress is the reciprocal process that was used in determining E_{gaged}. The equation

$$\sigma_{actual} = E_{gaged}\, \varepsilon_{measured}$$

is used (1) to determine E_{gaged} when σ_{actual} and the strain measured by the gages are known and (2) to determine the stress σ_{actual} after E_{gaged} has been determined for a given thickness and the strain measured. If the corresponding actual strain is desired, a second conversion must be made by using the actual modulus of elasticity, E_{actual} of Figure 14, or

$$\varepsilon_{actual} = \frac{\sigma_{actual}}{E_{actual}}$$

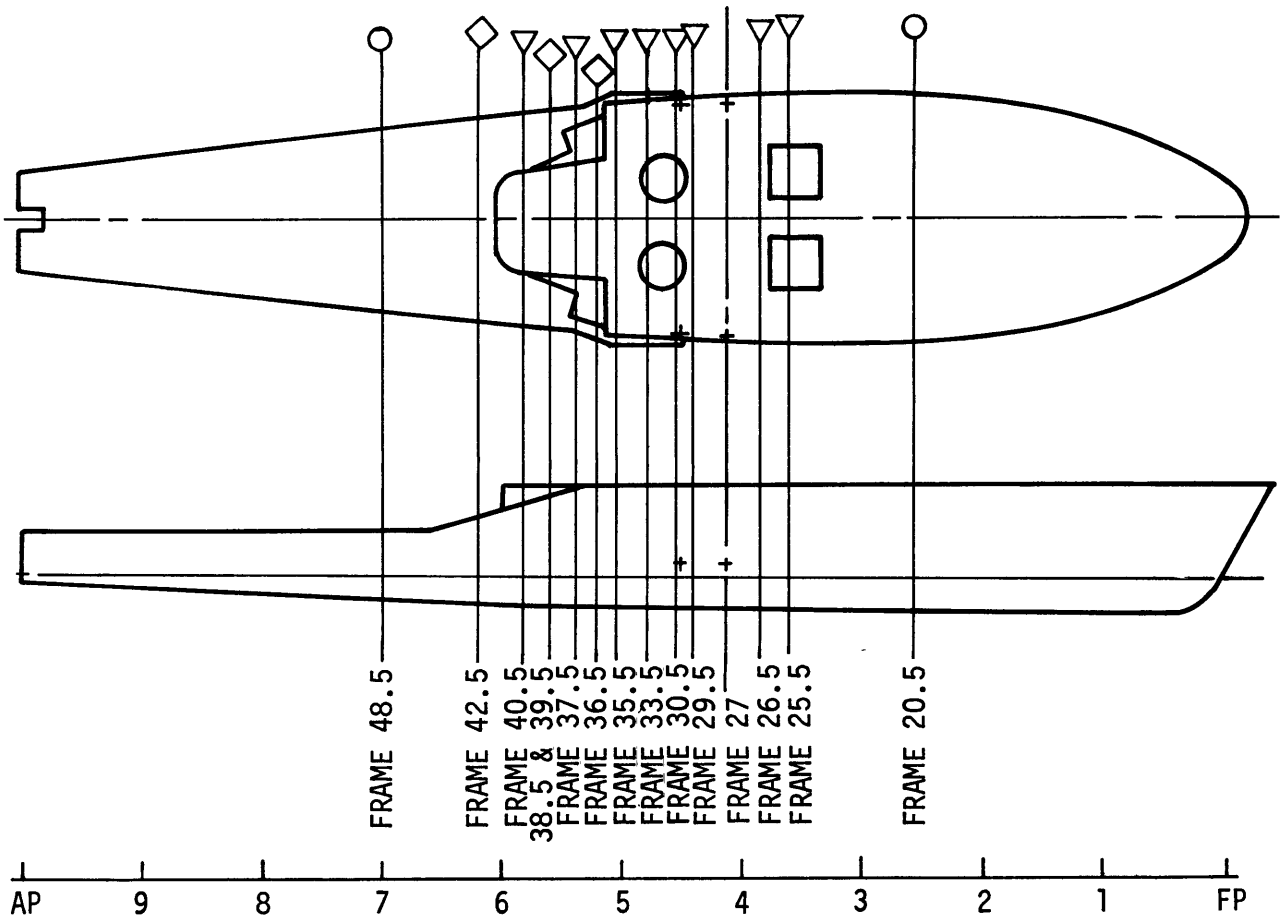

KEY

○ CROSS-SECTIONAL STRESS INVESTIGATION

▽ CROSS SECTIONAL AND SHEAR STRESS INVESTIGATION

◇ SHEAR STRESS INVESTIGATION

Figure 38 - Stress Investigation Locations for 1:20 AGEH PVC Model

TABLE 9 - LONGITUDINAL BENDING STRESS INVESTIGATION

(The circles indicate areas where gages are located)

Frame No.	Keel Gage	Main Deck Gage	0-1 Level Gage
13.5	0		0
18.5	0		0
20.5	0		0
21.5	0		0
22.5	0		0
23.5	0		0
24.5	0		0
25.5	0		0
26.5	0		0
28.5	0		0
29.5	0		0
30.5	0		0
32.5	0		0
33.5	0		0
34.5	0		0
35.5	0		0
36.5	0	0	0
37.5	0	0	0
39.5	0	0	0
40.5	0	0	0
42.5	0	0	
45.5	0	0	
52.5	0	0	

It must be remembered that the strain measured by the gage requires empirical conversion. In addition to strain readings, vertical deflections of the keel will be measured. Detailed procedural information will be included in the forthcoming report on the experimental program.

CONCLUSIONS

The AGEH-1 1:20 PVC Model was successfully designed, constructed, and instrumented, and is ready for experimental investigation.

The model is supported by strut mechanisms representative of full-scale behavior. It provides scaled longitudinal (vertical) and lateral bending and torsion to enable elastic strain and deflection measurements directly applicable to the prototype. The model instrumentation consists of approximately 400 data channels, including the strain-gage locations installed on the prototype.

The following conclusions are made:

1. Small-scale rigid vinyl models result in considerable savings of time and money over large-scale models and prototypes.

2. Complex geometries and details are easily fabricated and allow for the accurate modeling of virtually any structure.

3. In addition to being a structural model, the plastic model serves as a visual aid for design engineers in the modification and redesign of components and assemblies.

4. Rigid vinyl (PVC) is a relatively stable and effective plastic for structural model applications. PVC is nonhygroscopic and isotropic, and plastic creep is virtually nonexistent for all stress levels up to 500 psi. The AGEH-1 prototype equivalent of 500 psi is nearly 20 ksi, therefore, the majority of the elastic range of the aluminum ship can be investigated without any material creep. Stress values above 500 psi are relatively creep free after an appropriate waiting time. (Complete quantitative material properties will be reported independently.)

5. Vacuum-mold forming of heated PVC allows for very detailed representations of complex ship hull curvatures. Sharp corners and other similar forms may result in thinning of plastic; however, component forming provides a means of avoiding unwanted thinning.

6. PVC material thermal behavior is such that the elastic modulus varies less than 1 percent per degree F. (A temperature-controlled laboratory was established to eliminate any variation in results.)

7. Available stock thicknesses of vinyl plastic often require modifications and/or simplification of the full-scale structure. If this is the case, the modifications must be examined and possibly remodified to ensure accurate prototype representation. Elastic buckling tendencies as a result of structural simplification must also be eliminated.

8. The various methods of forming materials used in ship construction can be simulated on a PVC model with equivalent joint rigidity i.e., spot welding, fillet welding, threaded fasteners, etc. Reliable joints require snug fitting, proper cleaning, and full curing time of solvent or epoxy before handling. The use of solvent requires a great deal of care. Solvent over large surface areas is not recommended nor is excessive bodied solvent applications because deformation and material softening result. The use of epoxy is recommended for those applications.

9. Drafting and fabrication costs can be easily reduced through the use of solid (one price) frames and bulkheads in lieu of "built-up" members. Plastic thickness controls the frames bending stiffness.

ACKNOWLEDGMENTS

The author is grateful to Mr. E. Marmentini for initiation of the rigid vinyl program at NSRDC and to Mr. D.J. Clark for his valuable suggestions and support throughout the development and design of the model. The performance of Messrs. J.J. Metzger and B.E. Berwager in constructing the model was outstanding. The contributions of Messrs. W. Schafer, G. Lauver, and J. Hardison both in PVC research and model instrumentation are greatly appreciated. The assistance offered by Messrs J. Daniel and W. Bird in obtaining and interfacing the automatic data acquisition system is gratefully acknowledged. Finally, the author is indebted to Mr. B. Ball for the continuous photographic coverage used throughout the construction.

APPENDIX A

SCALING RELATIONSHIPS

DERIVATION FOR A STATICALLY LOADED, ELASTIC MODEL

The derivation of the geometrically similar scaling relationships used in the design of a statically loaded, elastic model is illustrated in the following examples:

Assume:
$$L_m = \lambda L_p \tag{1}$$

$$\varepsilon_m = \varepsilon_p \tag{2}$$

where: L_m is the length of the model,

L_p is the length of the prototype,

λ is the scaling factor,

ε_m is the model strain, and

ε_p is the prototype strain.

For derivation of stress (σ) using Hooke's Law:

$$\sigma = E\varepsilon \tag{3}$$

where E is the elastic modulus. Therefore

$$\sigma_m = E_m \varepsilon_m \tag{4}$$

and

$$\sigma_p = E_p \varepsilon_p \tag{5}$$

The ratio of σ_m/σ_p of Equations (4) and (5) becomes:

$$\frac{\sigma_m}{\sigma_p} = \frac{E_m \varepsilon_m}{E_p \varepsilon_p} \tag{6}$$

since $\varepsilon_m/\varepsilon_p = 1$ by Equation (2).
Then

$$\frac{\sigma_m}{\sigma_p} = \frac{E_m}{E_p} \quad (1) \tag{7}$$

and

$$\boxed{\sigma_m = e\,\sigma_p} \tag{8}$$

where $e = E_m/E_p$.

For derivation of force:

$$\sigma = F/A \tag{9}$$

in terms of Force (F) and Length (L), Equation (9) dimensionally becomes

$$\sigma \overset{|d|}{=} F/L^2 \tag{10}$$

Rearrangement of terms in Equation (10) gives:

$$F = L^2\,\sigma \tag{11}$$

Also

$$F_p = L_p^{\,2}\,\sigma_p \quad \text{and} \tag{12}$$

$$F_m = L_m^{\,2}\,\sigma_m \tag{13}$$

The ratio of F_m/F_p is

$$\frac{F_m}{F_p} = \frac{L_m^{\,2}\,\sigma_m}{L_p^{\,2}\,\sigma_p} \tag{14}$$

By introducing Equations (1), (2), and (3), Equation (14) becomes

$$\frac{F_m}{F_p} = \frac{\left(\lambda^2\,L_p^{\,2}\right)\left(e\,\sigma_p\right)}{L_p^{\,2}\,\sigma_p} \tag{15}$$

Reducing (15) gives:

$$\frac{F_m}{F_p} = \lambda^2 e \tag{16}$$

or

$$\boxed{F_m = e \lambda^2 F_p} \tag{17}$$

The rest of the equations of Table 2 can be derived in a similar manner.

MODIFICATION OF THICKNESS

The modification of thickness to allow for simplification without plate elastic buckling requires a change in the scaling relationships. Since the thickness was increased by a factor k, then the area was also increased by the same factor. The derivation is similar to the above; however, it was assumed that the scaled force would remain unchanged, thus causing a reduction in model strain:

For stress: Equation (9) becomes

$$\sigma_2 = P_2/A_2 \tag{18}$$

and since

$$A_2 = k A_1 \tag{19}$$

where

$k = t_2/t_1$,

t_2 = increased thickness, and

t_1 = scaled thickness (λt_p),

then

$$\sigma_2 = P_2/k A_1 \tag{20}$$

$$\sigma_1 = P_1/A_1 \tag{21}$$

Since $P_1 = P_2$ (as assumed)

$$\frac{\sigma_2}{\sigma_1} = 1/k \tag{22}$$

or

$$\sigma_2 = \sigma_1/k \tag{23}$$

Therefore Equation (8) becomes

$$\boxed{\sigma_m = e\,\sigma_p/k} \tag{24}$$

Similarly for strain: from Equation (3)

$$\varepsilon_2 = \sigma_2/E \tag{25}$$

From Equation (23)

$$\sigma_2 = \sigma_1/k \tag{26}$$

Substituting (26) into (25) gives

$$\varepsilon_2 = \sigma_1/E_1\ k$$

or

$$\varepsilon_2 = \varepsilon_1/k \tag{27}$$

Therefore Equation (2) becomes

$$\boxed{\varepsilon_m = \varepsilon_p/k} \tag{28}$$

The remainder of the relationships of Table 4 can be derived in a similar manner.

APPENDIX B

CALCULATION OF THICKNESS SCALING FACTOR

PANEL EXTRUSION A (from Figure 10)

Total Area = 3.19 in.^{2}

Effective plating thickness at 10 in. widths = 0.319 in.

Effective plating thickness at $\lambda = 1/20$ at 0.5 in. widths = 0.01595 in.

Factor to increase to 0.030 in.:

$$0.01595\ k = 0.030$$

$$\boxed{k = 1.881}$$

$$0.319\ \lambda_t = 0.030$$

$$\boxed{\lambda_t = 0.09404 \quad \lambda_t = 1/10.634}$$

PANEL EXTRUSION B (from Puget Sound Bridge and Dry Dock Company Drawing AGEH-1-800-2206521)

Total Area at 14 in. = 3.175 in.^{2}

Effective thickness at 14 in. = 0.2267 in.

Effective model thickness = 0.0213 $\approx$ 0.020 in.

PANEL EXTRUSION C

Total Area at 12 in. = 2.287 in.^{2}

Effective thickness at 12 in. = 0.091 in.

Effective model thickness = 0.0179 $\approx$ 0.020 in.

PANEL EXTRUSION D

Total Area at 6 in. = 0.705 $in.^2$

Effective thickness at 6 in. = 0.11750 in.

Effective model thickness = 0.011 in. ≈ 0.010 in.

Extrusion T-D	Prototype Effective Thickness, in.	Model* Effective Thickness, in.	Closest Available Plating in.
A	0.319	0.030	0.030
B	0.2267	0.0213	0.020
C	0.191	0.0179	0.015/0.020
D	0.1175	0.011	0.010

*Using λ_t = 0.09404.

APPENDIX C

LONGITUDINAL AND LATERAL MOMENTS OF INERTIA
FOR AGEH-1

The following curves and digitized data represent the longitudinal and lateral (or transverse) area moments of inertia.* Figure C.1 presents the longitudinal area moment of inertia distribution of the AGEH hull as calculated by two methods. The first, represented by Curve A of Figure C.1, assumes all hull structure as effective and openings as ineffective. The second, Curve B, also considers a triangular area forward and aft of the opening with a 4:1 slope as inefffective. Digitized values of Curves A and B at various frames are given in Tables C.1 and C.2, respectively. Figure C.2 presents the transverse area moment of inertia with the digitized form given in Table C.3.

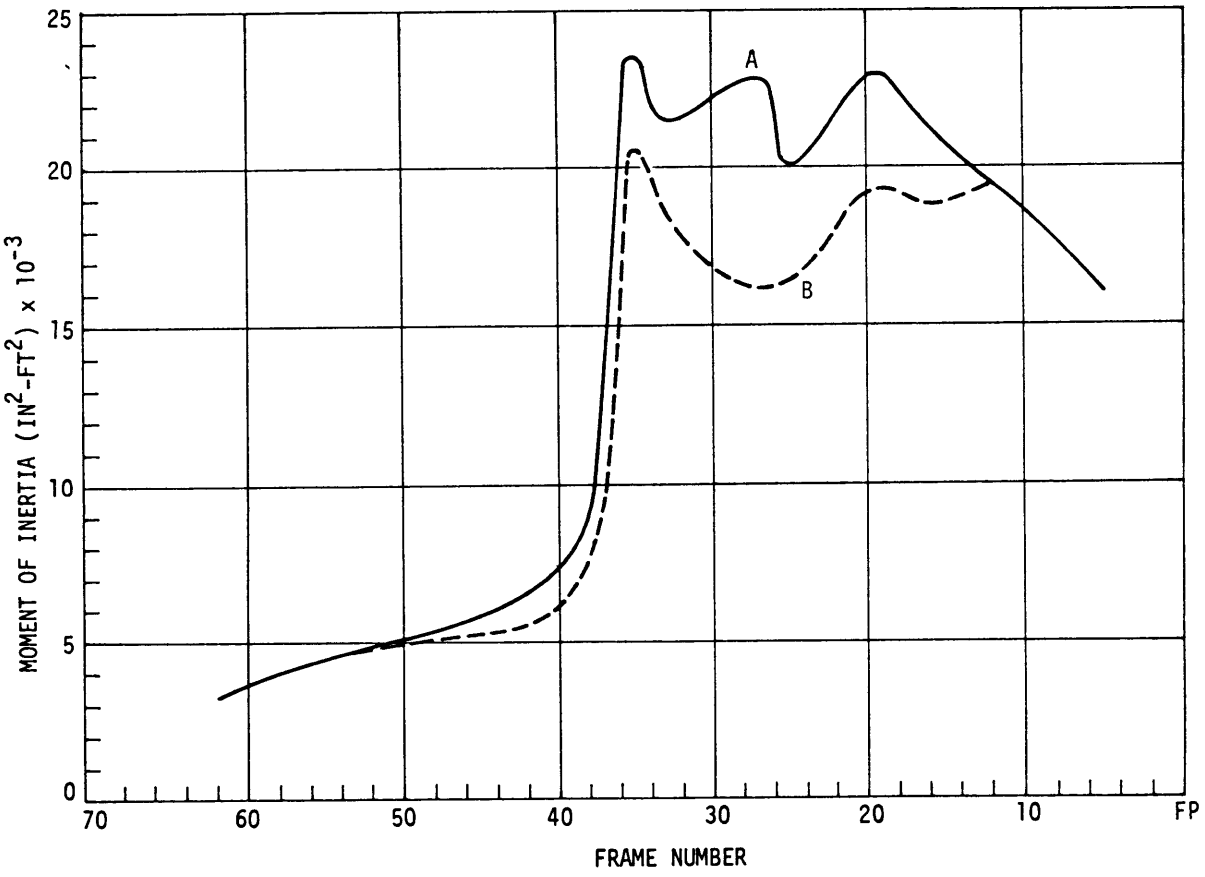

Figure C.1 - Distribution of Longitudinal Area Moment of Inertia for the AGEH-1 Hull Structure

*Reported informally by Clark et al. in NSRDC Tech Note SD 178.

TABLE C.1 - SUMMARY OF CALCULATED LONGITUDINAL MOMENT OF INERTIA WITH OPENINGS CONSIDERED INEFFECTIVE

Frame	Station	I_{YY} $in^2\text{-}ft^2$	Y_K ft	Y_{WD} ft	S_K $in^2\text{-}ft$	S_{WD} $in^2\text{-}ft$
5	0.73	16,000	13.77	8.02	1170	2010
12	1.76	19,750	11.84	9.95	1670	1980
16	2.35	21,100	11.49	10.30	1840	2050
19	2.79	22,900	11.57	10.22	1980	2240
25	3.66	20,100	10.26	11.53	1960	1740
33	4.79	21,400	10.44	11.18	2050	1910
35	5.08	23,400	10.85	10.44	2160	2240
37	5.38	13,600	9.11	10.14	1490	1340
42	6.10	6,600	7.15	5.55	920	1190
48	6.98	5,300	6.60	5.17	800	1020
55	8.00	4,400	6.32	4.40	700	1000
62	9.03	3,200	5.96	3.69	540	870

Y_K is distance from neutral axis to keel in ft.

Y_{WD} is distance from neutral axis to weather deck in feet.

S_K is section modulus for keel.

S_{WD} is section modulus for weather deck.

TABLE C.2 - SUMMARY OF CALCULATED LONGITUDINAL MOMENT OF INERTIA WITH OPENINGS AND ADDITIONAL* AREAS CONSIDERED INEFFECTIVE

Frame	Station	I_{YY} $in^2\text{-}ft^2$	Y_K ft	Y_{WD} ft	S_K $in^2\text{-}ft$	S_{WD} $in^2\text{-}ft$
5	0.73	16,000	13.77	8.02	1170	2010
12	1.76	19,400	11.76	10.03	1650	1930
16	2.35	18,800	10.88	10.91	1730	1720
19	2.79	19,400	10.66	11.13	1820	1740
25	3.66	16,300	10.01	11.78	1630	1380
27	4.00	16,200	8.91	12.88	1820	1260
33	4.79	18,500	9.53	12.09	1940	1530
35	5.08	20,600	10.04	11.25	2050	1830
37	5.38	9,700	8.32	10.93	1170	890
42	6.10	5,400	6.51	6.19	830	870
48	6.98	5,100	6.44	5.33	790	960
55	8.00	4,400	6.32	4.40	700	1000
62	9.03	3,200	5.96	3.69	540	870

Y_K is distance from neutral axis to keel in feet.

Y_{WD} is distance from neutral axis to weather deck in feet.

S_K is section modulus for keel.

S_{WD} is section modulus for weather deck.

*Refers to a triangular area forward and aft of the opening, with a 4:1 slope.

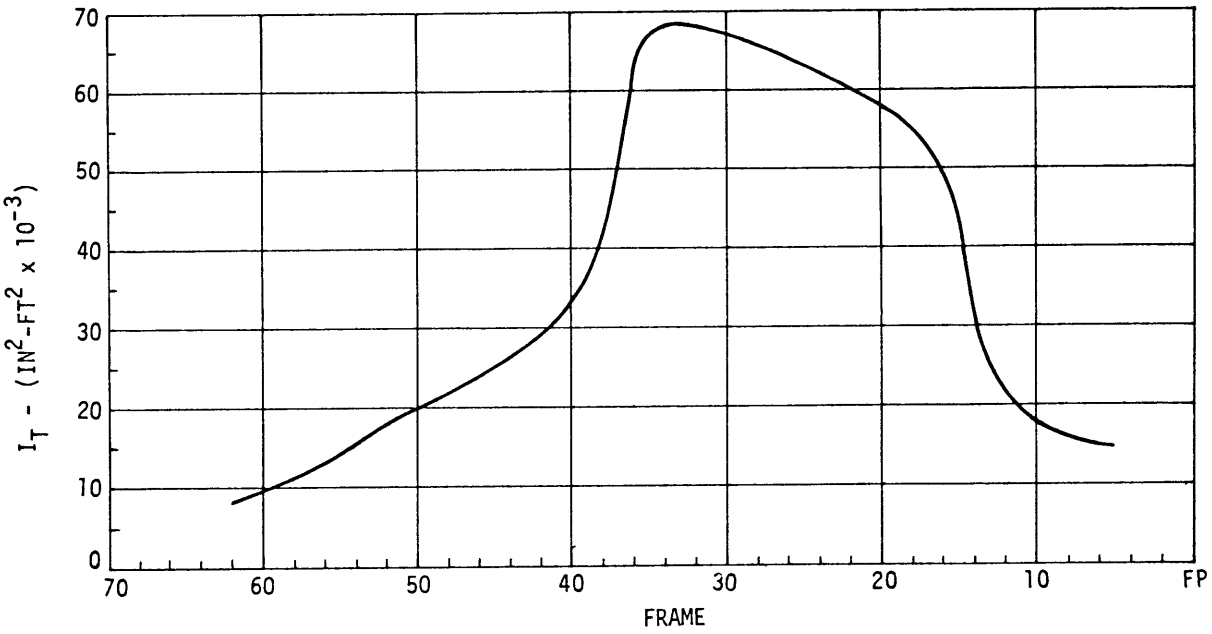

Figure C.2 - Distribution of Transverse Area Moment of Inertia for the AGEH-1 Hull Structure

TABLE C.3 - SUMMARY OF CALCULATED TRANSVERSE MOMENT OF INERTIA WITH OPENINGS CONSIDERED INEFFECTIVE

Frame	Station	I_{ZZ} in^2-ft^2
5	0.73	14,800
12	1.76	36,140
16	2.35	49,600
19	2.79	56,800
25	3.66	63,300
33	4.79	68,200
35	5.08	67,300
37	5.38	49,500
42	6.10	28,900
48	6.98	22,000
55	8.00	14,100
62	9.03	8,000

APPENDIX D

TORSIONAL-SHEAR FLOW INVESTIGATION

Oden[5] gives the rate of twist for a multicelled "tube," or the equation of consistent deformation, as:

$$\theta = \frac{1}{2G\,\Omega_j} \cdot \left[q_j \oint_{s_j} \frac{ds}{t} - \sum_{r=1}^{m} \left(q_r \int \frac{ds}{t} \right) \right] \tag{D1}$$

where θ is the rate of twist;

G is the torsional modulus;

Ω is as defined in Figure 23;

q is the shear flow;

s is the plating width (of cross section);

t is the plating thickness;

j is the number of cells, and

r is the number of common plating between cells.

The equation of consistent deformation for cell j becomes:

$$\sigma_{ji}\, q_i + \delta_{jj}\, q_j + \delta_{jk} - 2\,\Omega_j\,\theta = 0 \tag{D2}$$

where

$$\delta_{ji} = -\frac{1}{G} \int_{s_{ji}} \frac{ds}{t} \tag{D3}$$

$$\delta_{jk} = -\frac{1}{G} \int_{s_{jk}} \frac{ds}{t} \tag{D4}$$

$$\delta_{jj} = \frac{1}{G} \int_{s_j} \frac{ds}{t} \tag{D5}$$

(these are called "warping flexibilities")

---

[5] Oden, J.T., "Mechanics of Elastic Structures," Chapter 3, 3.10 in "Multicell Thin Walled Tubes," McGraw Hill Book Company, New York (1967), pp. 53-56.

Solving for q_i for the model

$$\begin{bmatrix} q_1 \\ q_2 \\ q_3 \\ q_4 \end{bmatrix} = \begin{bmatrix} 0.096\ G\ \theta \\ 0.092\ G\ \theta \\ 0.108\ G\ \theta \\ 0.092\ G\ \theta \end{bmatrix} \tag{D6}$$

Also the torque (M_t)

$$M_t = 2 \sum_{j=1}^{m} q_j\ \Omega_j \tag{D7}$$

Substituting (D6) into (D7) gives

$$M_t = 23.139\ G\theta \tag{D8}$$

or

$$\theta = 0.0432\ \frac{M_t}{G} \tag{D9}$$

Substitution of (D9) into (D6) gives

$$\begin{bmatrix} q_1 \\ q_2 \\ q_3 \\ q_4 \end{bmatrix} = \begin{bmatrix} 4.15 \times 10^{-3}\ M_t \\ 3.97 \times 10^{-3}\ M_t \\ 4.67 \times 10^{-3}\ M_t \\ 3.97 \times 10^{-3}\ M_t \end{bmatrix} \tag{D10}$$

Using prototype design of

$$M_t = 0.5 \times 10^3 \text{ ft-kip} \tag{D11}$$

or model equivalent

$$M_t = 37.5 \text{ in-lb} \tag{D12}$$

Note:

The actual value of the polar moment of inertia is

$$J_{AV} = 23.139 \text{ in.}^4$$

A true-to-scale value would be

$$J_{\pi s} = 11.83$$

the ratio $\sigma_{AV}/J_{\pi s} = 1.956$

This is 1.04 greater than the increased stiffness created by the thickness factor of Table 5. Therefore to obtain conformity of results the torsion must be increased by 1.04. Equation (D12) becomes:

$$M_t = 37.5 \ (1.04) = 39.0 \tag{D13}$$

Substitution of (D13) into (D10) gives

$$\left.\begin{aligned} q_1 &= 0.162 \text{ lb/in.} \\ q_2 &= 0.155 \text{ lb/in.} \\ q_3 &= 0.182 \text{ lb/in.} \\ q_4 &= 0.155 \text{ lb/in.} \end{aligned}\right\} \tag{D14}$$

In terms of the model the shear (τ) is:

$$\left.\begin{aligned} \tau_{\text{main deck}} &= 10.8 \text{ psi} \\ \tau_{\text{side plating}} &= 8.1 \text{ psi} \\ \tau_{\text{hull bottom}} &= 6.0 \text{ psi} \end{aligned}\right\} \tag{D15}$$

which is very low and well below the critical buckling stress.

APPENDIX E

CONSTRUCTION PHOTOGRAPHS OF AGEH 1:20 SCALE MODEL

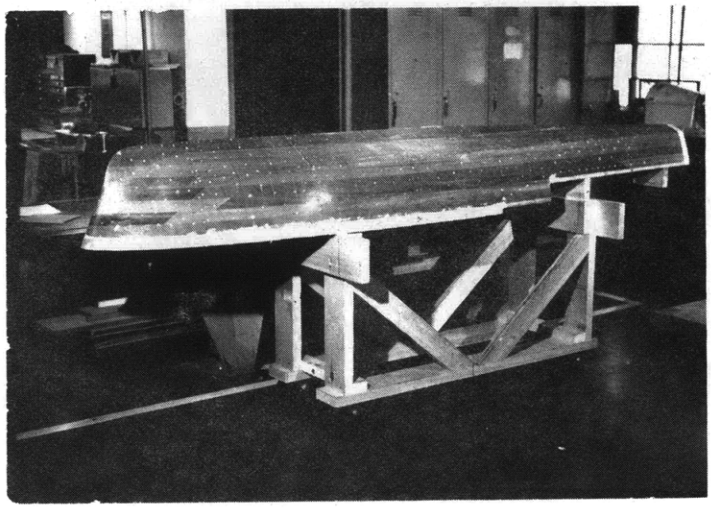

Figure E.1 - Male Vacuum Mold of AGEH Hull Form (Heated PVC is draped over mold and a vacuum applied to form the hull skin)

Figure E.2 - Hull Skin Elements (They are unitized in fiber-glass female construction alignment mold by using solvent and hypodermic needle)

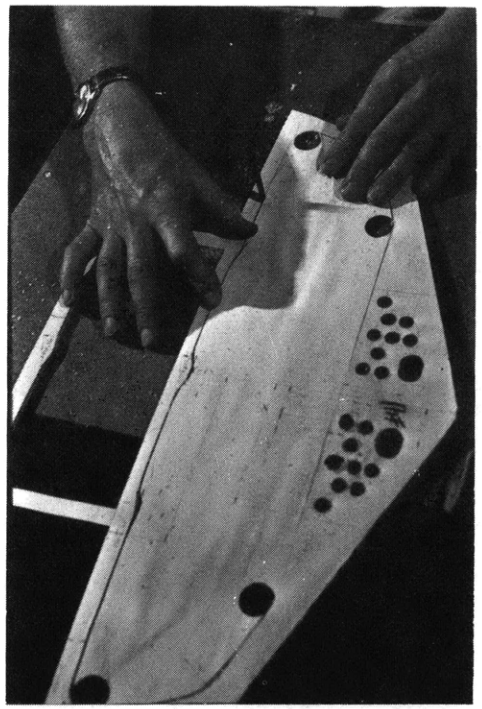

Figure E.3 - Rough Cut Frame (Plans are attached to the plastic and a frame is "rough cut" on a special saw)

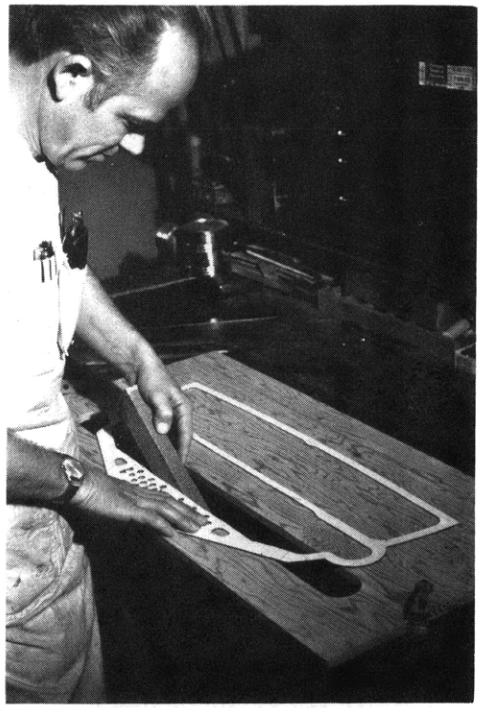

Figure E.4 - Finishing of Rough-Cut Frame (The rough cut frame is sanded to exact dimensions for snug fit in hull skin)

Figure E.5 - Frame Alignment (Frames are aligned by using the construction mold and alignment bar and attached with solvent)

Figure E.6 - The 0-1 Level and Main Deck "Cross-Frame" Structure is Removed for Installation of Strain Gages on the Lower or Second Deck

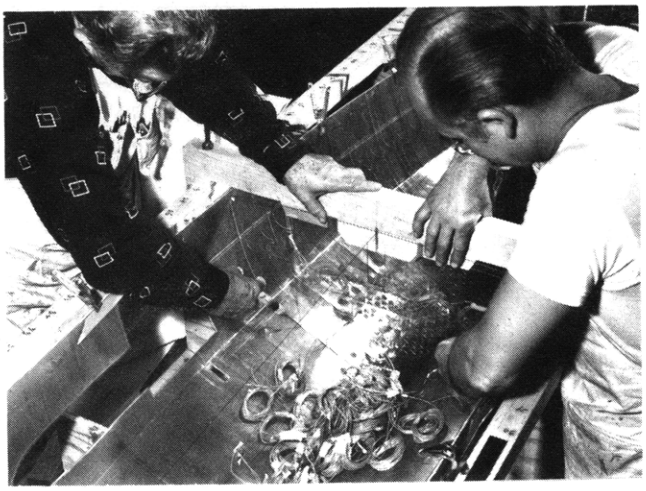

Figure E.7 - As Strain Gages are Installed, the Number of Wires Increase and Require Planning as to Their Passage Through the Model

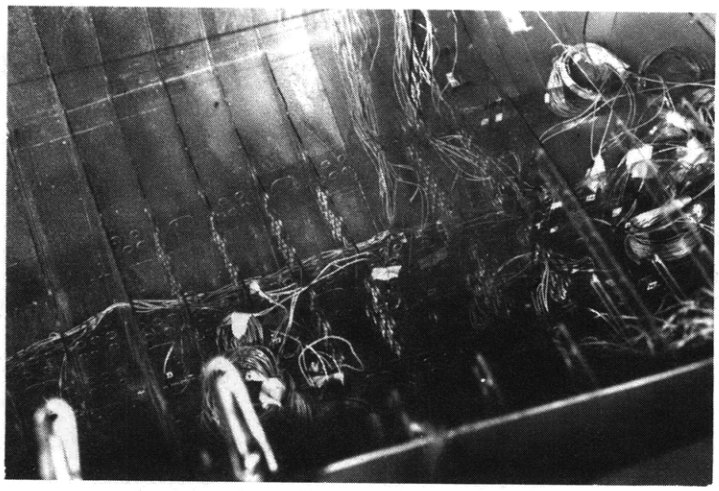

Figure E.8 - The Lightening Holes and Voids in the Frames Provide Passage for Gage Lead Wires below the Second Deck

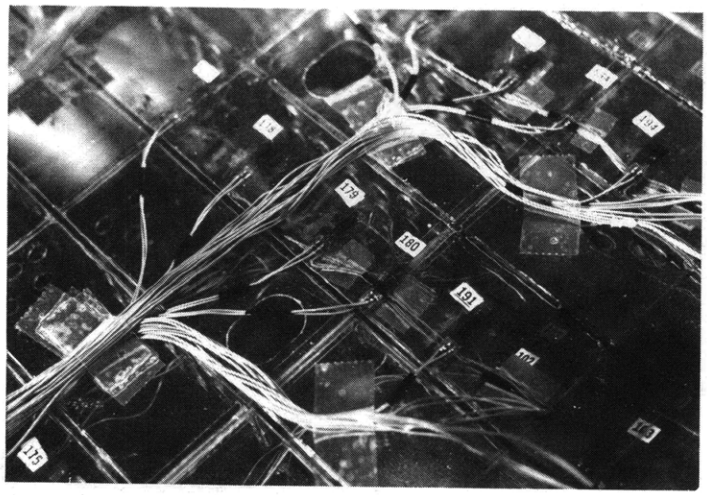

Figure E.9 - Typical Gage Installation on the Second Deck (The Gage Elements shown Run Parallel to the Ship Center-line)

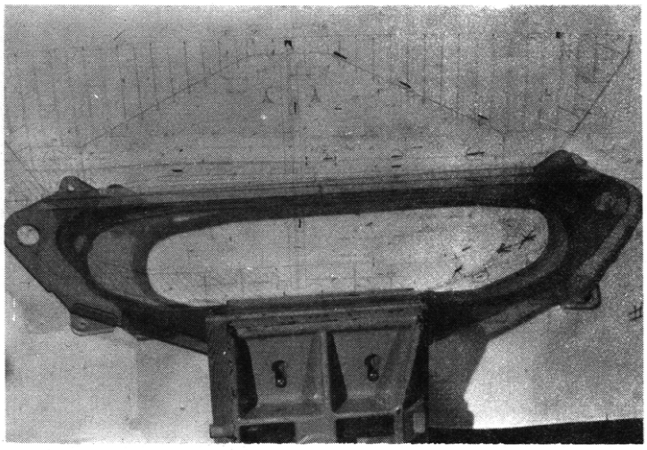

Figure E.10 - Detailed Structural Frame 27, Construction of Main Strut Support Region

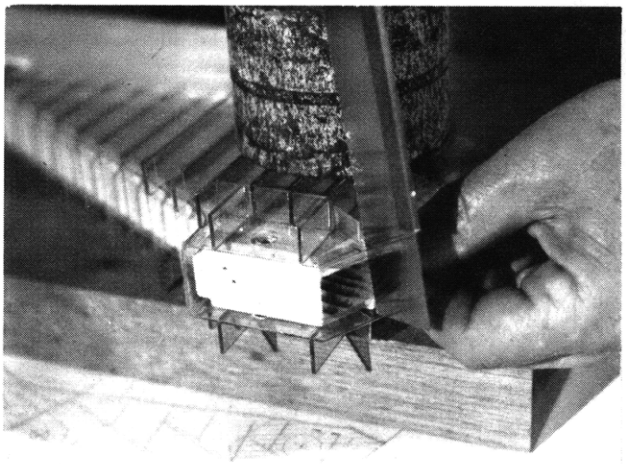

Figure E.11 - Final Fitting of Main Strut and Foil Retraction System Housing Before Completion of Frame 27

Figure E.12 - Solvent Bonding of Structural Support and Retraction Housing

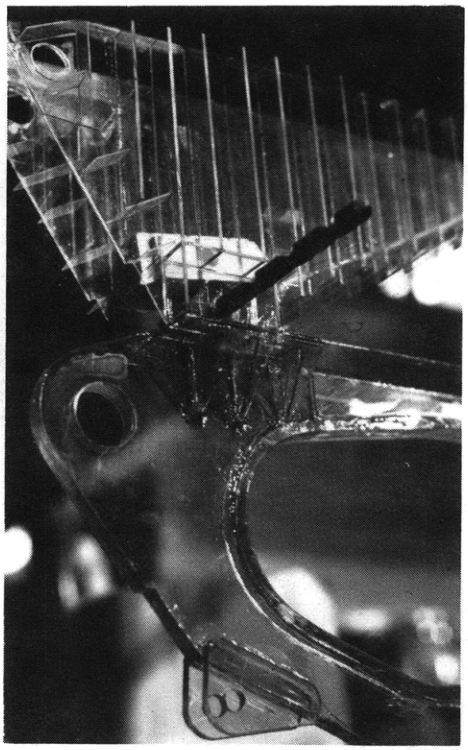

Figure E.13 - Portion of the Computed Structural Support Frame 27 (Note the Detail Potential of Rigid Vinyl Model)

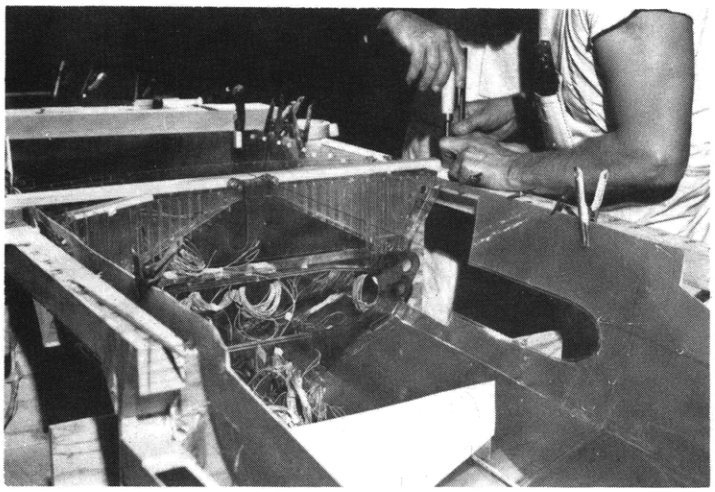

Figure E.14 - Installation of Frame 27 into Hull Skin

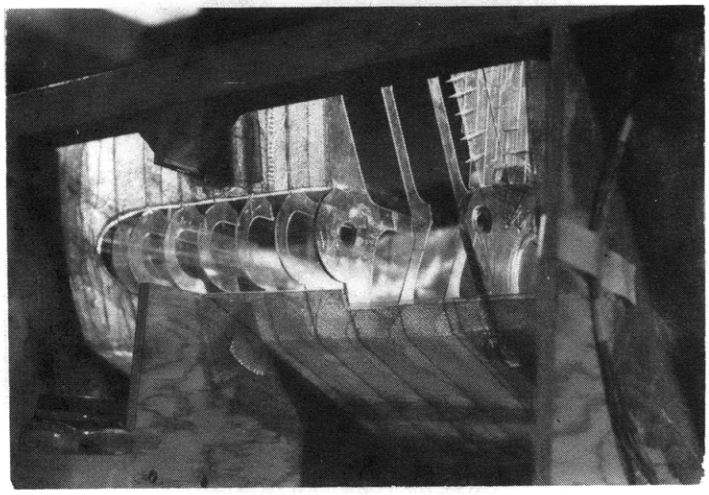

Figure E.15 - Starboard View of Main Strut Support Area of the AGEH Model

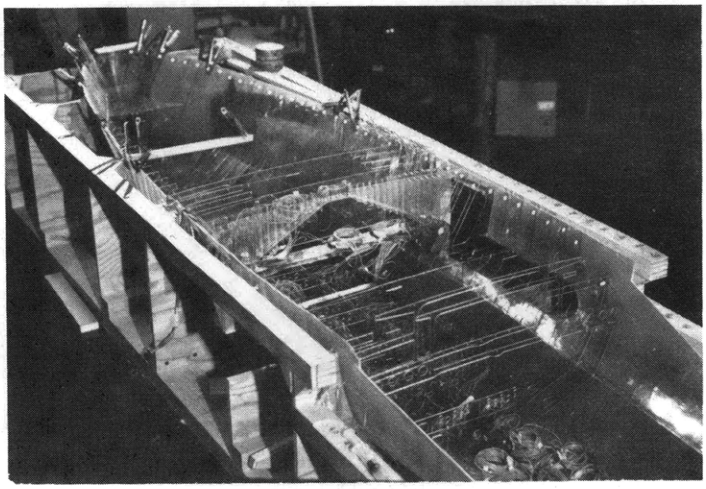

Figure E.16 - Installation of Transitional Area Frame Work

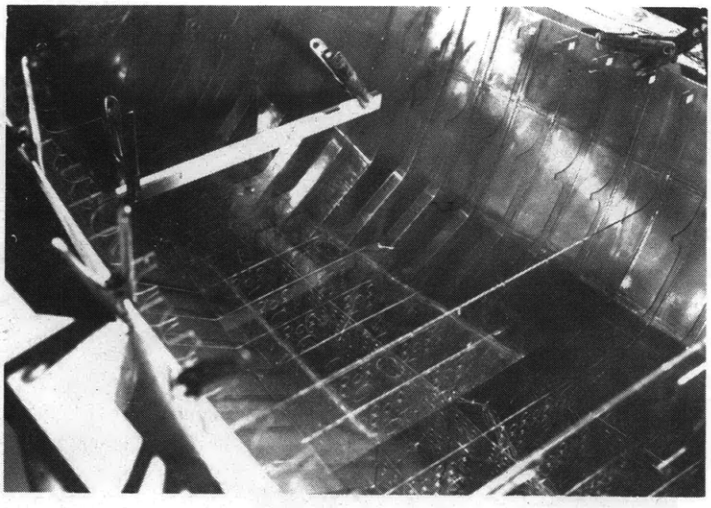

Figure E.17 - Second Deck in Place Forward of Transverse Bulkhead 18

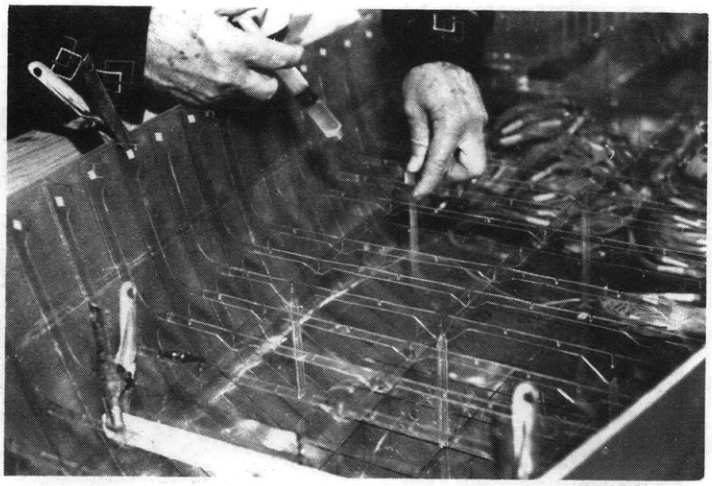

Figure E.18 - Installation of Main Deck Cross Structures and Stanchions

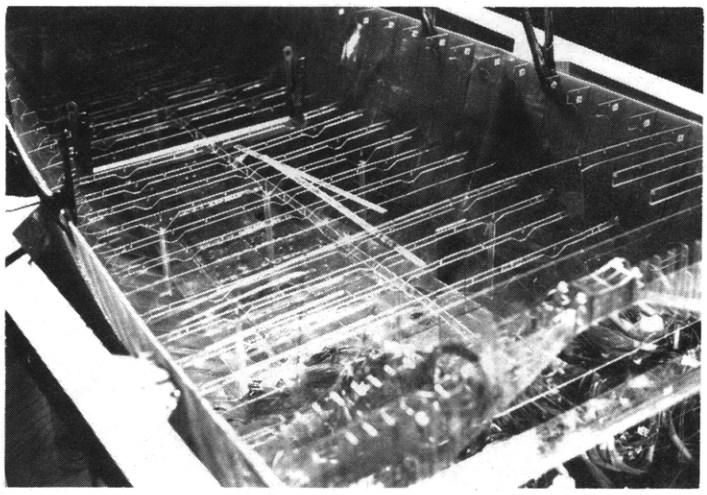

Figure E.19 - Main Deck Structure Forward of Frame 27 Before Decking is in Place

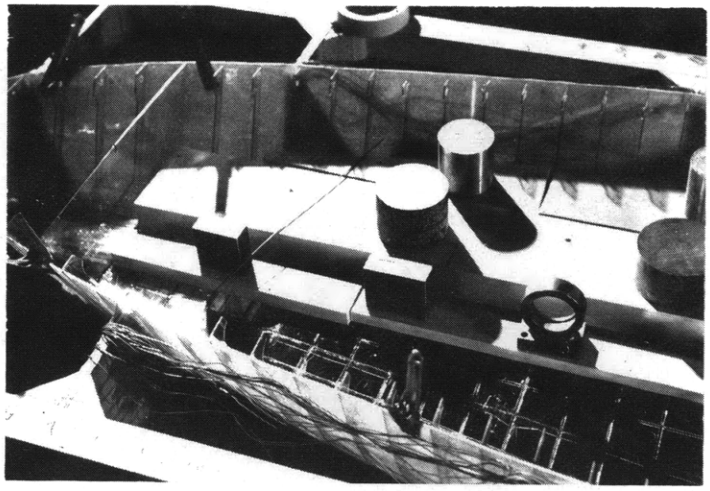

Figure E.20 - Weights to Ensure a Good Epoxy Bond and Representative Decking Stiffness

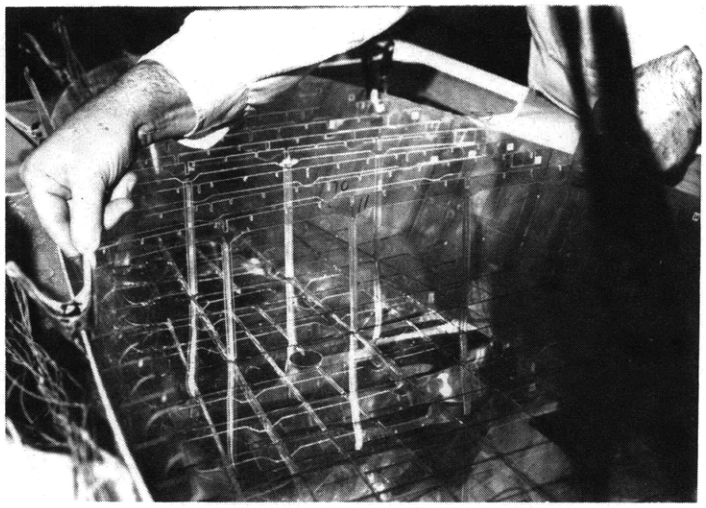

Figure E.21 - Transverse 0-1 Level Deck Framing and Stanchion Installation

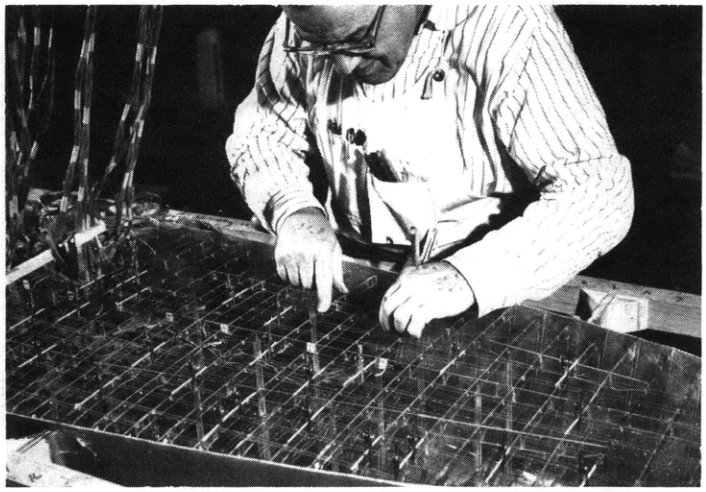

Figure E.22 - 0-1 Level Structural Support Being Completed with the Attachment of the Buckling Resisting Stringers

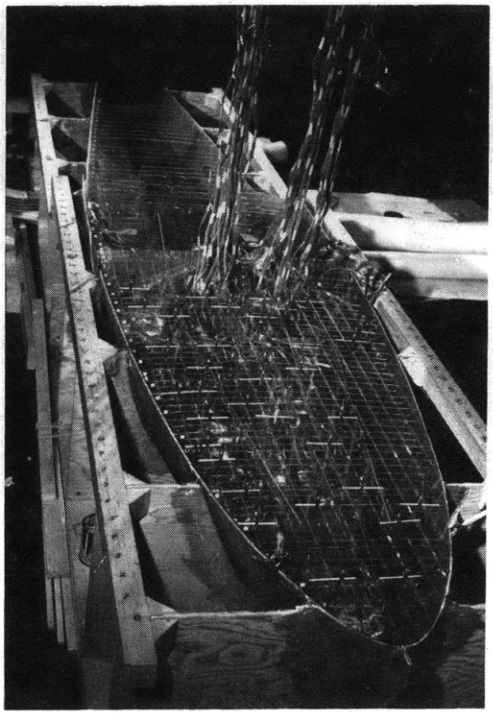

Figure E.23 - 0-1 Level Prior to Attachment of Deck Plating (Note the Strain Gage Lead Wires Passing through the Air Intake Openings)

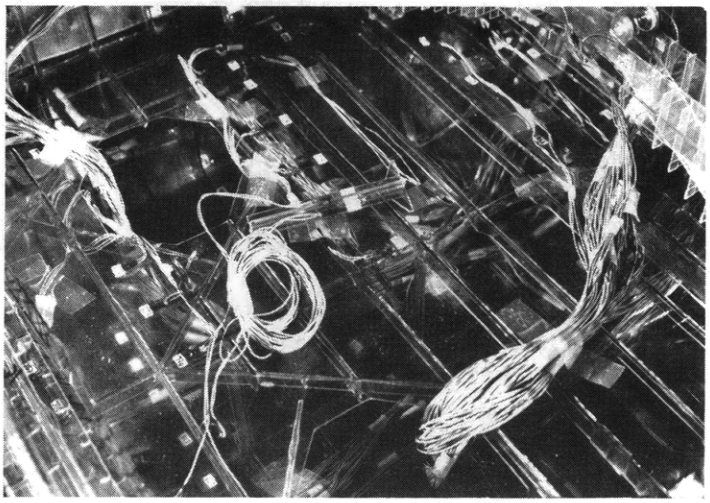

Figure E.24 - Main Deck Structure Aft of Frame 27 and Forward of Bulkhead 36 (Lead Wires are Passed through Exahust Openings)

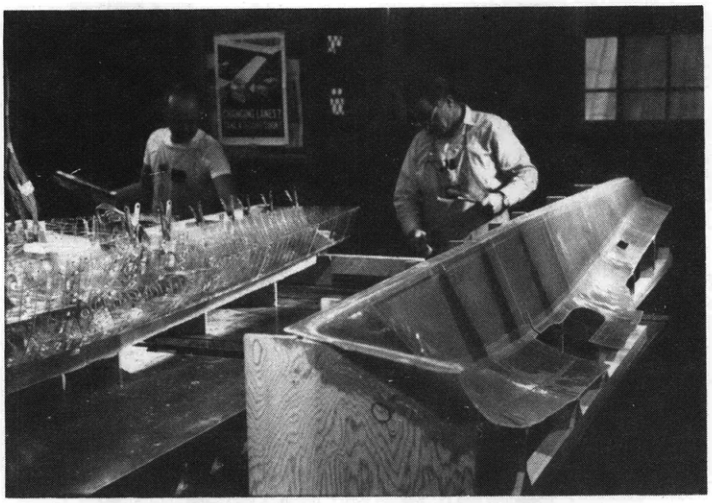

Figure E.25 - Removal of Port Construction Mold for External Work on Main Strut Attachment Area

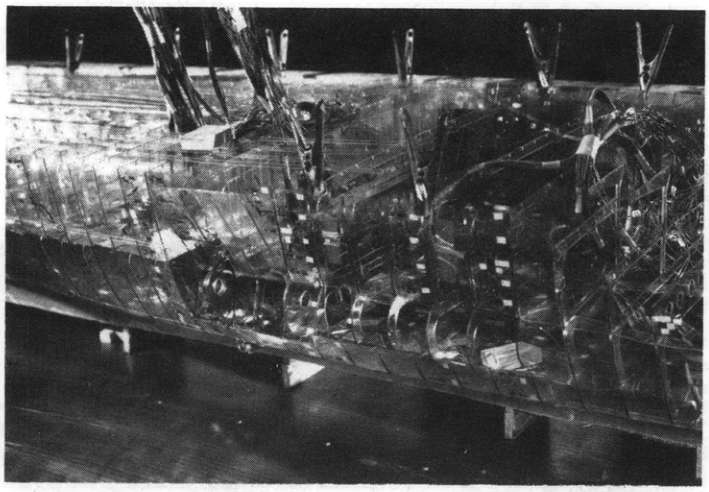

Figure E.26 - Detailed View of Port Strut Attachment Area with Construction Mold Removed

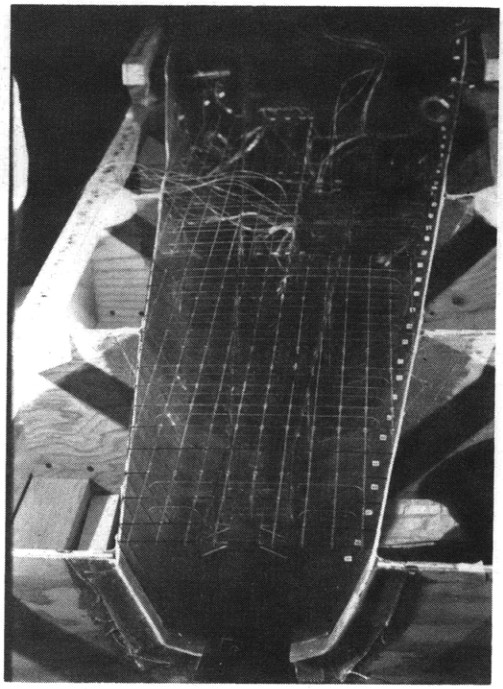

Figure E.27 - Main Deck Support Structure Aft of the Transition Area

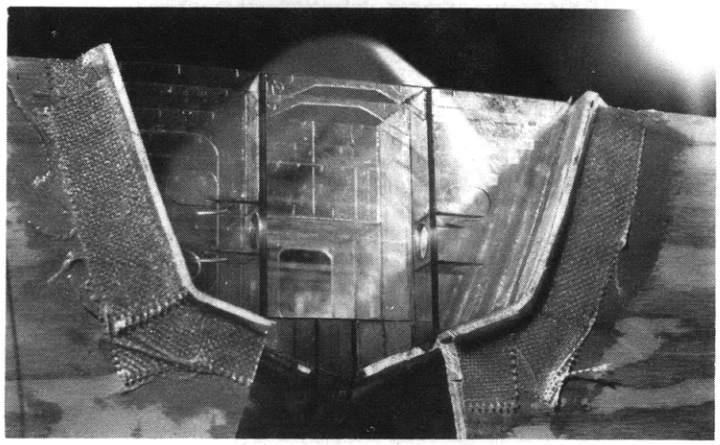

Figure E.28 - Detailed View of the Rear Strut Support Area

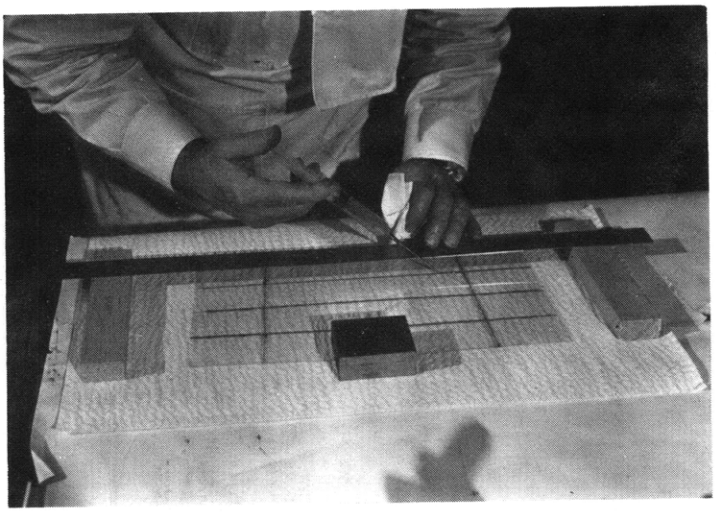

Figure E.29 - Application of Epoxy Bead to Main Deck Plating

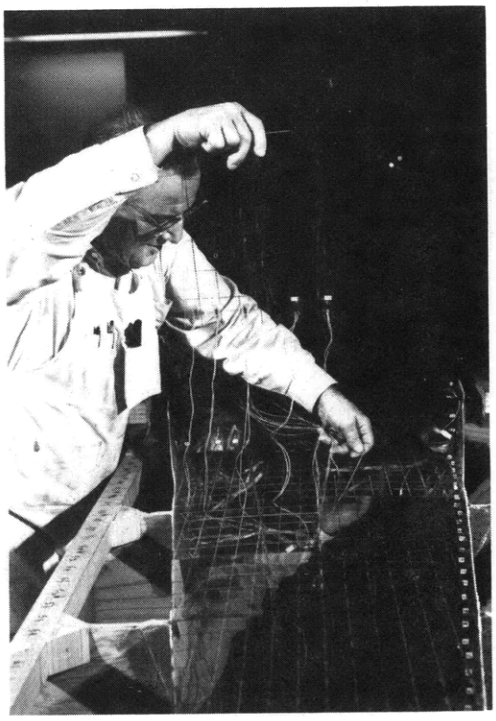

Figure E.30 - Installation of Main Decking Aft of the Transition Area Including Pre-Application of Epoxy Bead and Passing of Gage Lead Wires

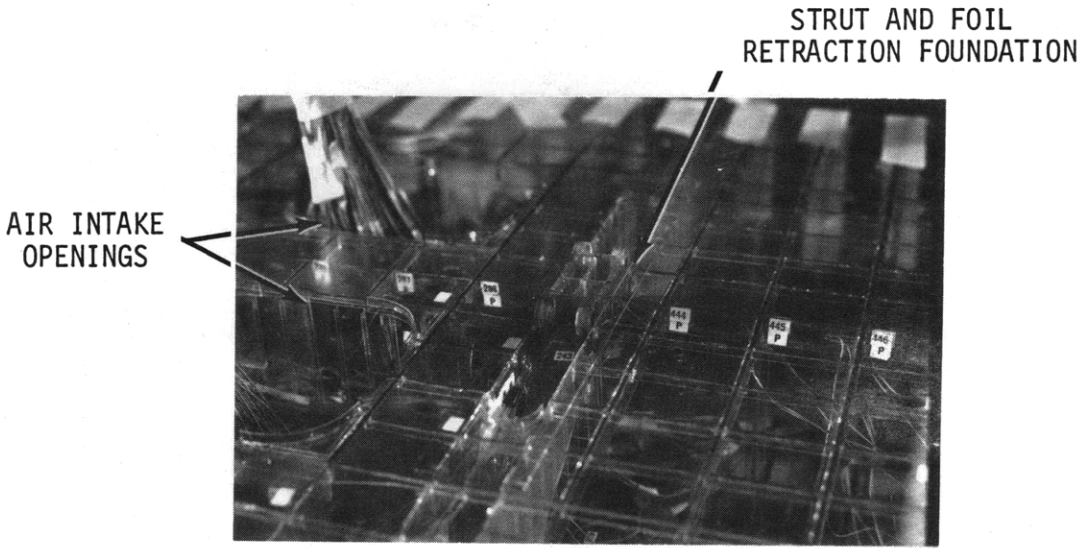

Figure E.31 - Complete 0-1 Level between Frames 24 and 31 (Note Air Intake Openings and Main Strut and Foil Retraction Foundation)

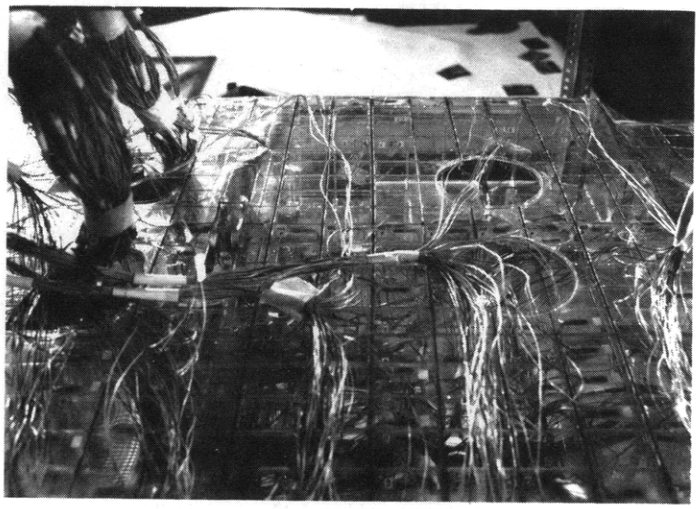

Figure E.32 - 0-1 Level between Frames 24 and 36 with External Gages in Place

Figure E.33 - Starboard View of AGEH Model, Foilborne Configuration

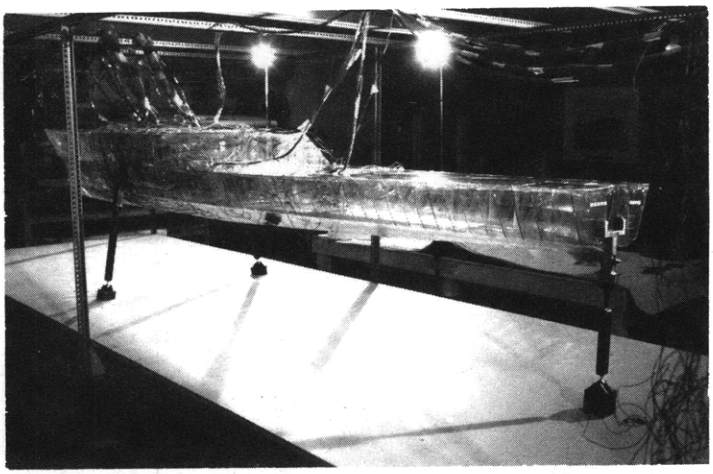

Figure E.34 - Port View of Completed AGEH Model Looking Forward, Foilborne Configuration

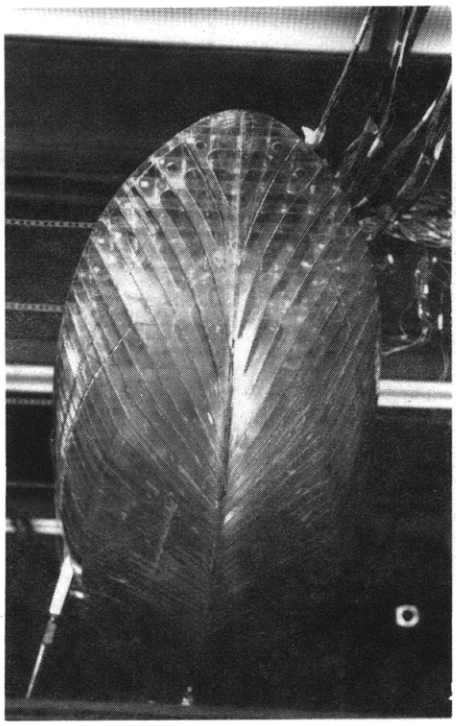

Figure E.35 - Keel-Bow View,
Straight On

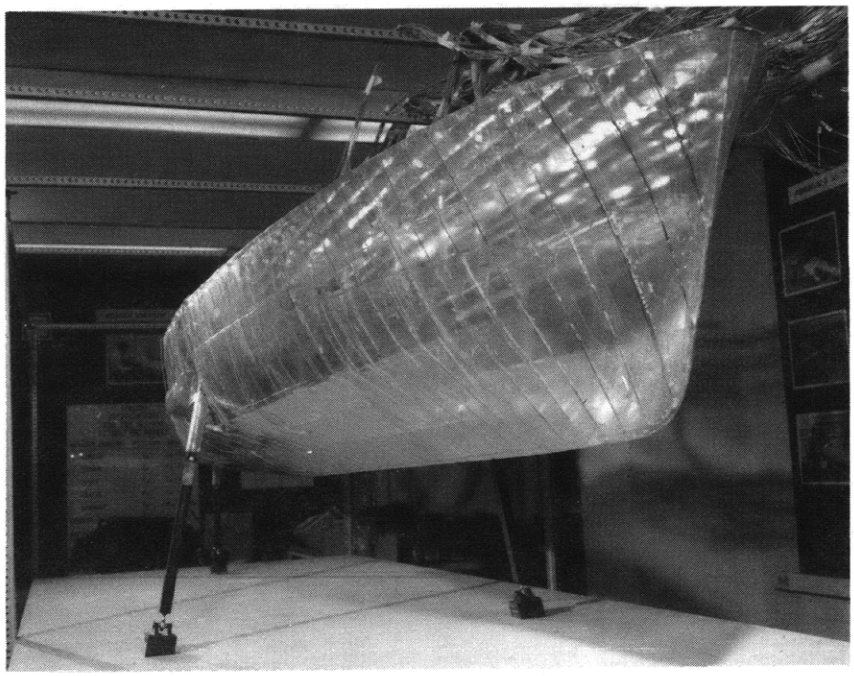

Figure E.36 - Starboard Bow View of Hull
Plating

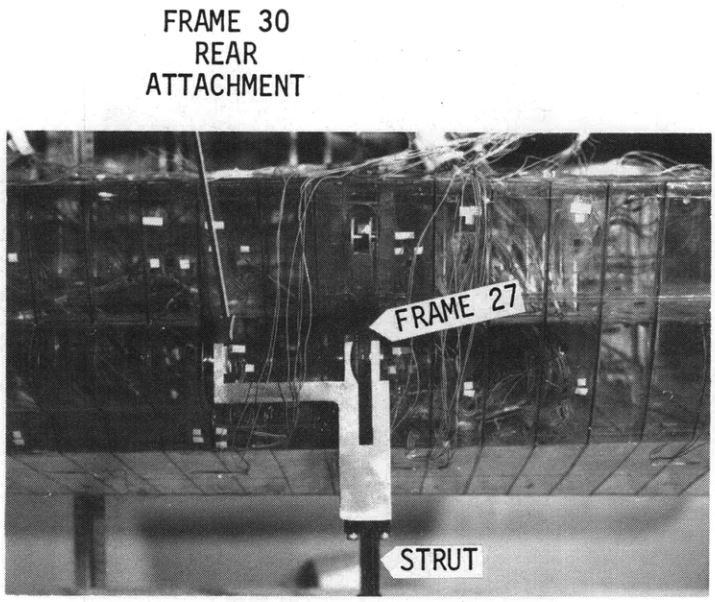

Figure E.37 - Starboard Main Strut Attachment

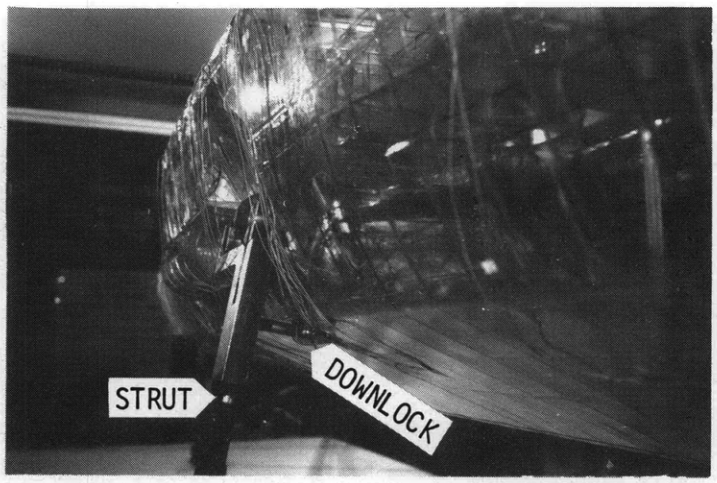

Figure E.38 - Starboard Main Strut Attachment and Downlock Looking Aft

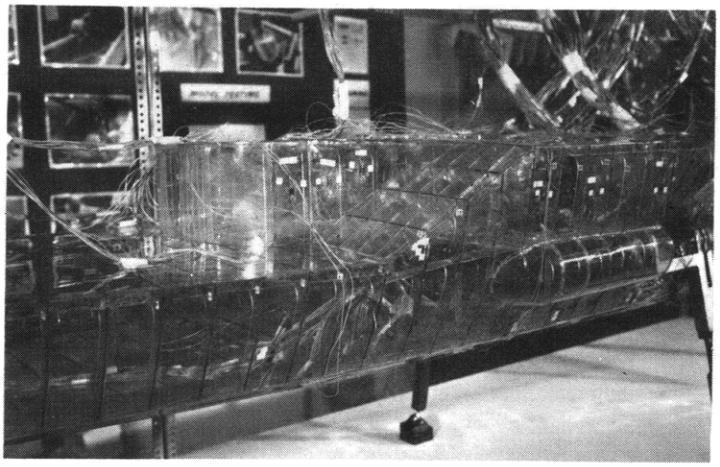

Figure E.39 - Transition Area of AGEH,
Starboard Side Looking Forward

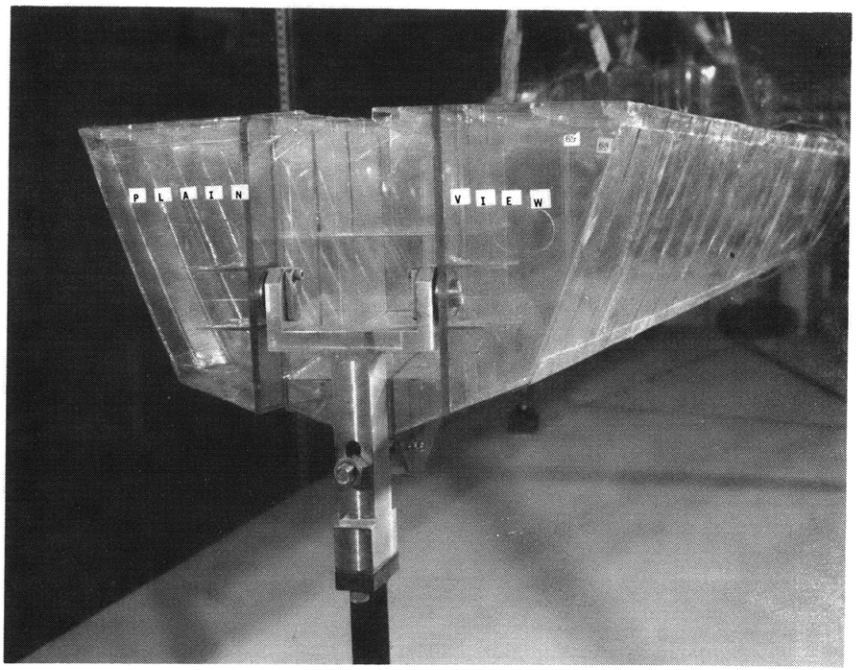

Figure E.40 - Rear Strut and
Strut Support

APPENDIX F

STRAIN-GAGE LOCATIONS ON AGEH 1:20 PVC MODEL

The following figures present the location of the strain gages of the AGEH model. The scale of the drawings are 1 in. ≅ 4 in. and the frames are observed as if looking in the aft direction. The following key is observed throughout the appendix unless otherwise indicated:

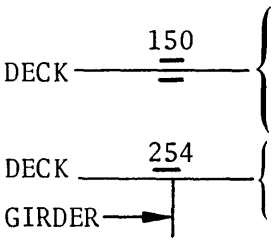

indicates a back-to-back gage (configuration 150), with elements fore and aft to measure strain in a line perpendicular to the paper.

indicates a single gage number (Gage 354) with strain direction read as above

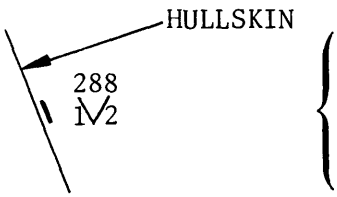

indicates a shear bridge, (No. 288). The 1V2 indicates the elements as they would appear if observed perpendicularly to the hull stern from the side indicated by the V.

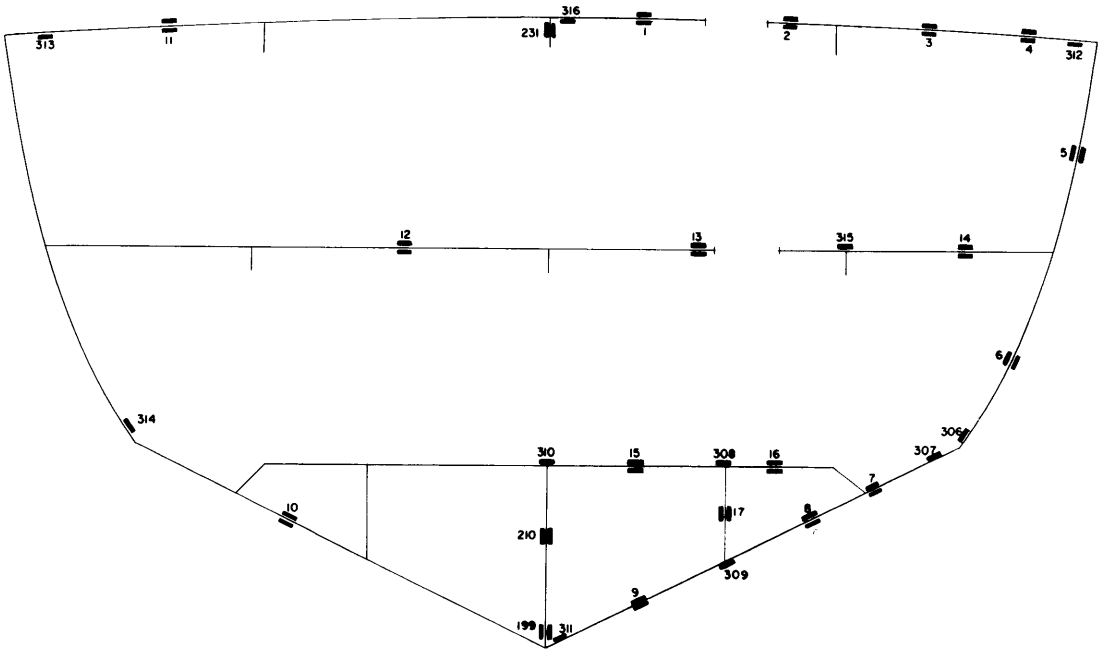

Figure F.1 - Frame 20 1/2

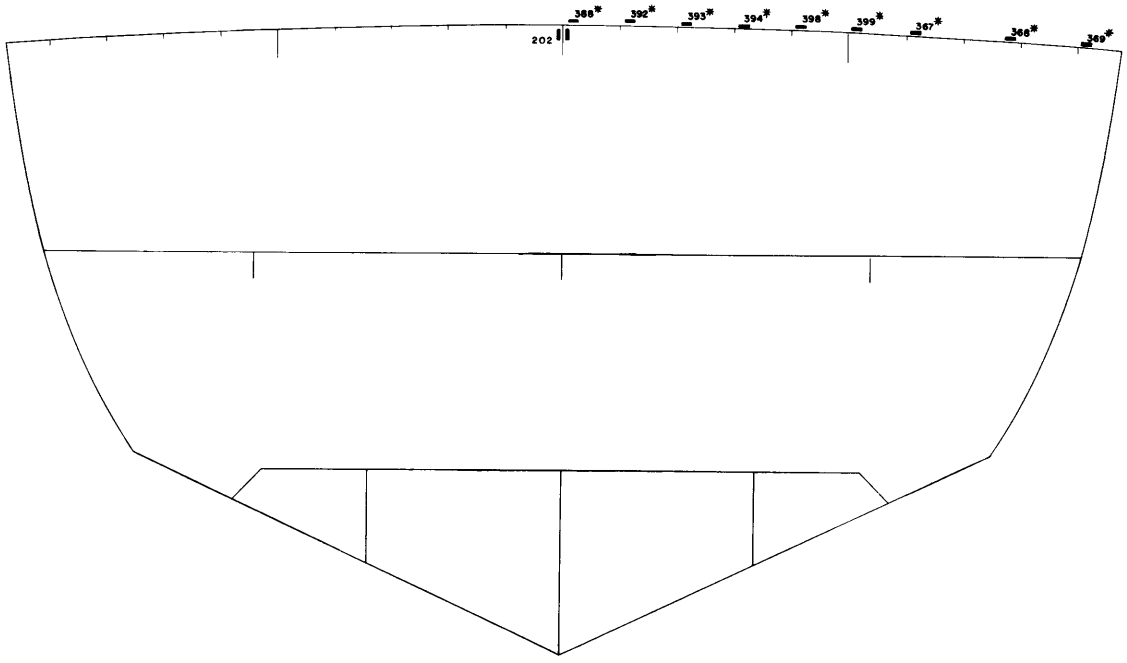

Figure F.2 - Frame 22 1/2

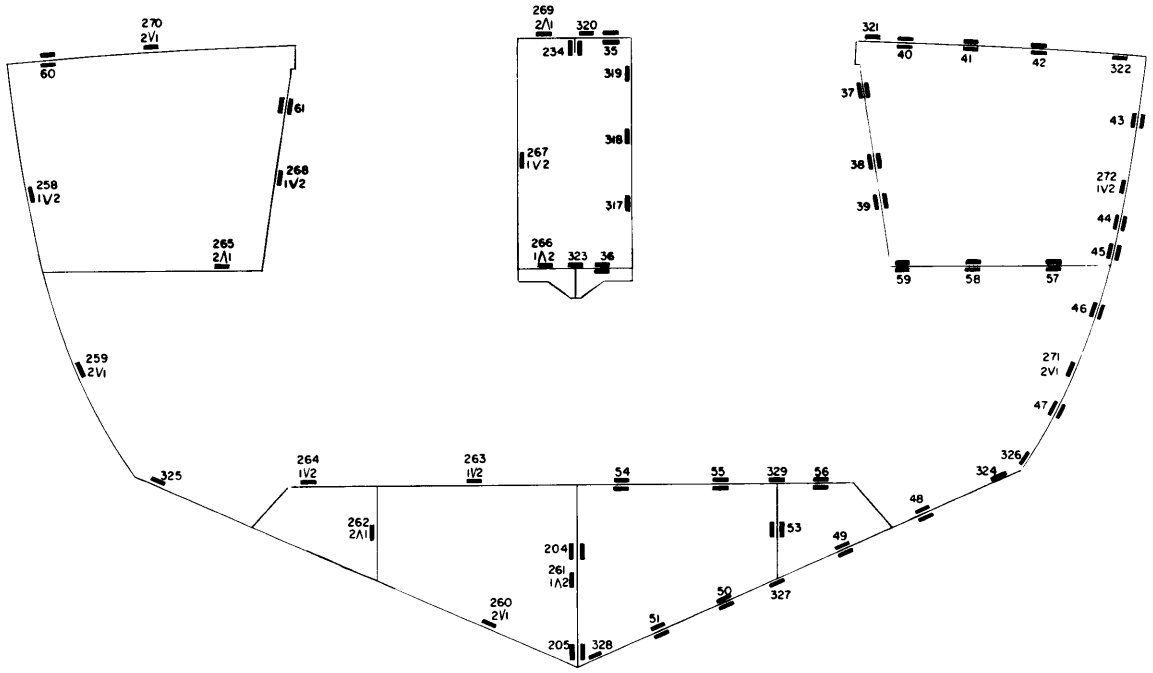

Figure F.3 - Frame 25 1/2

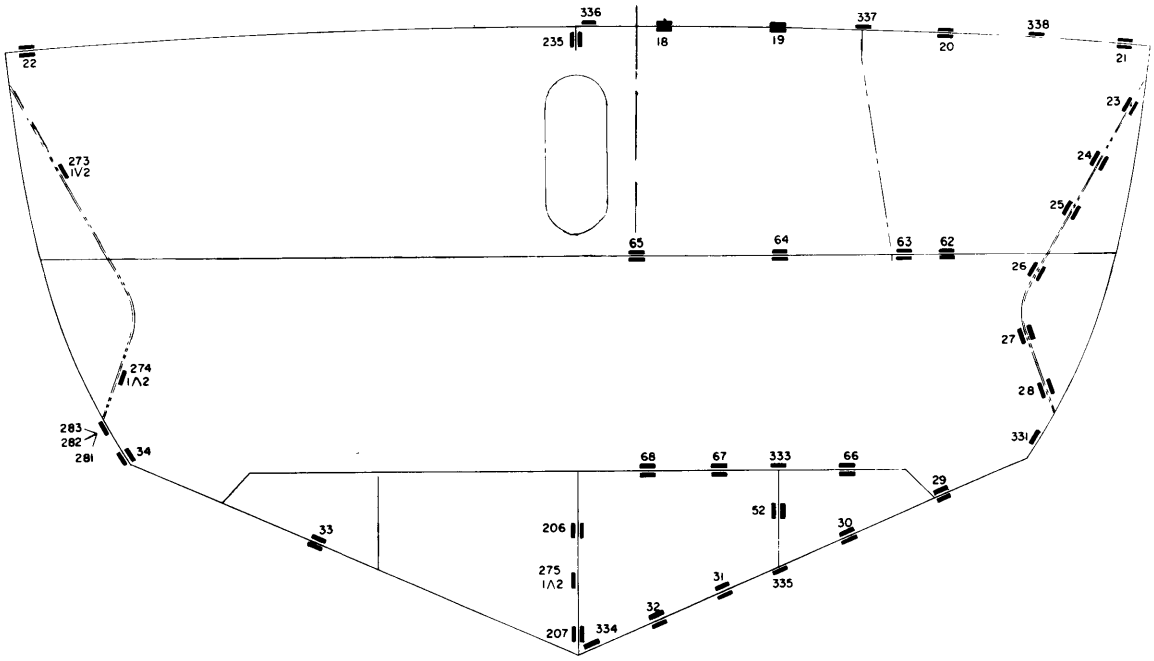

Figure F.4 - Frame 26 1/2

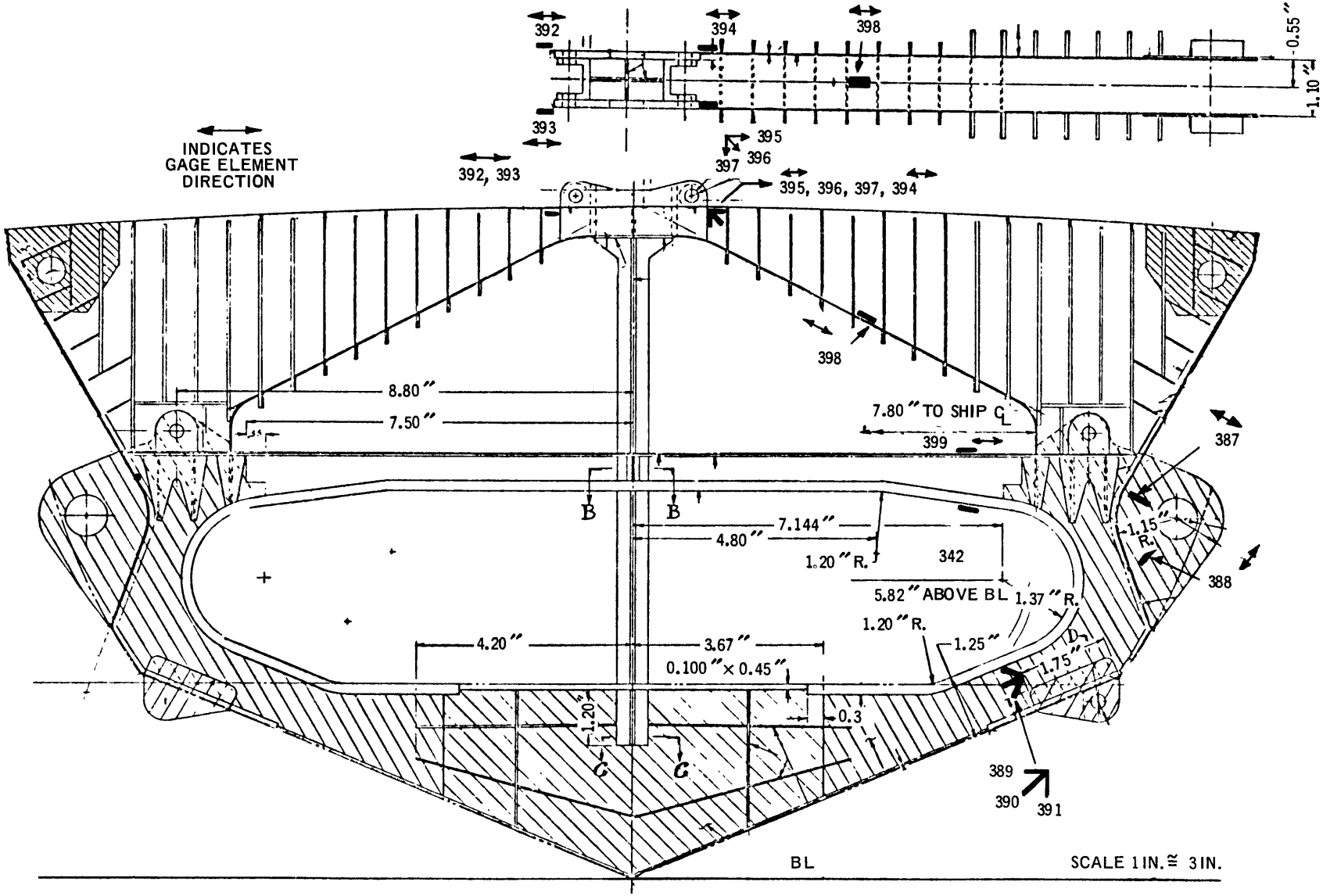

Figure F.5 - Frame 27 2.19 In. Aft of Frame 26

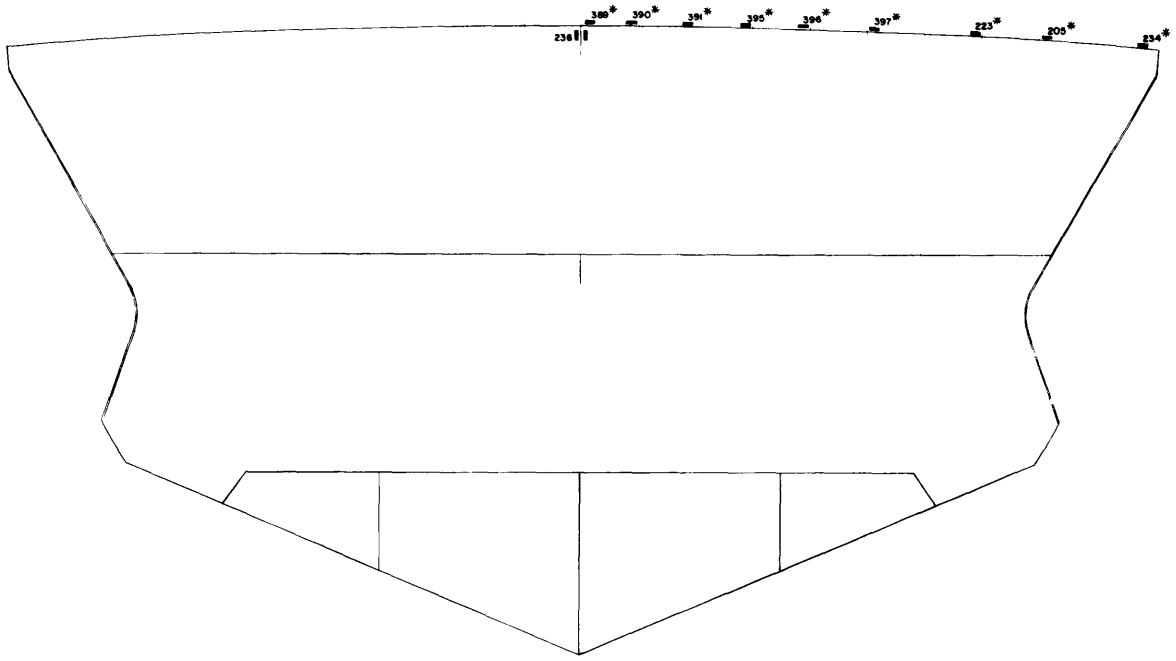

Figure F.6 - Frame 28 1/2

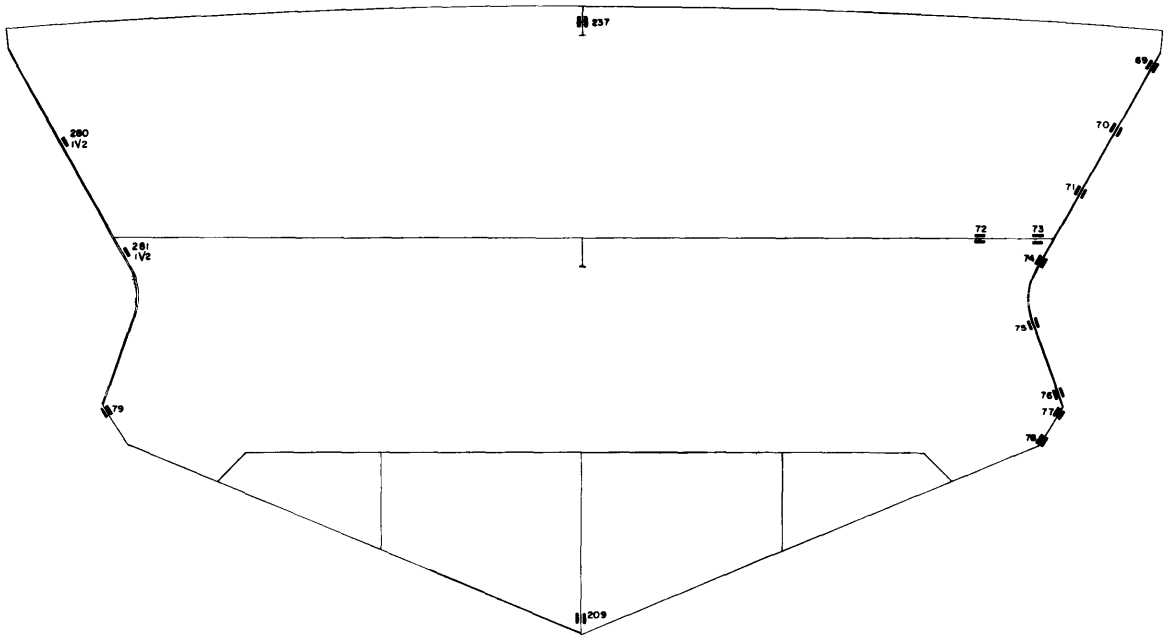

Figure F.7 - Frame 29 1/2

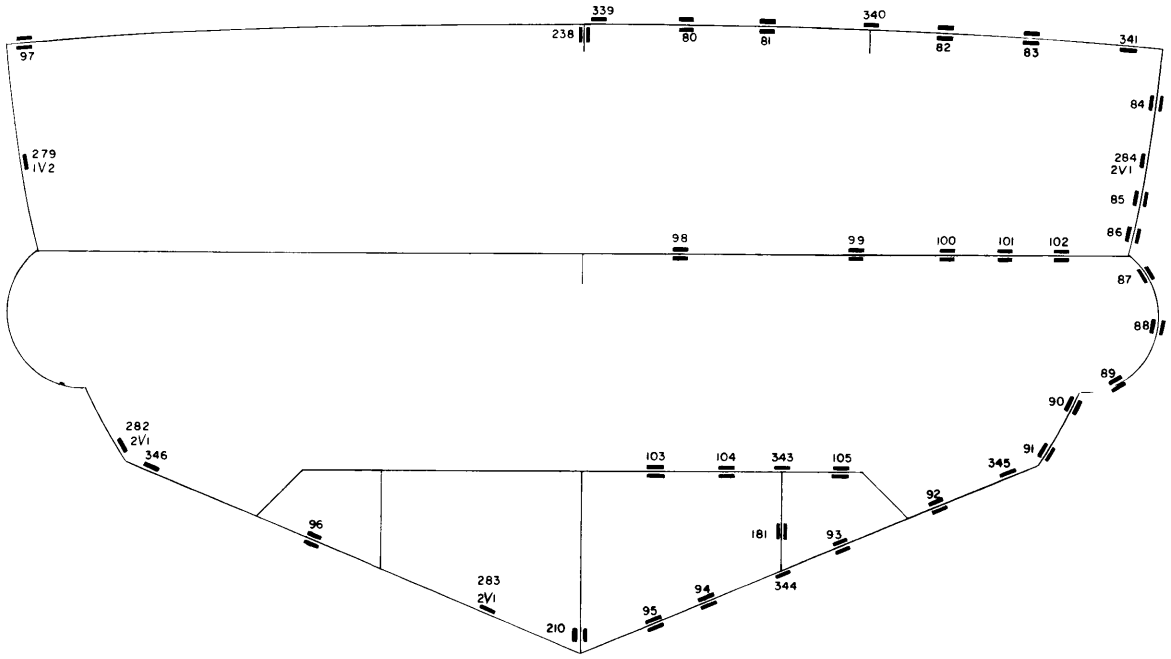

Figure F.8 - Frame 31 1/2

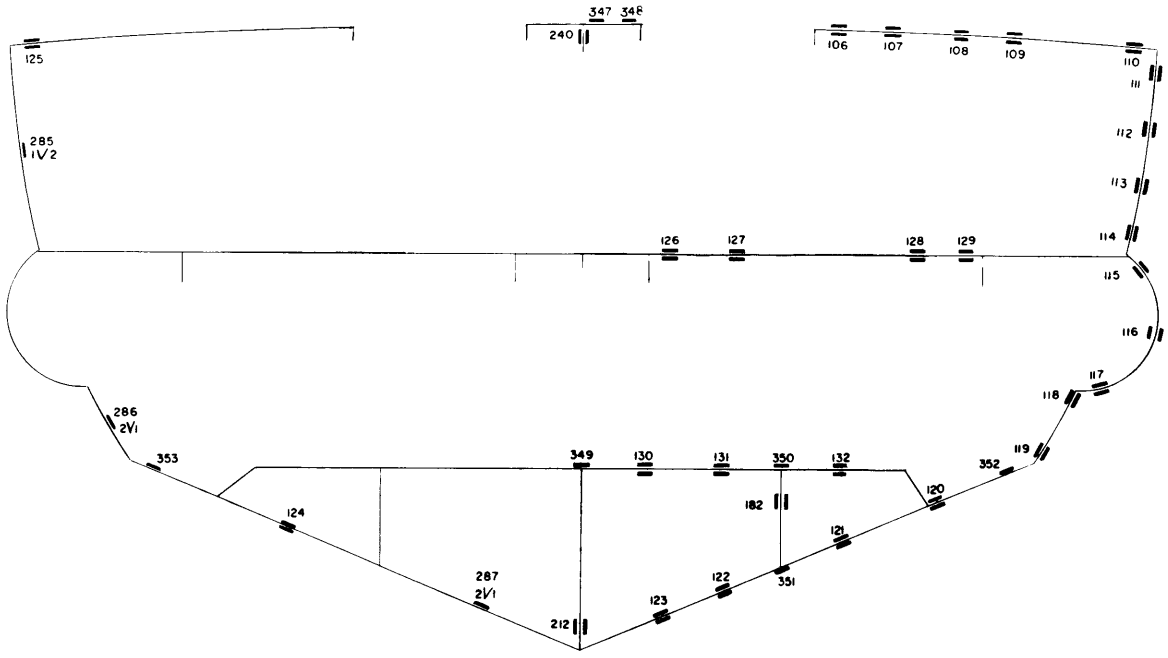

Figure F.9 - Frame 33 1/2

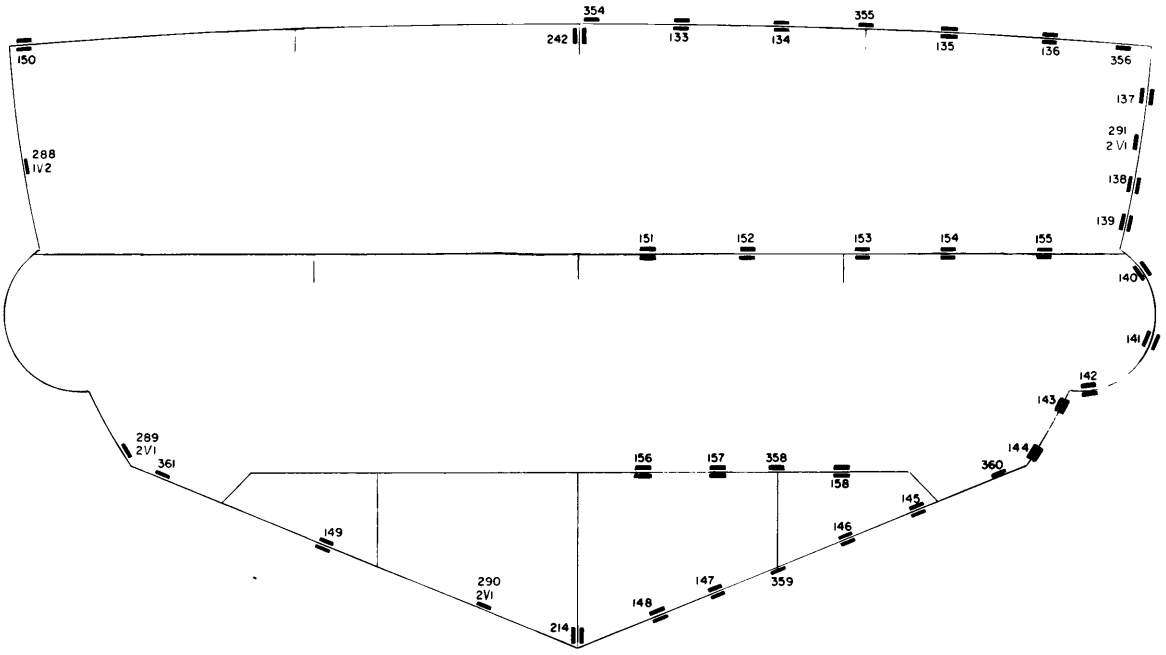

Figure F.10 - Frame 35 1/2

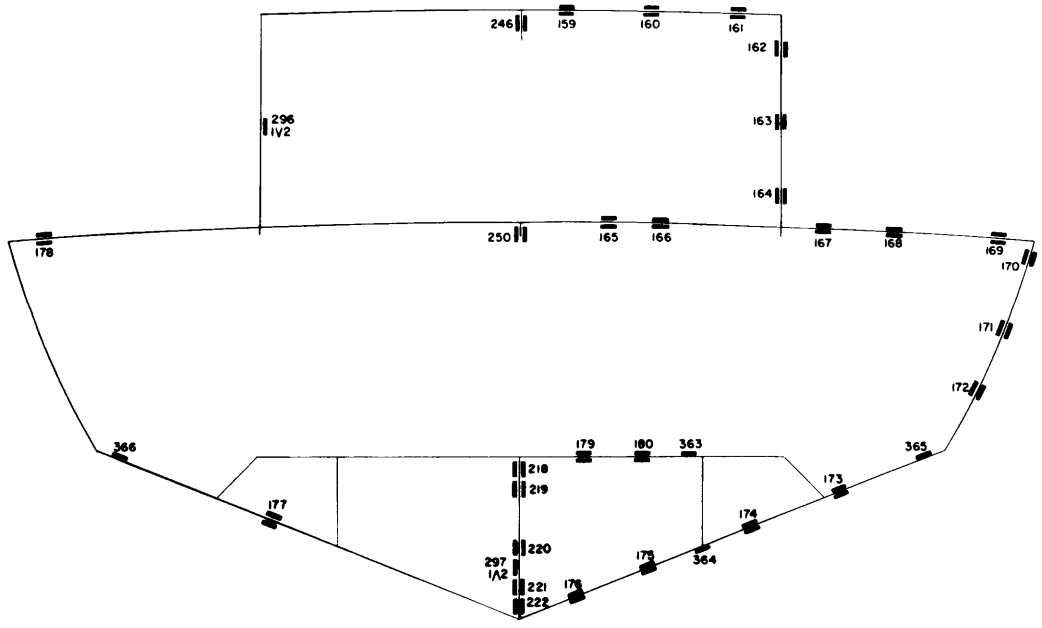

Figure F.11 - Bulkhead 40 1/2

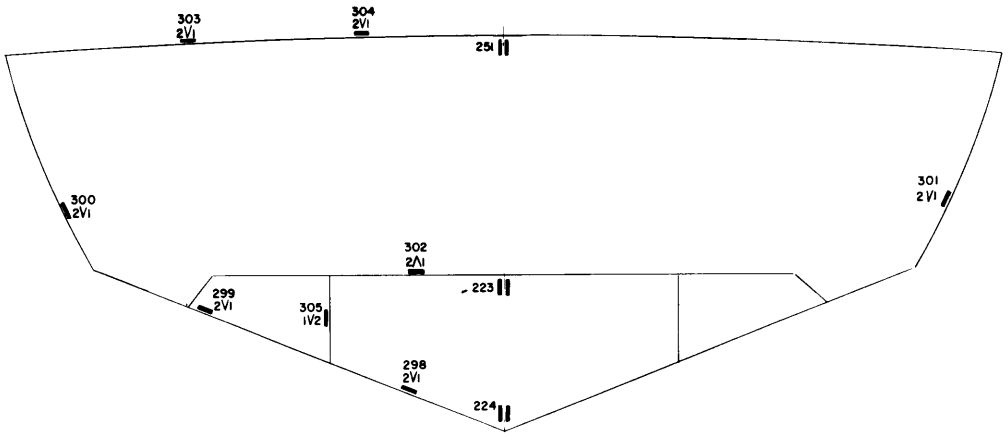

Figure F.12 - Frame 42 1/2

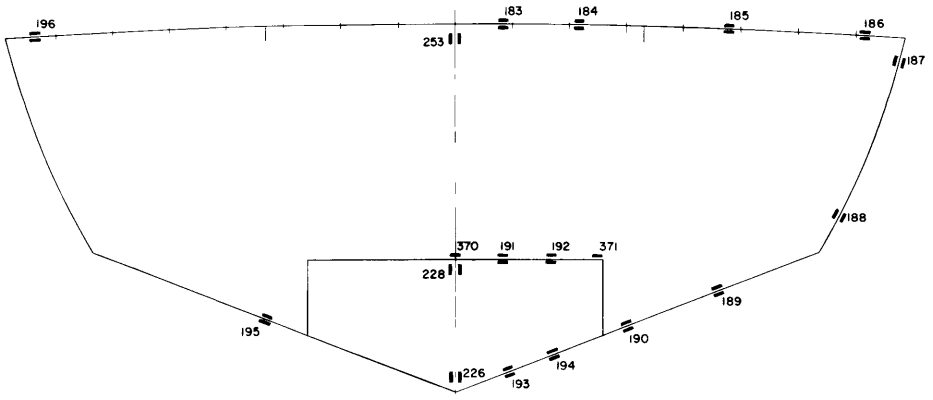

Figure F.13 - Frame 48.5

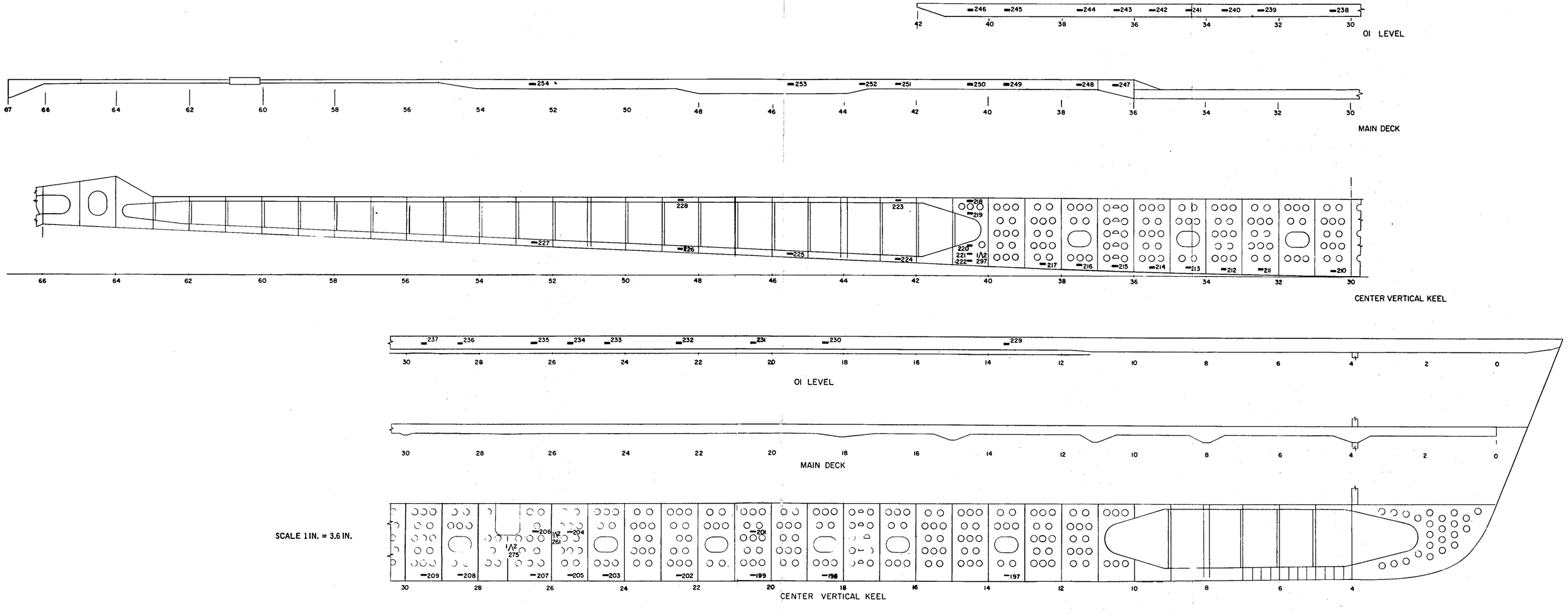

Figure F.14 - Centerline Longitudinal Bending Section

INITIAL DISTRIBUTION

Copies	
3	CNO 1 OP 07T 1 OP 343 1 OP 723H
2	ONR 1 Code 439 1 Code 459
2	NAVMAT 1 MAT 0331 1 MAT 033A
1	NRL, Tech Lib
1	DNL
9	NAVSHIPSYSCOM 2 SHIPS 2052 1 SHIPS 031 1 SHIPS 0342 1 SHIPS 034 2 SHIPS 034-12 2 PMS 382A
3	NAVAIRSYSCOM 1 Aero & Hydro Br (Code 5301) 1 Str Br (Code 5302) 1 Engr Div (Code 520)
1	NAVORDSYSCOM ORD 913
1	NADC
1	NELC Attn: Mr. D. Washburn
1	NURDC Attn: Mr. C. Miller (D602)
2	NWC 1 Code 556 1 Code 5056
1	NOL, Code 730
1	NUSC, New London
1	USNA
1	PGSCHOL, Monterey
1	ROTC, MIT
1	Naval War College
1	NAVAIRENGCEN

Copies	
1	NAVSHIPYD BREM
1	NAVSHIPYDBSN
1	NAVSHIPYDCHASN
1	NAVSHIPYD LBEACH
1	NAVSHIPYD NORVA
1	NAVSHIPYD PEARL
1	NAVSHIPYD PTSMH
1	NAVSHIPYD SFRANBAY VJO
1	SUPSHIP 13th Naval District (Code 6233D)
12	NAVSEC 4 SEC 6110 1 SEC 6115 1 SEC 6120 1 SEC 6128 1 SEC 6132 1 SEC 6139 1 SEC 6137 1 SEC 6101 1 SEC 6114D
12	DDC
1	ARPA
1	Air Force
2	USCG 1 Chief Testing & Development Div 1 Ship Structures Comm.
1	Lib of Congress
3	MARAD 1 Director 1 Chief Div of Ship Design 1 Office of R&D
1	Nat'l Research Council Nat'l Academy of Sci Ship Hull Research Comm.
1	Nat'l Sci Foundation Engr Div

Copies	
1	Director, Dept of Naval Arch College of Engr Univ of Calif
2	Catholic Univ 1 Prof S.R. Heller, Jr.
1	Director, Iowa Inst of Hydraulic Research, State Univ of Iowa
1	Dept of Mechanics Lehigh Univ
1	MIT, Dept of NAME
1	Univ of Michigan Dept of NAME
1	Univ of Minnesota St. Anthony Falls Hydraulic Lab
1	Director, Davidson Lab, SIT
1	SWRI
1	Virginia Polytechnic Inst & State Univ Dept of Engr Mechanics Attn: Prof. C.W. Smith
1	American Bureau of Shipping 45 Broad Street New York, N.Y. 10004 Attn: S.G. Stiansen
1	The Boeing Co., Aerospace Grp P.O. Box 3999 Seattle, Wash 98124
1	Gibbs & Cox, Inc
1	Grumman Aerospace Corp Bethpage, Long Island, New York 11714
1	President, Hydronautics Inc Pindell School Rd Laurel, Md. 20810
2	Secretary, SNAME 74 Trinity Place New York, N.Y. 10006 1 Slamming Panel

CENTER DISTRIBUTION

Copies	Code
1	11
1	115
1	1151
1	1153
1	1154
1	1170
1	1180
1	15
1	156
1	16
1	17
1	1703
1	172
1	173
1	1731
1	1735
1	174
1	177
1	178
1	19
1	196
1	1962
1	1966
	Annapolis
1	27
1	28

DOCUMENT CONTROL DATA - R & D

(Security classification of title, body of abstract and indexing annotation must be entered when the overall report is classified)

1 ORIGINATING ACTIVITY (Corporate author)	2a. REPORT SECURITY CLASSIFICATION
Naval Ship Research & Development Center Bethesda, Maryland 20034	UNCLASSIFIED
	2b. GROUP

3 REPORT TITLE

DESIGN HISTORY OF THE RIGID VINYL MODEL OF THE HYDROFOIL PLAINVIEW (AGEH-1)

4 DESCRIPTIVE NOTES *(Type of report and inclusive dates)*

NAVSHIPRANDCEN Report

5 AUTHOR(S) *(First name, middle initial, last name)*

Steven L. Austin

6. REPORT DATE	7a. TOTAL NO. OF PAGES	7b. NO OF REFS
October 1972	111	5

8a. CONTRACT OR GRANT NO.	9a. ORIGINATOR'S REPORT NUMBER(S)
b. PROJECT NO. In-House	3883
c.	9b. OTHER REPORT NO(S) *(Any other numbers that may be assigned this report)*
d.	

10 DISTRIBUTION STATEMENT

APPROVED FOR PUBLIC RELEASE: DISTRIBUTION UNLIMITED

11 SUPPLEMENTARY NOTES	12. SPONSORING MILITARY ACTIVITY
	Hydrofoil Advanced Development Program

13 ABSTRACT

This report presents the method and the rationale used in the design and construction of a small-scale rigid vinyl (PVC) statically loaded, elastic structural model of the hydrofoil PLAINVIEW (AGEH-1).

14 KEY WORDS	LINK A		LINK B		LINK C	
	ROLE	WT	ROLE	WT	ROLE	WT
Structural Modeling						
Plastic Models						
Rigid Vinyl (PVC)						
Model Design and Construction						
Model Instrumentation						
Hydrofoil PLAINVIEW (AGEH-1)						